1-37A Copy No. ____________

Guide for Mechanistic-Empirical Design

OF NEW AND REHABILITATED PAVEMENT STRUCTURES

FINAL REPORT

PART 3. DESIGN ANALYSIS

CHAPTER 4. DESIGN OF NEW AND RECONSTRUCTED RIGID PAVEMENTS

NCHRP

Prepared for
National Cooperative Highway Research Program
Transportation Research Board
National Research Council

Submitted by
ARA, Inc., ERES Consultants Division
505 West University Avenue
Champaign, Illinois 61820

March 2004

ACKNOWLEDGMENT OF SPONSORSHIP

This work was sponsored by the American Association of State Highway and Transportation Officials, in cooperation with the Federal Highway Administration, and was conducted in the National Cooperative Highway Research Program, which is administered by the Transportation Research Board of the National Research Council.

PART 3—DESIGN ANALYSIS

CHAPTER 4
DESIGN OF NEW AND RECONSTRUCTED RIGID PAVEMENTS

3.4.1 INTRODUCTION

This chapter describes the mechanistic-empirical design procedures for new and reconstructed jointed plain concrete pavements (JPCP) and continuously reinforced concrete pavements (CRCP). The process requires an iterative hands-on approach by the designer. The designer must select a trial design and then analyze the design in detail to determine if it meets the established performance criteria. The performance measures considered in this guide include joint faulting and transverse cracking for JPCP, punchouts for CRCP, and International Roughness Index (IRI) for both pavement types. If the trial design does not satisfy the performance criteria at a given reliability level, the design should be modified and reanalyzed until the design does satisfy the criteria. The designs that meet the applicable performance criteria at the selected reliability level are then considered feasible from a structural and functional standpoint and can be further considered for other evaluations, such as life cycle cost analysis (LCCA) and environmental impacts.

This chapter provides a detailed description of the design procedure for JPCP, followed by the design procedure for CRCP. Also included in this chapter are sensitivity analyses for factors that affect JPCP and CRCP design and recommendations for changes if a particular design does not meet the performance criteria. The contents of this chapter are as follows:

1. Introduction (section 3.4.1).
2. An overview of the design procedure (section 3.4.2).
3. Design inputs for new rigid pavement design (sections 3.4.3).
4. JPCP design considerations (section 3.4.4).
5. JPCP design procedure (section 3.4.5).
6. CRCP design considerations (section 3.4.6).
7. CRCP design procedure (section 3.4.7).
8. Special loading considerations (section 3.4.8)
9. Calibration to local conditions (section 3.4.9).

The procedures described in this chapter can be used for design of JPCP and CRCP on new alignment or for reconstruction of existing pavements. There are no fundamental differences in the way pavements are designed for new alignment or reconstruction. However, one practical aspect is that for reconstruction, the potential reuse of the materials from the existing pavement structure is an important issue that should be considered. The effects of using the materials recycled from the existing pavement structure in various modified layers of the new pavement can be evaluated using the procedures described in this Guide.

3.4.2 OVERVIEW OF THE DESIGN PROCESS

The overall iterative design processes for JPCP and CRCP are illustrated in figures 3.4.1 and 3.4.2, respectively. The main steps include the following:

1. Assemble a trial design for a specific site conditions including traffic, climate, and foundation—define layer arrangement, portland cement concrete (PCC) and other paving material properties, and design and construction features.
2. Establish criteria for acceptable pavement performance at the end of the design period (i.e., acceptable levels of faulting and cracking for JPCP, punchouts for CRCP, and IRI for both).
3. Select the desired level of reliability for each of the applicable performance indicators (e.g., select design reliability levels for cracking, faulting, and IRI for JPCP).
4. Utilize design guide software to accomplish the following:
    a. Process input to obtain monthly values of traffic, material, and climatic inputs needed in the design evaluations for the entire design period.
    b. Compute structural responses (stresses and deflections) using finite element based rapid solution models for each axle type and load and for each damage-calculation increment throughout the design period.
    c. Calculate accumulated damage at each month of the entire design period.
    d. Predict key distresses (joint faulting, slab cracking, CRCP punchouts) month-by-month throughout the design period using the calibrated mechanistic-empirical performance models provided in the Guide.
    e. Predict smoothness (IRI) as a function of initial IRI, distresses that occur over time, and site factors at the end of each time increment.
5. Evaluate the expected performance of the trial design at the given reliability level for adequacy.
6. Modify the design and repeat the steps 4 through 5 above as necessary until the design does meet the established criteria.

The designs that satisfy the target performance criteria at the specified reliability are considered feasible from a structural and functional viewpoint and can be further considered for other evaluations, such as LCCA.

3.4.2.1 Design Inputs

<u>Trial Design Inputs and Site Conditions</u>

The design procedure offers the capability to consider a wide variety of structural layer arrangements (as illustrated in figure 3.4.3) and design features, including joint spacing, dowels, tied PCC shoulder, widened slabs, base type, and drainage. The design is accomplished iteratively by analyzing trial designs in detail to identify a design that satisfies the performance criteria (i.e., joint faulting, slab cracking, punchouts, IRI) over the analysis period. A trial design includes all details needed to perform design evaluations using the procedures prescribed in this Guide, including pavement layers, joint design, reinforcement design, and materials properties.

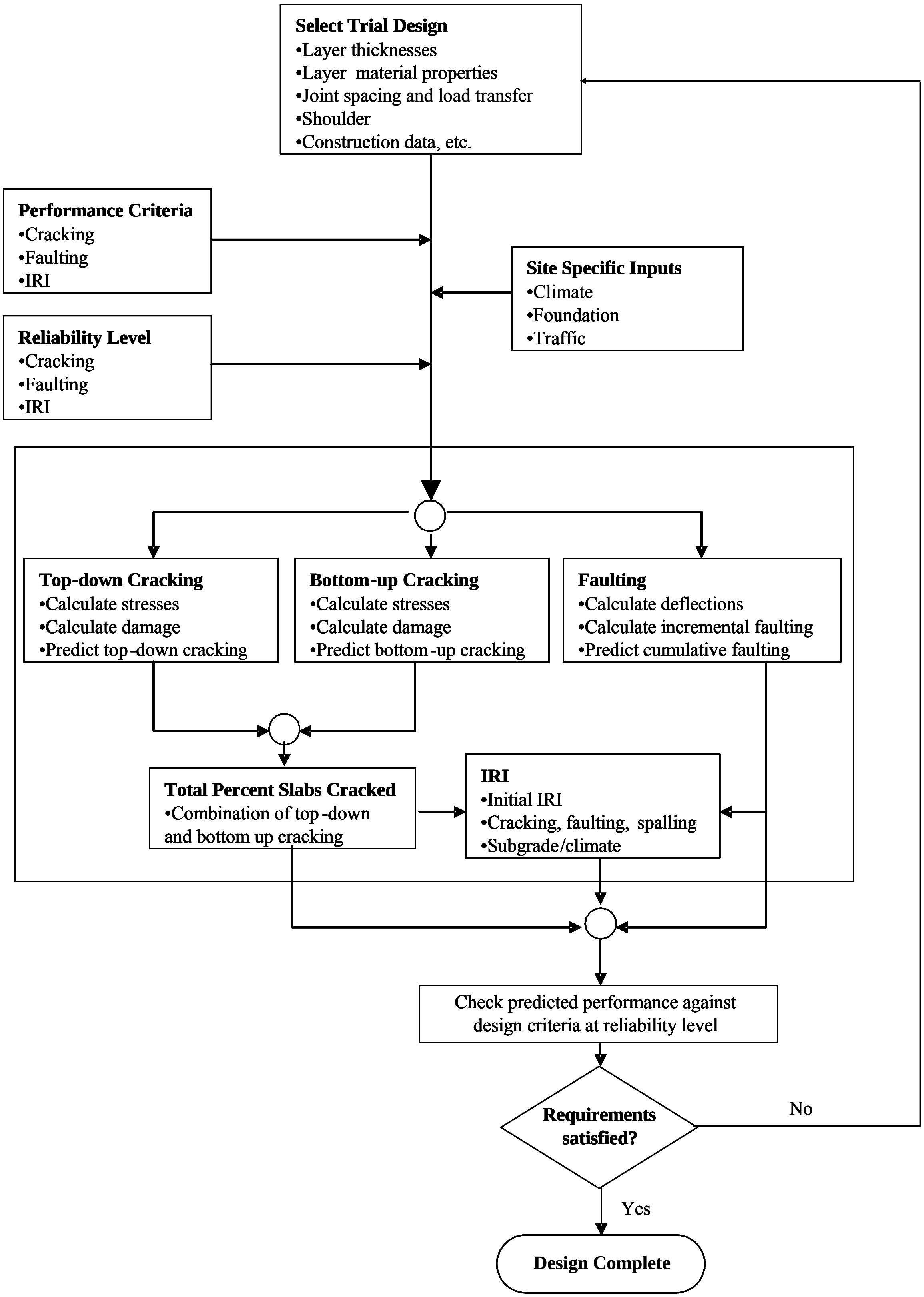

Figure 3.4.1. Overall design process for JPCP.

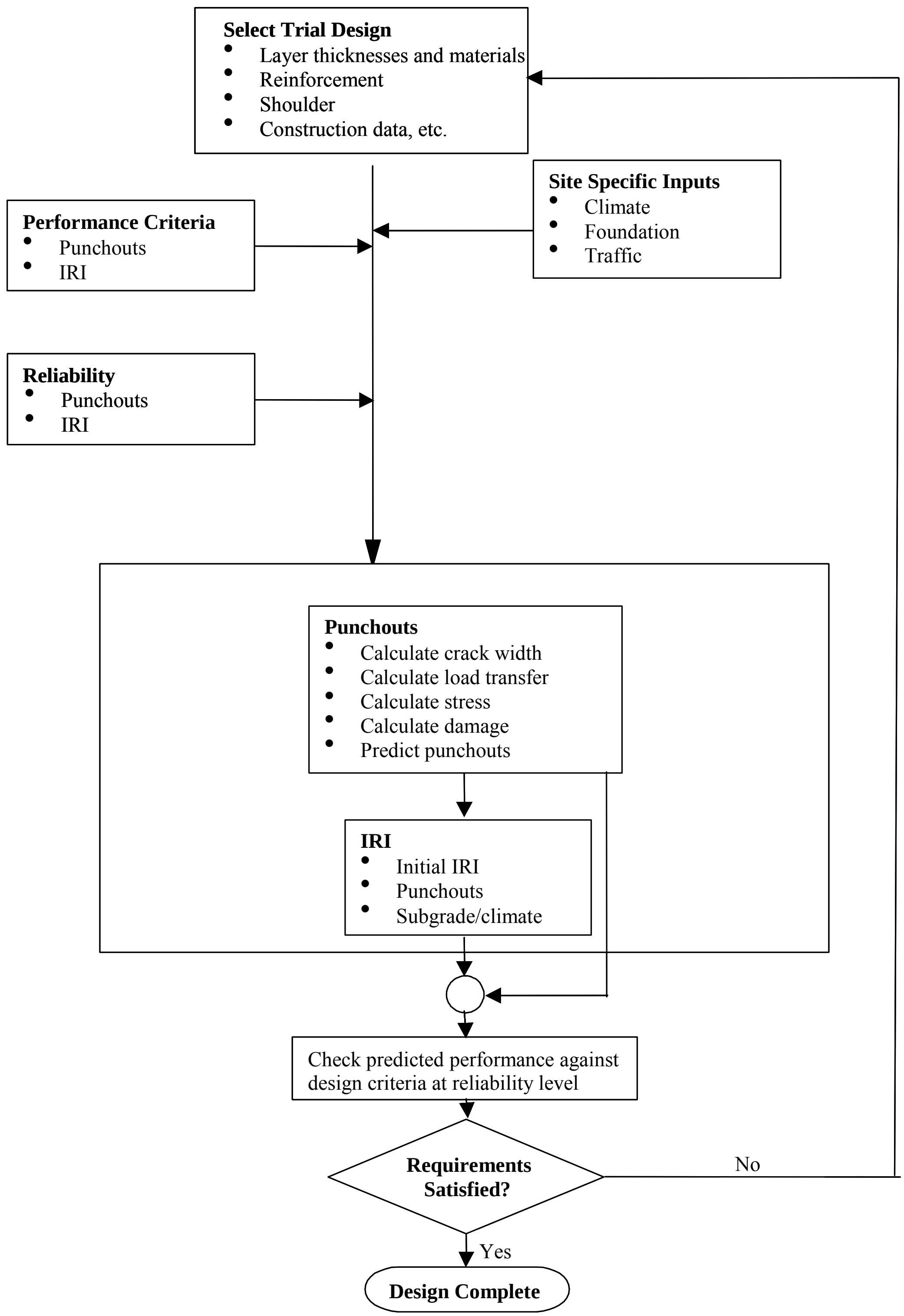

Figure 3.4.2. Overall design process for CRCP.

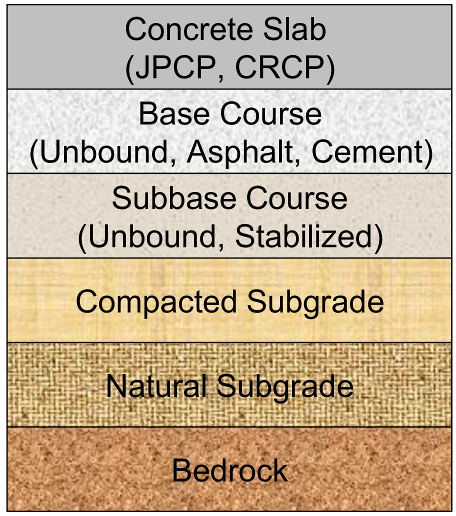

Figure 3.4.3. Illustration of possible rigid pavement layered system.

In addition to the trial design, the designer must provide inputs for the project site conditions including subgrade properties (including presence of bed rock), traffic, and climatic data. There are also several design inputs related to construction such as the initial smoothness (initial IRI), estimated month of PCC paving, estimated month that the pavement will be opened to traffic, and estimated permanent curl/warp of the PCC slab.

A major difficulty in obtaining adequate design inputs is that the desired project specific information is not generally available at the design stage and must often be estimated several years in advance of construction. The actual materials used in a project may not even be known until a few weeks before construction begins. The designer should obtain as much data as possible on material properties, traffic, and other inputs for use in design to obtain as realistic a design as possible. The designers should also conduct a sensitivity analysis to identify which inputs affect pavement performance the most. Based on sensitivity analysis results, provisions could be made in the contract documents for stringent control of the quality of key material properties (e.g., PCC CTE), or the design could be modified to make the pavement performance less sensitive to the input in question (e.g., slab joint spacing).

Design Input Levels

For many of the design inputs, the designer can choose from multiple (generally three) levels of data quality. These are briefly identified below:

1. Level 1—site and/or material specific inputs for the project obtained through direct testing or measurements. Examples of Level 1 data include material properties obtained through laboratory testing and measured traffic volumes and weights near or at the project site.
2. Level 2—the use of correlations to establish or determine the required inputs. Examples of Level 2 data include the resilient modulus of the subgrade or unbound base materials estimated from California Bearing Ratios (CBR) or R-values using empirical correlations.

3. Level 3—the use of national default values or local experience to define the inputs. Examples of Level 3 input include the use of AASHTO soil classifications to determine a typical resilient modulus value or the use of roadway type and truck type classifications to determine normalized axle weight and truck classification distributions.

The input levels can vary from input parameter to input parameter. For example, subgrade resilient modulus can be obtained from a lab test (Level 1) and traffic axle load distribution from national data (Level 3). The input level selection for a specific parameter depends on several factors, including the following:

- Sensitivity of the pavement performance to a given input.
- The criticality of the project.
- The information available at the time of design.
- The resources and time available to the designer to obtain the inputs.

The input levels for the various design parameters are described in PART 2 of this Guide. The level chosen for each input parameter, however, may have a significant effect on project design, costs, and reliability. Sensitivity analysis can be used to determine which parameters should be determined more precisely for a given project.

<u>Processing of Inputs over Design Analysis Period</u>

The raw design inputs are processed by the software to obtain monthly values of the traffic, material, and climatic inputs needed in the design evaluations, which consist of the following:

- Average hourly number of single, tandem, tridem, and quad axles in each axle weight category for each month of the analysis period.
- Temperatures at 11 evenly spaced nodes in the PCC layer for every hour of the available climatic data. A minimum of 1 year's weather station data are required.
- Average monthly relative humidity for each calendar month.
- PCC strength and modulus at each month of the analysis period.
- Monthly average moduli values of the base layer.
- Monthly average effective subgrade modulus of reaction (k-value) determined based on subgrade resilient modulus (the raw design input).

PART 2, Chapter 4 describes the details of traffic calculations. PART 2, Chapter 3 describes details of climatic calculations.

The monthly layer moduli and the hourly temperatures profiles in the PCC layer are obtained using the Enhanced Integrated Climatic Model (EICM), which is a part of the Design Guide software. Major layer types included in the design procedure are PCC slab, asphalt stabilized base, cement stabilized base, other cementitious and lime-treated layers, unbound aggregate base/subbase, and subgrade soils. PART 2, Chapter 2 describes the materials inputs required for each of these layer types in detail. PART 2, Chapter 3 describes how each of these materials are affected by seasonally changing temperature and moisture conditions.

Temperature and moisture variations through the PCC slab are directly considered in the design procedure through a "permanent" component and "transitory" (hourly and monthly) component.

- A constant permanent curl/warp (modeled through an effective temperature difference through slab) is estimated for the PCC slab based on the cracking model calibration results.
- The transitory curling due to the changes in the temperature conditions in the slab is modeled using the EICM computed hourly temperature profiles in the PCC slab. The transitory warping due to the changes in relative humidity is converted into equivalent temperature differences on monthly basis as described in section 3.4.4 and added to the effects of transitory curling.

Long-term PCC strength gain and corresponding changes in PCC elastic modulus (E_C) are considered in the rigid design procedure. The PCC strength (modulus of rupture, compressive strength, and indirect tensile strength) and E_C for each month of the analysis period can be determined based on either direct input (Level 1) or using the default PCC strength gain model (see PART 2, Chapter 2).

Seasonally adjusted modulus values of the subgrade and other sublayers from the EICM are converted into an average monthly effective k-value for structural response calculation and damage analysis. This conversion is made internally in the Design Guide software program. The methodology used to perform this conversion is explained later in this section.

The input processing is automated in the Design Guide software, and the processed inputs feed directly into the structural response calculation modules that compute critical pavement responses on a month-by-month basis over the entire design period.

3.4.2.2 Structural Response Model

Finite element analysis has been proven to be a reliable tool for solving many engineering problems, including the computation of PCC pavement responses, such as stresses and deflections under the influence of traffic and environmental loads. However, the incremental design procedure adopted in this Guide requires hundreds of thousands of stress and deflection calculations to compute monthly damage (for the different loads, load positions, and equivalent temperature differences) over a design period of many years. These computations would take days to complete using existing finite element programs. To reduce computer time to a practical level, neural networks (NNs) have been developed, based on the ISLAB2000 finite element (FE) structural model (*1*), to accurately compute critical stresses and deflections virtually instantaneously. This makes it possible to conduct detailed, month-by-month, incremental analysis within a practical time frame (within a few minutes). A series of neural networks were developed for different analyses that accurately reproduce the results given by direct FE analysis (R^2 of 0.99). Appendix QQ provides a detailed description of the finite element models and neural networks.

3.4.2.3 Incremental Damage Accumulation

The trial design is analyzed for adequacy by dividing the design analysis period into monthly time increments beginning with the traffic opening month.

- Traffic loads are divided into types of axles and axle loads. Axle load increments are 1,000 lb for single axles, 2,000 lb for tandem axles, and 3,000 lb for tridem and quad axles.
- Lateral truck wander is assumed normally distributed and modeled using mean wheelpath and standard deviation of lateral traffic wander.
- Equivalent temperature difference through the PCC slab (which includes permanent and transitory temperature and moisture gradient effects) is accounted for in increments of 2 °F for both positive (daytime) and negative (nighttime) top-to-bottom temperature differences.

Within each increment (each month), all other factors that affect pavement responses and damage are held constant. These include:

- PCC strength and modulus.
- Base modulus.
- Subgrade modulus.
- Joint load transfer (transverse and longitudinal).
- Base erosion and loss of support (for CRCP).

Thus, within each increment a critical stress or deflection can be calculated, as well as the damage incurred in that increment. Damage is summed over all increments and output at the end of each month by the Design Guide software.

3.4.2.4 Distress Prediction

The damage calculated and accumulated as described in section 3.4.2.3 is a mechanistic parameter that represents a relative index of load associated damage within the pavement structure. When "damage" is very small (e.g., 0.0001) the pavement structure would not be expected to have any physical distress like cracking, faulting, or punchouts. As computed "damage" increases to a significant value (e.g., 0.1 or greater), visible distress may be expected to develop in a few locations along the project.

The incremental damage is accumulated month by month and is converted to physical pavement distresses such as transverse cracks, faulting, and punchouts using calibrated models that relate the calculated damage to observable distresses. An example of one such model that relates bottom-up fatigue damage to percent slabs cracked in JPCP is shown in figure 3.4.4. Calibrated distress prediction models were developed using the Long Term Pavement Performance (LTPP) database and other long-term pavement performance data obtained for a wide range of JPCP and CRCP structures located in a variety of climatic conditions and subject to various traffic and environmental loading situations.

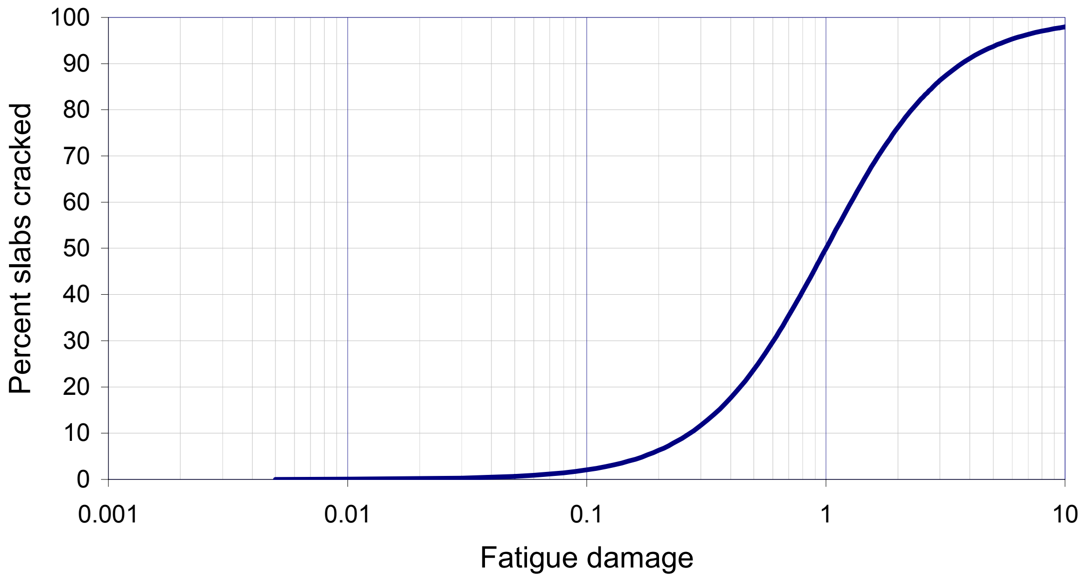

Figure 3.4.4. Relationship between fatigue damage and percent slabs cracks in JPCP.

The structural distresses considered for JPCP design are fatigue-related transverse cracking of PCC slabs and differential deflection related transverse joint faulting. Transverse cracking of PCC slabs can initiate either at the top surface of the PCC slab and propagate downward (top-down cracking) or vice versa (bottom-up cracking) depending on the loading and environmental conditions at the project site, as well as material properties, design features, and the conditions during construction. Both top-down and bottom-up cracking are considered in this Guide. For CRCP, the principal structural distress considered is edge punchouts. Damage accumulates differently for each of these different distresses and hence needs to be considered separately. The following sections explain the damage accumulation process of these distresses.

<u>Bottom-Up Transverse Cracking (JPCP)</u>

When the truck axles are near the longitudinal edge of the slab, midway between the transverse joints, a critical tensile bending stress occurs at the bottom of the slab, as shown in figure 3.4.5. This stress increases greatly when there is a high positive temperature gradient through the slab (the top of the slab is warmer than the bottom of the slab). Repeated loadings of heavy axles under those conditions result in fatigue damage along the bottom edge of the slab, which eventually result in a transverse crack that propagates to the surface of the pavement. Over time, transverse cracks in JPCP may deteriorate and cause roughness. The most effective means of limiting bottom-up transverse cracking include the following:

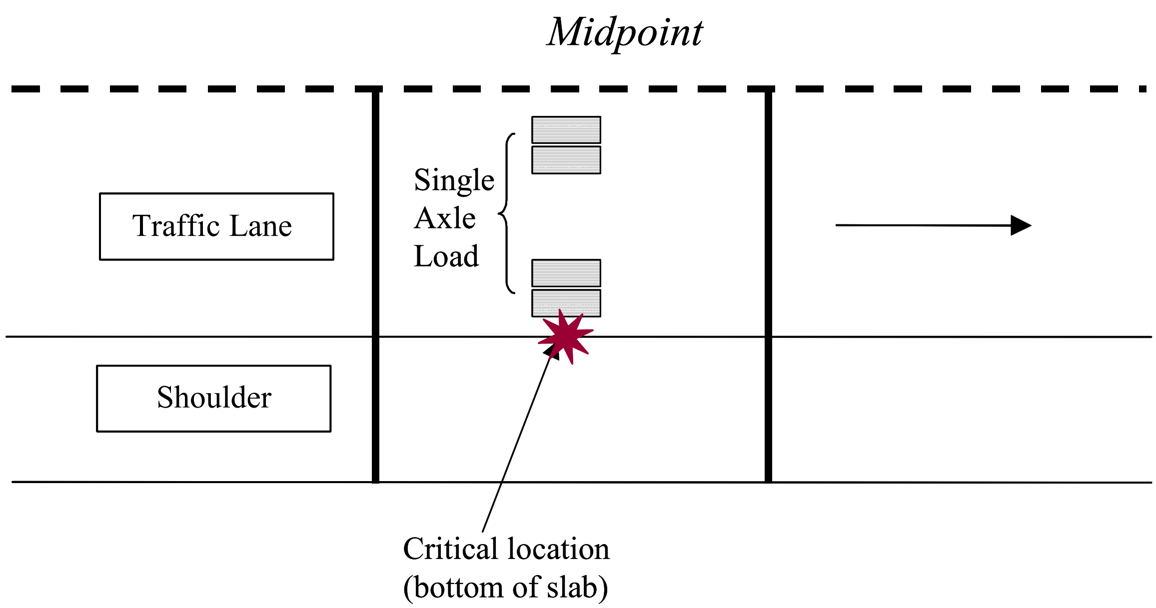

Figure 3.4.5. Critical load and structural response location for JPCP bottom-up transverse cracking.

- Increase slab thickness.
- Reduce joint spacing.
- Use widened slab.
- Use PCC mix with lower CTE.
- Provide tied PCC shoulder.
- Use a higher strength PCC mix (mixed results due to higher PCC elastic modulus, CTE, and shrinkage).
- Use a stabilized base.

Top-Down Transverse Cracking (JPCP)

Repeated loading by heavy truck tractors with certain axle spacings when the pavement is exposed to high negative temperature gradients (the top of the slab cooler than the bottom of the slab) result in fatigue damage at the top of the slab, which eventually results in a transverse or diagonal crack that is initiated on the surface of the pavement. The critical loading condition for top-down cracking involves a combination of axles that loads the opposite ends of a slab simultaneously. In the presence of a high negative temperature gradient, such load combinations cause a high tensile stress at the top of the slab near the critical edge, as shown in figure 3.4.6 (*2, 3*). This type of loading is most often produced by the combination of steering and drive axles of truck tractors and other vehicles. Multiple trailers with relatively short trailer-to-trailer axle spacing are other common sources of critical loadings for top-down cracking. The top-down stress becomes critical when significant amount of permanent upward curl/warp is present. Thus, the top-down cracking is controlled most effectively by the following means:

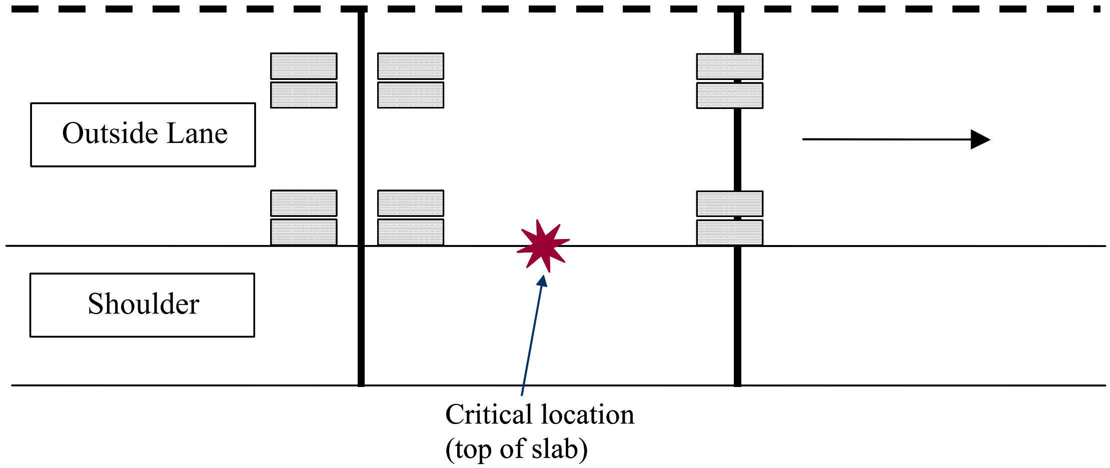

Figure 3.4.6. Critical load and structural response location for JPCP top-down transverse cracking.

- Increase slab thickness.
- Reduce joint spacing.
- Provide tied PCC shoulder.
- Use widened slab.
- Use a higher strength PCC mix with lower CTE and shrinkage.
- Use a stabilized base.
- Reduction in built-in curling after placement.

Joint Faulting (JPCP)

Repeated heavy axle loads crossing transverse joints creates the potential for joint faulting, as shown in figure 3.4.7 (*4*). Faulting can become severe and cause loss of ride quality and require premature rehabilitation if any of the following conditions occurs:

- Repeated heavy axle loads.
- Poor joint load transfer efficiency (LTE).
- Presence of pumpable fines beneath the joint—an erodible base, subbase, or subgrade.
- Presence of free moisture under the joint.

The most effective means of controlling faulting include the following:

- Provide dowels.
- Increase dowel size.
- Use widened slabs.
- Provide a less erodible base.
- Specify shorter joint spacing.
- Improve large aggregate properties (size of maximum aggregate and so on).
- Provide tied PCC shoulder.
- Provide subdrainage (particularly for undoweled pavements).

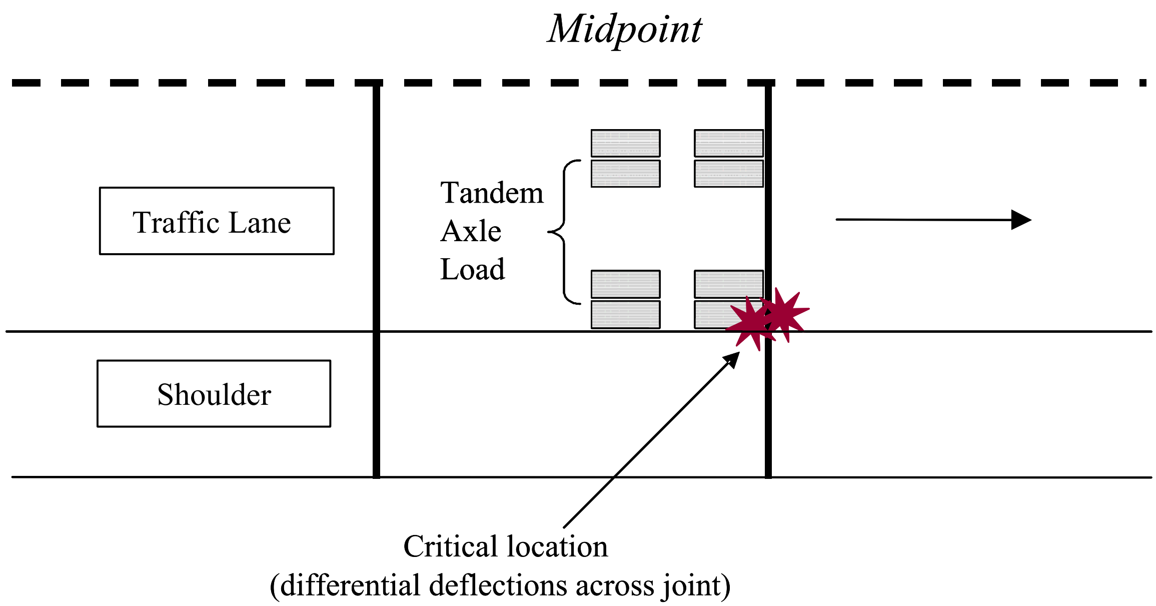

Figure 3.4.7. Critical load and structural response location for JPCP joint faulting analysis.

Punchouts (CRCP)

When truck axles pass along near the longitudinal edge of the slab between two closely spaced transverse cracks, a high tensile stress occurs at the top of the slab, some distance from the edge (say from 40 to 60 in from the edge), transversely across the pavement, as shown in figure 3.4.8. This stress increases greatly when there is loss of load transfer across the transverse cracks or loss of support along the edge of the slab.

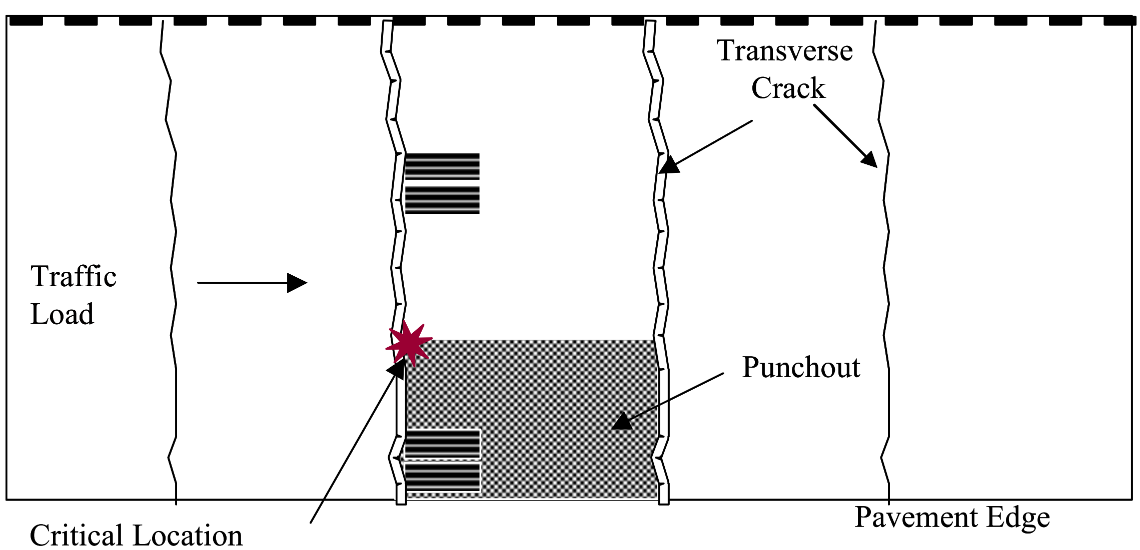

Figure 3.4.8. Critical load and structural response location for CRCP punchout analysis.

Repeated loading of heavy axles results in fatigue damage at the top of the slab, which results first in micro-cracks that initiate at the transverse crack and propagate longitudinally across the slab to the other transverse crack (see figure 3.4.8). The punchouts in CRCP are predicted considering the loss of crack LTE and erosion along the edge of the slab over the design life, and the effects of permanent and transitory moisture and temperature gradients. The transverse crack width is the most critical factor affecting LTE and, therefore, punchout development.

The most effective means of controlling punchouts in CRCP include the following:

- Increase longitudinal steel content (reduces crack width).
- Place reinforcement above mid-depth.
- Reduce PCC CTE.
- Increase slab thickness.
- Provide tied PCC shoulder.
- Use a stabilized base.
- Reduction in built-in curling after placement.
- Increase PCC strength.

3.4.2.5 Smoothness (IRI) Prediction

The IRI over the design period depends upon the initial, as-constructed, profile of the pavement from which the initial IRI is computed and the subsequent development of distresses over time (*5*). These distresses include transverse slab cracking, joint faulting, and joint spalling for JPCP and punchouts for CRCP. The IRI model uses the distresses predicted using the models included in this Guide and an empirical JPCP spalling model, initial IRI, and site factors to predict smoothness over time. The site factors include subgrade and climatic factors to account for the roughness caused by shrinking or swelling soils and frost heave conditions. IRI is estimated incrementally over the entire design period on a monthly basis.

3.4.2.6 Assessment of Performance and Design Modifications

A feasible design is obtained iteratively in a mechanistic design procedure. The process involves the following steps:

1. Establish performance criteria (e.g., level of cracking, faulting, punchouts and crack width, and smoothness at the end of the design life and the desired level of reliability for each).
2. Assemble a trial design.
3. Predict performance over the design life.
4. Evaluate the predicted performance against the design requirements.
5. If the design criteria are not satisfied, revise design and repeat steps 3 and 4 until the design does satisfy the performance requirements.

The key design factors that affect each individual the performance criterion have been briefly mentioned in section 3.4.2.4 of this chapter. Those are the main factors the designers may adjust to obtain a design that satisfies all design requirements. More details are provided in section 3.4.4 for JPCP design and in section 3.4.5 for CRCP design, including the sensitivity of pavement performance to key design factors.

3.4.2.7 Design Reliability

A large amount of uncertainty and variability exists in pavement design and construction, as well as in the application of traffic loads and climatic factors over the design life. In the mechanistic-empirical design, the key outputs of interest are the individual distress quantities (e.g., faulting, transverse cracking, and smoothness for JPCP). Therefore, the predicted distress is the random variable of interest in reliability design. Quantification of the distribution this variable assumes for all possible estimates of the mean and its associated moments is of interest for reliability estimation. In this Guide, the variability associated with the predicted distress quantity is estimated based on calibration results, after a careful analysis of the differences between the predicted versus actual distresses in the field. For design purposes, the design reliability is established based on knowledge of variation of a given performance around the mean prediction.

Design reliability for the individual pavement distress models (i.e., top-down cracking, bottom-up cracking, faulting, and CRCP punchouts) are based on the standard error of the estimates of each individual model obtained through the calibration process. These estimates of error include a input estimation variability, construction process variability, model error, and pure replication error.

The desired level of reliability is specified along with the acceptable level of distress at the end of design life in defining the performance requirements for a pavement design in this Guide. For example, one criterion might be to limit percent slabs cracked to 10 percent at a design reliability of 90 percent. Thus, if a designer designed 100 projects, 90 of these projects would exhibit slab cracking less than 10 percent at the end of the design life. Different reliability levels may be specified for different distresses in the same design. For example, the designer may choose to specify 95 percent reliability for slab cracking, but 90 percent reliability for faulting and IRI. Of course, increasing the design reliability will increase the higher the initial cost of the pavement; however, the future maintenance cost would be lower for the higher-reliability design.

3.4.2.8 Life Cycle Costs Estimation

After a trial design has passed the structural (distress) and functional (smoothness) requirements, it becomes a technically feasible design alternative. At this point, the pavement can be analyzed for its life cycle costs and other considerations for comparison with other feasible designs. A general procedure for life cycle costing is provided in Appendix C. The predicted distress and IRI of the feasible design alternatives can be used in estimating the mean lives of the design alternatives and their standard deviations, along with a designer-defined maintenance and rehabilitation policy, in conducting a LCCA.

3.4.3 INPUTS FOR NEW RIGID PAVEMENT DESIGN

Input data used for the design of new rigid pavements presented in this chapter are categorized as follows:

- General information.
- Site/project identification.
- Analysis parameters.
- Traffic.
- Climate.
- Drainage and surface properties.
- Pavement structure
- Design features.

Several of these inputs (e.g., traffic, climate) are identical to those used for flexible pavement design discussed in PART 3, Chapter 3. However, there are variations in how some these inputs are processed for use in JPCP and CRCP design. The focus of this section is to summarize all the inputs required for the design of rigid pavements using this Guide with appropriate commentary on how they relate to the design process.

Detailed descriptions for several of these inputs were presented in previous chapters of the Guide as indicated below:

- PART 2 – Design Inputs, Chapter 1: Subgrade/Foundation Design Inputs.
- PART 2 – Design Inputs, Chapter 2: Material Characterization.
- PART 2 – Design Inputs, Chapter 3: Environmental Effects.
- PART 2 – Design Inputs, Chapter 4: Traffic.
- PART 3 – Design Analysis, Chapter 1: Drainage.

These chapters should be consulted for more detailed guidelines on the applicable inputs.

3.4.3.1 General Information

The following inputs define the analysis period and type of design:

- Design life – expected pavement design life (years).
- Construction month – see description in PART 2, Chapter 3. Selecting June means construction occurs on June 1 and all aging is keyed to this date. Selecting hot months results in higher "zero-stress" temperatures and wider crack openings. By avoiding construction during the most adverse months (the months that will result in the PCC achieving the highest "zero-stress" temperatures), the risk of early pavement failures may be significantly reduced.
- Traffic opening month – see description in PART 2, Chapter 3. This can be a sensitive input because it determines the PCC strength at which traffic is applied to the pavement. Note that PCC strength increases at a relatively high rate during the first few months after PCC placement.

- Pavement type – JPCP or CRCP. This input determines the method of design evaluations and the applicable performance models.

3.4.3.2 Site/Project Identification

This group of inputs includes the following:

- Project location.
- Project identification – Project ID, Section ID, begin and end mile posts, and traffic direction.

3.4.3.3 Analysis Parameters

Initial IRI

The initial IRI defines the as-constructed smoothness of the pavement. This parameter is highly dependent on the project smoothness specifications and has a significant impact on the long-term ride quality of the pavement. Typical values range from 50 to 100 in/mi.

Performance Criteria

The JPCP design is based on transverse cracking, transverse joint faulting, and pavement smoothness (IRI). The designer may select some or all of these performance indicators and establish criteria to evaluate a design. For CRCP design, crack width and LTE, punchouts and smoothness are the key performance indicators. The performance criteria should be selected in consideration with the design reliability. For example, specifying a high reliability level and low distress level will result in a very conservative design.

Transverse Slab Cracking (JPCP)

Cracks in JPCP slabs may eventually lead to a loss of smoothness. Inadequate design to control transverse cracking has resulted in the premature failure of JPCP. Thus, it is desirable to limit transverse cracking to ensure that the pavement will perform as required over the design period.

The performance criterion for transverse cracking defines the maximum allowable percentage of cracked slabs at the end of design life and determines the level of slab cracking that may occur over the design period. The allowable level of transverse cracking depends on the individual highway agency's tolerance for the amount of slab cracking over the design period. Typical values of allowable cracking range from 10 to 45 percent, depending on the functional class of the roadway and design reliability.

Transverse Joint Faulting (JPCP)

The mean transverse joint faulting is a critical factor affecting ride quality. Thus, it is desirable to limit mean faulting to ensure that a pavement will remain smooth over the design period. The performance criterion for joint faulting defines the allowable amount of mean joint faulting at the end of the design life and determines the level of joint faulting over the design period. The acceptable level of faulting depends on the individual highway agency's tolerance for roughness and maintenance policy. Typical values of allowable JPCP mean faulting range from 0.1 in to 0.2 in, depending on the functional class of the roadway and design reliability.

Crack Width and Crack LTE

Crack width in the cold weather is the most critical design parameter. The wider the crack the greater the probability it will loose load transfer efficiency. The design guide software calculates the crack width at the depth of reinforcement. This should be limited to 0.02 in or less. The crack LTE is the ultimate strength parameter and depends on crack width and number of heavy axles applied. The crack LTE should be limited to greater than 95 percent throughout the design life.

Punchouts (CRCP)

Development of punchouts is the principal mode of failure for CRCP. Punchouts is a major cause of loss of smoothness in CRCP. The performance criterion for punchouts defines the acceptable number of punchouts per mile at the end of design life and also determines the number of punchouts that may develop over the design period. Note that the observed punchouts on sections used to calibrate the CRCP model were mostly of low severity, which is defined by LTPP as a fine longitudinal crack formed between two transverse cracks that are tight with less than 3 in spalling or 0.25 in faulting. Further deterioration of such a punchout will likely require several years of trafficking. The selection of the punchout performance criteria for design should reflect this low severity condition. Typical values of allowable CRCP punchouts (all severities) range from 10 to 20 per mile (depending on the functional class of the roadway and design reliability).

Smoothness (JPCP and CRCP)

Functional adequacy is quantified most often by pavement smoothness. Rough roads not only lead to user discomfort but also to increased travel times and higher vehicle operating costs. Although the structural performance of a pavement, in terms of pavement distress, is important the public complaints generated by rough roads often contribute to a large part of the rehabilitation decisions that are made by State highway agencies. In a simplistic way, smoothness can be defined as "the variation in surface elevation that induces vibrations in traversing vehicles." The IRI is the most common way of measuring smoothness in managing pavements.

As with the structural distresses, the performance criterion for smoothness defines the acceptable IRI at the end of design life. Terminal IRI values are chosen by the designer and should not be exceeded at the design level of reliability. Typically values in the range of 150 to 250 in/mile are used for terminal IRI, depending on the functional class of the roadway and design reliability.

3.4.3.4 Traffic

Traffic data is one of the key data elements required for the analysis and design of pavement structures. The Design Guide considers truck traffic loadings in terms of axle load spectra, as described in detail in PART 2, Chapter 4. The full axle load spectra for single, tandem, tridem, and quad axles are considered. The Design Guide software outputs on a monthly basis the cumulative number of heavy trucks in the design lane as an overall indicator of the magnitude of truck traffic loadings (FHWA class 4 and above). This parameter can be considered as a general indicator of the level of truck traffic. For example, a pavement can be described as carrying 1 million heavy trucks or 100 million trucks over its design life.

A summary of the traffic data required for JPCP and CRCP design is presented below along with the basic definitions of the variables and references to default values. Detailed discussion and guidance on traffic inputs is presented in PART 2, Chapter 4.

Basic Information

- Annual Average Daily Truck Traffic (AADTT) for base year – the total number of heavy vehicles (classes 4 to 13) in the traffic stream.
- Percent trucks in the design direction (directional distribution factor).
- Percent trucks in the design lane (lane distribution factor).
- Operational speed of vehicles – this input is used in the calculation of moduli of asphalt bound layers.

PART 2, Chapter 4 discusses the recommended procedures to configure these inputs at each of the three hierarchical levels. Default values based on national traffic studies are presented in the chapter for use at Level 3 for the directional and lane distribution factors.

Traffic Volume Adjustment

Monthly Adjustment Factors

The truck monthly distribution factors are used to determine the monthly variation in truck traffic within the base year. These values are simply the ratio of the monthly truck traffic to the AADTT. Naturally, the average of the ratios for the 12 months of the base year must equal 1.0. PART 2, Chapter 4 discusses the monthly adjustment in more detail. If no information is available, assume even distribution (i.e., 1.0 for all months for all vehicle classes).

Vehicle Class Distribution

The normalized vehicle class distribution represents the percentage of each truck class (classes 4 through 13) within the AADTT for the base year. The sum of the percent AADTT of all truck classes should equal 100. PART 2, Chapter 4 discusses the procedures to determine this input at each of the input levels. It is important to note that if site-specific (Level 1) or regional data (Level 2) data are not available, truck traffic classification (TTC) can be used in conjunction with the functional class of the roadway to estimate the vehicle class distribution. Each TTC represents a traffic stream with unique truck traffic characteristics, and a default vehicle class distribution was established for each TTC using a national traffic database for use at Level 3. The default values are provided in PART 2, Chapter 4 and Appendix AA. They are also a part of the Design Guide software.

Hourly Truck Traffic Distribution

The hourly distribution factors represent the percentage of the AADTT within each hour of the day. These factors are important in the prediction of JPCP cracking, JPCP faulting, and CRCP punchouts. They help accurately account for daytime and nighttime traffic streams required for performance prediction. PART 2, Chapter 4 discusses this input in more detail and describes the ways estimate it at each of the three input levels.

Traffic Growth Factors

The traffic growth function allows for the growth or decay in truck traffic over time (forecasting or backcasting truck traffic). Three functions are available to estimate future truck traffic volumes:

- No growth.
- Linear growth.
- Compound growth.

Different growth functions may be used for different functional classes. Based on the function chosen, the opening date of the roadway to traffic (excluding construction traffic), and the design life (discussed in *Basic Information* input category), the traffic is projected into the future. The growth functions are presented in PART 2, Chapter 4.

<u>Axle Load Distribution Factors</u>

The axle load distribution factors simply represent the percentage of the total axle applications within each load interval for a specific axle type and vehicle class (classes 4 through 13). This data needs to be provided for each month for each vehicle class. A definition of load intervals for each axle type is provided below:

- Single axles – 3,000 lb to 41,000 lb at 1,000 lb intervals.
- Tandem axles – 6,000 lb to 82,000 lb at 2,000 lb intervals.
- Tridem and quad axles – 12,000 lb to 102,000 lb at 3,000 lb intervals.

The estimation of axle load distribution factors at different input levels is presented in PART 2, Chapter 4.

<u>General Traffic Inputs</u>

Most of the inputs under this category define the axle load configuration and loading details for calculating pavement responses. The exceptions are "Number of Axle Types per Truck Class" and "Wheelbase" inputs, which are used in the traffic volume calculations. Although these inputs have been described in PART 2, Chapter 4, additional discussion specific to JPCP and CRCP design is presented below.

Mean Wheel Location

Distance from the outer edge of the wheel to the pavement marking. This input is very important in computing fatigue damage for both JPCP cracking and CRCP punchout predictions. The sensitivity of JPCP transverse cracking to mean wheel location is shown in figure 3.4.9. As shown in this figure, mean wheel location is a very sensitive factor that affects JPCP cracking and CRCP punchouts. Depending on the mean wheel location, the slab cracking can vary by a factor of 4 or more. If a typical-width (8.5-ft) truck were perfectly centered in a standard-width (12-ft) lane, the mean wheelpath would be 21 in. Site conditions and pavement design features such as tied PCC shoulder or widened slab may affect the mean wheelpath.

The estimation of this input at the three input levels is discussed in PART 2, Chapter 4. At Level 3, 18 inches may be used for this input unless more accurate information is available.

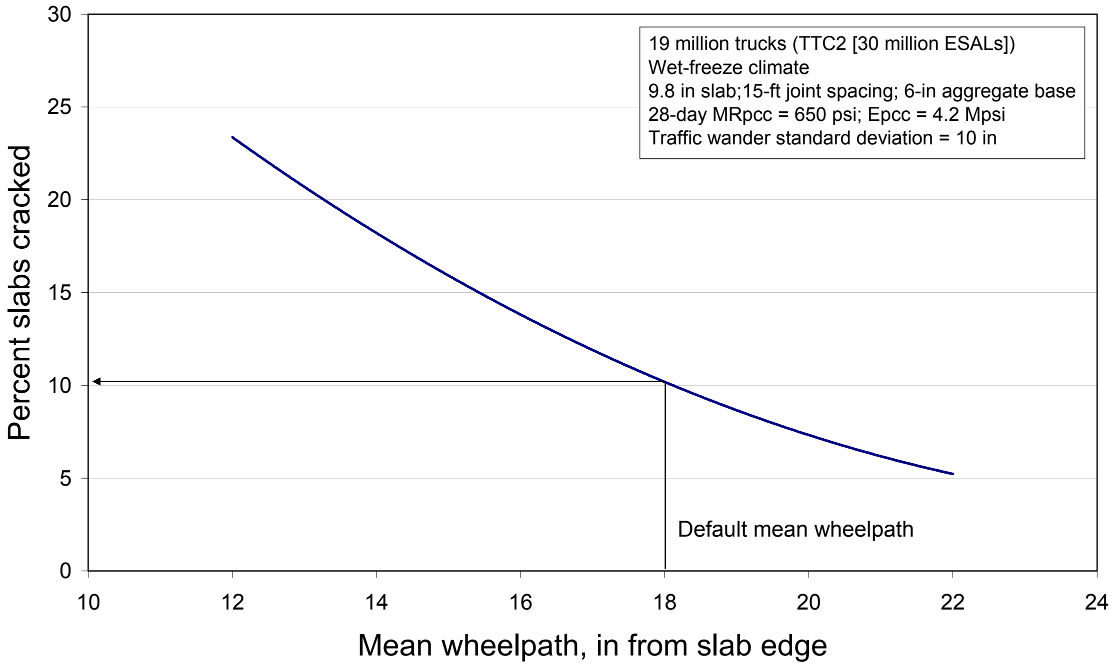

Figure 3.4.9. Sensitivity of JPCP transverse cracking to mean wheelpath location.

Traffic Wander Standard Deviation

This is the standard deviation of the lateral traffic wander. The wander is used to determine the number of axle load applications over a point for predicting distress and performance. This parameter affects prediction of all pavement distresses, but it is a relatively insensitive factor, as shown in figure 3.4.10. Site conditions and pavement design features such as tied PCC shoulder or widened slab may affect the traffic wander standard deviation. The estimation of this input at the three input levels is discussed in PART 2, Chapter 4. At Level 3, 10 inches may be used for this input unless more accurate information is available.

Design Lane Width

This is the distance between the lane markings on either side of the design lane. This input may or may not equal the slab width. The default value for standard-width lanes is 12 ft. It should be emphasized that this parameter refers to the actual traffic lane width, and not the “slab width,” which has a very significant effect on both faulting and cracking performance of JPCP.

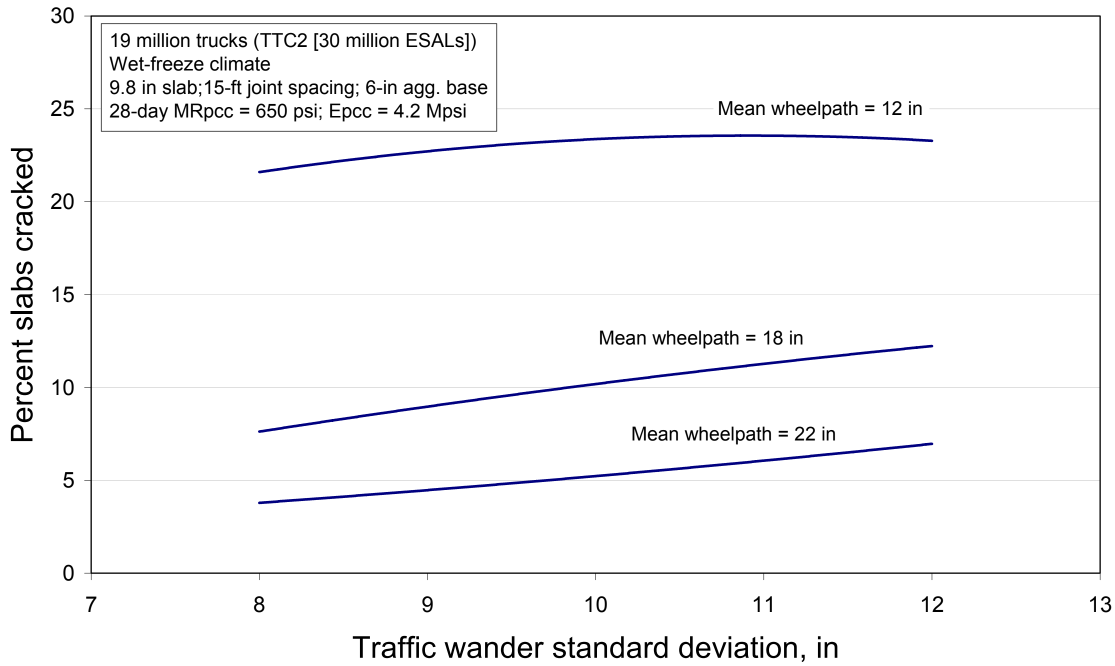

Figure 3.4.10. Sensitivity of JPCP transverse cracking to traffic wander standard deviation.

Number of Axle Types per Truck Class

This input represents the average number of axles for each truck class (class 4 to 13) for each axle type (single, tandem, tridem, and quad). The estimation of this input at the three input levels is discussed in PART 2, Chapter 4. Default values derived from a national traffic database for use at Level 3 are provided in PART 2, Chapter 4.

Axle Configuration

A series of data elements are needed to describe the details of the tire and axle loads for use in the pavement response module. Typical values are provided for each of the following elements; however, site-specific values may be used, if available.

- Average Axle-Width – the distance between two outside edges of an axle. For typical trucks, 8.5 ft may be assumed for axle width.
- Dual Tire Spacing – the distance between centers of a dual tire. Typical dual tire spacing for trucks is 12 in.
- Tire Pressure – the hot inflation pressure or the contact pressure of a single tire or a dual tire. For heavy trucks, typical hot inflation pressure is 120 psi which was used in calibration.
- Axle Spacing – the distance between the two consecutive axles of a tandem, tridem, or quad. The average axle spacing is 51.6 in for tandem and 49.2 in for tridem axles.

Wheelbase

This information is used in determining the number of load applications for JPCP top-down cracking. For top-down cracking, the critical loading is caused by a combination of axles that places an axle load close to both ends of a slab at the same time (figure 3.4.6). In general, the steering and drive axles of truck tractors or other trucks are the most common sources of these load combinations, but multiple trailers can also cause this type of loading. The inputs in this category include the following:

- Average axle spacing (ft) – short, medium, or long. The recommended values are 12, 15, and 18 ft for short, medium, and long axle spacing, respectively.
- Percent of trucks – the percent of trucks with the short, medium, and long axle spacing. Use even distribution, unless more accurate information is available (e.g., 33, 33, and 34 percent for short, medium, and long axles, respectively was used in calibration).

The percent of trucks is the axle spacing distribution of truck tractors (Class 8 and above). If other vehicles in the traffic stream also have the axle spacing in the range of the short, medium, and long axles defined above, the frequency of those vehicles should be added to the axle-spacing distribution of truck tractors. For example, if 10 percent of truck traffic is from multiple trailers (Class 11 and above) that have the trailer-to-trailer axle spacing in the "short" range, 10 percent should be added to the percent trucks for "short" axles. Thus, the sum of percent trucks in the short, medium, and long categories can be greater than 100.

<u>Input Processing</u>

The traffic inputs are further processed to produce the following "processed input" for every month over the entire design period:

- Number of single axles under each load category.
- Number of tandem axles under each load category.
- Number of tridem axles under each load category.
- Number of quad axles under each load category.
- Number of truck tractors (Class 8 and above) under each load category (for top-down cracking).

The load combination for top-down cracking is assumed to consist of a steering axle and a tandem axle. The steering axle is assumed to have a fixed load of 12,000 lb, while the tandem axle is assumed to have the same load distribution as other tandem axles.

The hourly traffic distribution factors are applied to the processed traffic input (the traffic counts by axle type for every month of the design period) to obtain hourly traffic at the time of damage calculation for each distress. More discussion on the additional processing of traffic inputs is provided in sections 3.4.4 and 3.4.5, as well as in Appendices JJ, KK, LL, and NN.

3.4.3.5 Climate

Environmental conditions have a significant effect on the performance of rigid pavements. The interaction of the climatic factors with pavement materials and loading is complex. Factors such as precipitation, temperature, freeze-thaw cycles, and depth to water table affect pavement and subgrade temperature and moisture content, which, in turn, directly affects the load-carrying capacity of the pavement layers and ultimately pavement performance. Detailed guidance on environmental inputs required for pavement design is presented in PART 2, Chapter 3. This section provides a summary of the climatic inputs required for rigid pavement analysis and a brief discussion of the effects of climate on rigid pavement behavior.

<u>Climatic Inputs</u>

The following weather related information is required to perform rigid pavement design:

- Hourly air temperature over the design period.
- Hourly precipitation over the design period.
- Hourly wind speed over the design period.
- Hourly percentage sunshine over the design period.
- Hourly ambient relative humidity values.
- Seasonal or constant water table depth at the project site.

The first five inputs above are obtained from weather station data for a given site, if available. For locations within the United States, they can be obtained from the National Climatic Data Center (NCDC) database. The Design Guide software includes an extensive climatic database for over 800 cities in the U.S. and a capability to interpolate between the available sites. All of the necessary climatic information at any given location within the U.S., with the exception of the seasonal water table depth, can be generated by simply providing the following inputs:

- Pavement location – latitude and longitude.
- Elevation.

Designers may use data from the closest weather station (called actual weather station [AWS]) or data interpolated from up to six closest weather stations (to create a virtual weather station [VWS]) for design at the specific pavement location. The VWS is the strongly recommended approach, because the data are interpolated to the actual project location and this approach more adequately compensates for missing data from any one weather station.

<u>Input Processing</u>

The climatic inputs are combined with the pavement material properties, layer thicknesses, and drainage-related inputs by the EICM to yield the following information for use in the design analysis:

- Hourly profiles of temperature distribution through PCC slab—EICM produces temperatures at 11 evenly spaced points through slab thickness for JPCP analysis.

- Hourly temperature and moisture profiles (including frost depth calculations) through other pavement layers—obtained using EICM.
- Temperature at the time of PCC zero-stress temperature for JPCP and CRCP design.
- Monthly or semi-monthly (during frozen or recently frozen periods) predictions of layer moduli for asphalt, unbound base/subbase, and subgrade layers.
- Annual freezing index values.
- Mean annual number of wet days.
- Number of ambient freeze-thaw cycles.
- Monthly relative humidity values.

Effects of Climate on Rigid Pavement Behavior

Both temperature and moisture have a significant effect on performance of rigid pavements. Therefore, a discussion highlighting the impact of climate on the behavior of rigid pavements is provided. Discussions on the interaction of climatic factors on unbound pavement layers are provided in PART 2, Chapter 3 of the Design Guide and on asphalt bound layers is presented in PART 2, Chapters 2 and 3, and PART 3, Chapter 3.

Temperature Difference from Solar Radiation

Temperature differences from top to bottom through the JPCP or CRCP slabs have a very significant effect on critical stresses at the top and bottom of the slab. On a hot sunny day, the top of the PCC slab is much warmer than the bottom (a positive temperature difference through the slab). The result is an elongation of the top of the slab relative to the bottom and a convex curvature, as shown in figure 3.4.11. This is equivalent to having a void beneath the middle of the slab. Because self weight of the slab resists slab curling, actual voids may not develop except under extreme temperature conditions. However, any forces (including self weight) that restrain free slab movements cause stress, and in this case, the restraint to slab curling results in increased tensile stress at the slab bottom. Under traffic loads, any actual loss of support due to temperature differences further increases the critical tensile stresses at the slab bottom.

During nighttime, the top of the PCC slab is typically cooler than the bottom (a negative temperature difference through the slab). This results in a concave curvature of the slab, as shown in figure 3.4.12. This is equivalent to having voids beneath the edges of the slab, which when combined with traffic load, increases tensile stress at the top that can lead to fatigue cracking initiating from top down.

Because of the extreme sensitivity of critical stresses in rigid pavements to temperature gradients, consideration of hourly variation in temperature conditions is necessary. This is accomplished automatically in the Design Guide software using the EICM. Based on the hourly historical climatic data, pavement structure, and material properties, the EICM produces a file that includes historical hourly temperature profiles in the PCC slab for every year of the design period (8,760 profiles per design year [365 days * 24 hours]).

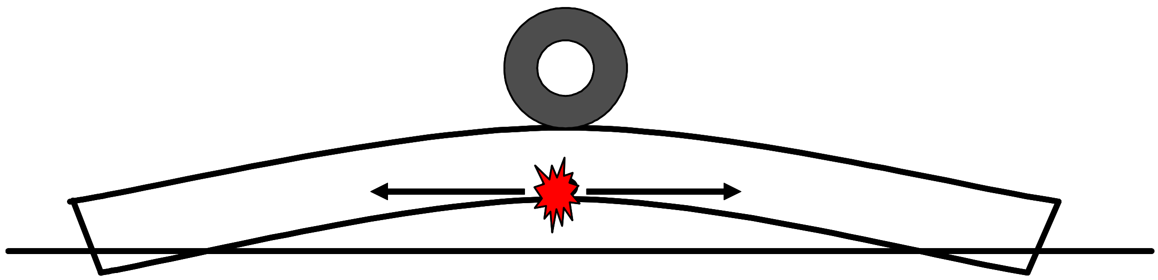

Figure 3.4.11. Curling of PCC slab due to daytime positive temperature difference plus critical traffic loading position resulting in high tensile stress at slab bottom.

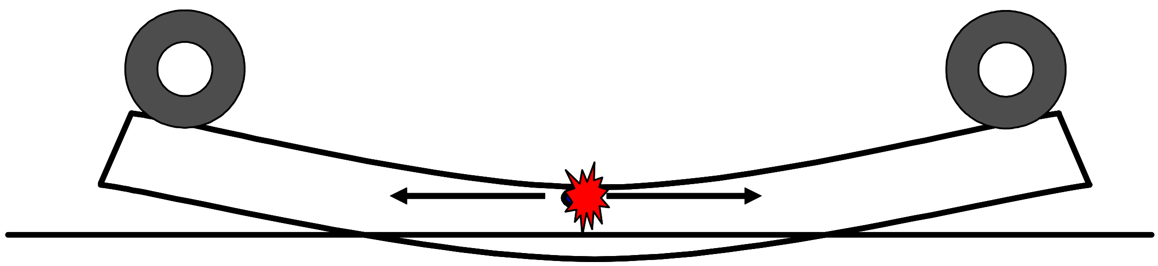

Figure 3.4.12. Curling of PCC slab due to nighttime negative temperature difference plus critical traffic loading position resulting in high tensile stress at slab top.

An example of nonlinear temperature profiles through a 10 in PCC slab within a 24-hour period is shown in figure 3.4.13. The available climatic data are recycled to fill out the design period. For example, if the design period is 20 years, but only 5 years of climatic data are available, EICM determines the temperature profiles for the available 5 years, and then reuses the results 4 times to fill out the design period.

Each hourly nonlinear temperature profile is converted in the Design Guide software automatically to an effective linear temperature difference (difference) for computational efficiency. Using only the linear component (difference between temperatures at top and bottom of slab) can result in significant errors in estimating PCC stresses. These historical effective hourly temperature differences are use to create monthly daytime (positive) and nighttime (negative) temperature difference probability distributions for use in analysis.

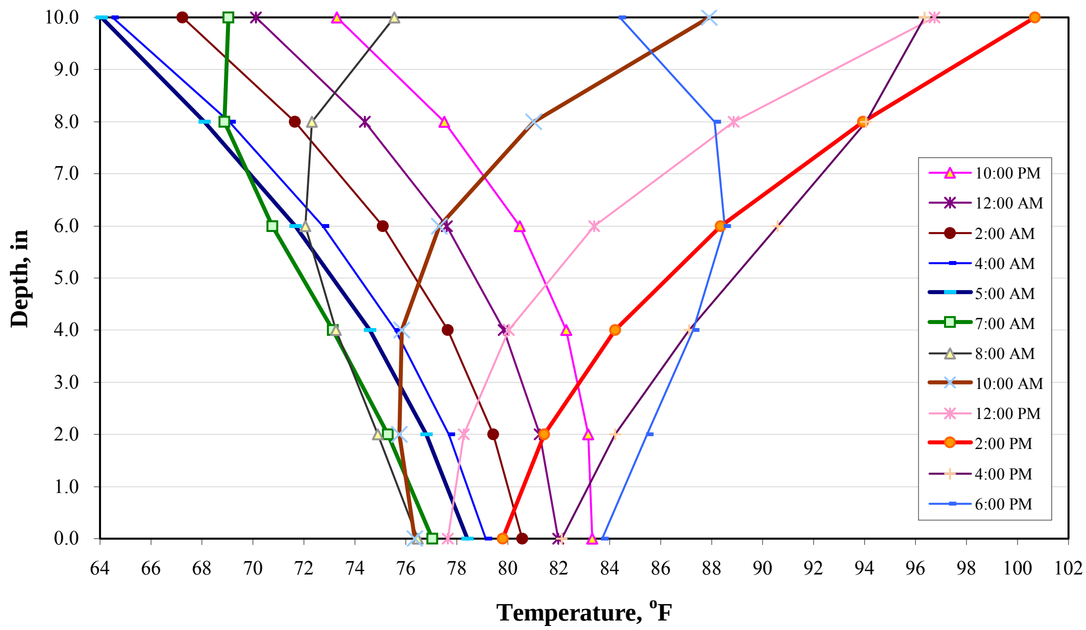

Figure 3.4.13. Example of temperature profile through a 10 in PCC slab for a typical spring day.

Moisture Warping

Hardened concrete expands with an increase in moisture and contracts with a loss of moisture. The surface of PCC pavements can dry out, but below about the 2-inch level, the moisture level remains at a relatively constant high level (85 percent relative humidity or higher), even in very dry areas. This results in upward warping of the slab as shown in figure 3.4.12. The amount of drying shrinkage that takes place in the upper portion of the slab depends on many factors, including the type of curing and the PCC mix components.

A part of the drying shrinkage in PCC is irreversible, but there is a reversible portion that varies with the ambient relative humidity (*6, 7, 8*). The irreversible shrinkage causes the permanent moisture warping, while the reversible shrinkage causes seasonal variation in moisture warping (seasonal moisture warping).

Permanent Curling and Warping

PCC paving is often performed during the mornings of hot sunny days, a condition that tends to expose the newly paved PCC slabs to a high positive temperature difference from intense solar radiation plus the heat of hydration. The PCC slabs are flat when they harden, but depending on the exposure conditions a significant amount of positive temperature gradient (upper portion of the slab is much warmer than bottom) may be present at the time of hardening. This temperature has been termed the “zero-stress temperature gradient” (*9, 10, 11, 38*). Whenever the temperature gradient in the slabs falls below the amount locked into the slab at the time of construction (the zero-stress gradient), the slabs will attempt to curl upward causing tensile stress at the top of the slab which can lead to top down cracking of JPCP or CRCP. Thus, an effective negative temperature gradient is permanently “built” into the slabs. The upward curling of pavement slabs is restrained by several factors, including the slab self weight, dowels, and the weight of any base course bonded to the slab. This hypothesis has been supported using data from instrumented field slabs located in different climatic conditions (*8*). These factors affect the amount of actual permanent curl, as well as the amount of creep relaxation that may take place.

If PCC paving is performed later in the afternoon or at night so that the highest temperature from the heat of hydration does not correspond with the most intense solar radiation, the amount of permanent temperature gradient "built" into the slab will be much lower and could potentially even be negative. Also, moist curing with water spray, wet burlap, and curing with reflective curing compounds can also produce a lower "zero-stress" or "built" in permanent temperature gradient than regular curing compound.

As discussed under "Moisture Warping," differential shrinkage also produces permanent warping, which is superimposed on the zero-stress thermal gradient and is basically indistinguishable from permanent curling. The permanent components of curling and warping are, therefore, considered together. The magnitude of permanent curling and warping is estimated from calibration of JPCP cracking and is expressed in terms of effective temperature difference from the top to bottom of the slab (called "permanent curl/warp"). It is important to note that only a portion of permanent curl/warp actually affects pavement response, because PCC creep that occurs over time negate the effects of permanent curvature present in PCC slabs. The magnitude of permanent curl/ warp estimated from calibration reflects the effects of long term creep.

Consideration of Climatic Effects in Rigid Pavement Design

The temperature and moisture effects are directly considered in the design of the JPCP and CRCP as follows:

- The permanent built-in curling that occurs during construction (the zero-stress temperature gradient) is combined with the permanent warping due to differential permanent shrinkage and expressed in terms of effective temperature difference between top and bottom (called "permanent curl/warp"). This parameter is a direct and influential input to the design of JPCP and CRCP and was established through national calibration for typical construction and mixture condition.
- Transient hourly negative and positive non-linear temperature differences (from top to bottom of the slab) caused by solar radiation are computed using the EICM.
- Transient negative moisture shrinkage in the top of the slab caused by changes in relative humidity during each month of the year is converted to an equivalent temperature difference for every month.

All three of the above temperature and moisture differences through the PCC slab are predicted and appropriately combined along with axle loads to compute critical slab stresses, which are used within a monthly increment to accumulate damage.

Both temperature and moisture changes are also directly considered in JPCP joint opening and closing and for CRCP crack opening and closing. The zero-stress temperature is considered the temperature at which the concrete hardens sufficiently to cause joints and cracks to open when the PCC temperature drops below this value. Thus, a slab which is placed and hardens at a higher temperature would experience wider joints and cracks at lower temperatures. Wider joints and cracks loose LTE at a higher rate leading to increased joint faulting and crack deterioration.

3.4.3.6 Drainage and Surface Properties

Information required under this category includes the following:

- Pavement surface layer (PCC) shortwave absorptivity.
- Potential for infiltration.
- Pavement cross slope.
- Length of drainage path.

The first item in the list above is essentially a PCC material property that interacts with the climatic inputs in defining the temperature regime in pavement layers. The remaining three inputs are related to infiltration and drainage. Guidance is not provided here for any detailed drainage designs or construction methods. The design of drainage components and how the overall pavement drainage is incorporated into structural design is presented in PART 3, Chapter 1. The inputs discussed in this section, however, have a significant impact on the amount of moisture that enters the pavement structure from a given rainfall event and help define some of the other parameters required for drainage calculations.

<u>PCC Pavement Shortwave Absorptivity</u>

The short wave absorptivity of a pavement surface depends on pavement composition, color, and texture. The short wave absorptivity is the ratio of the amount of solar energy absorbed by the pavement surface to the total energy the surface was exposed to, which naturally affects the temperature regime within the pavement structure and the associated structural response. This input ranges from 0 to 1. Generally the lighter and more reflective the surface is, the lower the short wave absorptivity will be. Refer to PART 2, Chapter 2 for more information on short wave absorptivity. The typical values for PCC surface range from 0.7 to 0.9. The recommended default value is 0.85, which is the value used in the calibration of rigid pavement performance models. PART 3, Chapter 3 discusses this input and its role in defining the temperature and moisture regime within the pavement system.

<u>Infiltration</u>

This input quantifies the amount of water infiltrating the pavement structure. Three choices are available for quantifying this input – minor, moderate, and extreme. The amount of infiltration from a given rain event is a function of the amount of precipitation, pavement condition, and shoulder type. However, for simplicity, the general guidelines for selecting this input are based on the shoulder type, since the lane-shoulder joint is the largest single source of moisture entry into the pavement structure:

- Minor – this value is valid when tied concrete shoulders are used or when an aggressive policy is pursued to keep the lane-shoulder joint sealed. This value can also be used when edgedrains are present under the shoulder.

- Moderate – this value is valid for all other shoulder types.
- Extreme – generally not used for new or reconstructed pavement design.

More discussion on this parameter can be found in PART 2, Chapter 3.

<u>Drainage Path Length</u>

This is the horizontal distance between the highest point in the pavement cross-section to the point where drainage occurs. For crowned pavement systems with longitudinal edgedrains, this would be the distance from the top of the crowned cross-section to the center of the pipe edgedrain. PART 2, Chapter 3 discusses this input in more detail.

<u>Pavement Cross-Slope</u>

The cross slope is the slope of the pavement surface perpendicular to the direction of traffic. This input is used in computing the time required to drain a pavement base or subbase layer from an initially wet condition.

3.4.3.7 Pavement Structure

The rigid pavement design procedure allows a wide variety of PCC, base (layer directly underneath the PCC slab), and subbase material properties and layer thicknesses as shown in figure 3.4.3. For example, a rigid pavement structure could consist of a PCC slab, an asphalt treated base, an aggregate subbase, compacted subgrade, natural subgrade, and bedrock. The Design Guide software can be used to analyze a maximum of 20 layers; however, because of automatic sub-layering of certain layers a maximum of 10 actual input layers is recommended, comprising the pavement structure and subgrade (or bedrock). The following rules or constraints need to be satisfied in defining a rigid pavement structure for design:

- The surface layer in rigid pavement design is always a PCC layer.
- Slab-on-grade (two layers) is the minimum structure that can be analyzed.
- Only one unbound granular layer can be placed between two stabilized layers.
- The last two layers in the pavement structure must be unbound layers. To satisfy this constraint, the Design Guide software automatically sublayers the subgrade into two identical layers for slab-on-grade pavements and for pavements where a bound layer rests directly on the subgrade.

Defining a trial design involves defining all pavement layers and material properties for each individual layer, including subgrade. Depending on the selected trial design, sub-layering may be necessary to satisfy the layering requirements of the analysis procedures. The Design Guide software performs the sub-layering internally based on the material type, layer thickness and the location of the layer within the pavement structure. The sub-layering scheme is discussed for each material type along with a summary of the materials inputs required in the following paragraphs. More detailed guidelines on material properties are provided in detail in PART 2, Chapter 2.

Portland Cement Concrete Layer

The PCC layer is not sub-layered for design and analysis purposes. The properties required for the PCC layer are divided into three categories—general and thermal properties, PCC mixture properties, and strength and stiffness properties. These are explained below. More detailed information on these inputs is provided in PART 2, Chapter 2.

General and Thermal Properties

- Layer thickness. The range for design thickness for new pavement design is approximately 6 to 17 inches.
- Poisson's ratio, μ – typical values for PCC range from 0.15 to 0.25.
- Coefficient of thermal expansion, α_{PCC} – PCC coefficient of thermal expansion can range from 4 to 7 x 10^{-6} / °F, depending on aggregate type and the amount of cement in the mix. Determining this value through direct testing of the project mix (Level 1 input) is recommended since this parameter is extremely significant (see PART 2, Chapter 2 for details).
- Thermal conductivity – the quantity of heat that flows normally across a surface of unit area per unit of time of temperature gradient normal to the surface. The recommended value is 1.25 BTU/hr-ft-°F which is used in calibration.
- Heat capacity – the heat required to raise the temperature of a unit mass of material by a unit temperature. The recommended value is 0.28 BTU/lb-°F which is used in calibration.

PCC Mix-Related Properties

The design procedure requires the following PCC mix-related inputs for modeling material behavior, including shrinkage, PCC zero-stress temperature, and load-transfer deterioration:

- Cement type (Types I, II, or III).
- Cement content.
- Water/cement (or w/c) ratio.
- Aggregate type.
- PCC zero-stress temperature, T_z – Defined as the temperature (after placement and during the curing process) at which the PCC layer exhibits zero thermal stress. If the PCC temperature is less than T_z, tensile stress occurs in the slab. The T_z is not actually a single temperature but varies throughout the depth of the slab (termed a zero-stress gradient). However, when referring to T_z for purposes of joint and crack opening, it will be called simply the zero-stress temperature and could be considered as approximately the mean slab temperature. T_z can be input directly or can be estimated from monthly ambient temperature and cement content using the equation shown below, which is based on daytime construction with curing compound (40).

$$T_z = (CC*0.59328*H*0.5*1000*1.8/(1.1*2400) + MMT) \qquad (3.4.1)$$

where,

T_z = temperature at which the PCC layer exhibits zero thermal stress (allowable range: 60 to 120 ^{0}F).

CC $=$ cementitious content, lb/yd^3.
H $=$ -0.0787+0.007*MMT-0.00003*MMT^2
MMT $=$ mean monthly temperature for month of construction, ^{0}F.

Table 3.4.1 shows an illustration of the zero stress temperatures for different mean monthly temperatures and different cement contents in the PCC mix design. Note that the T_z equation has many limitations. It does not consider the effect of many factors on heat of hydration including mineral admixtures (flyash, slag), cement composition and fineness, chemical admixtures, and others. This equation was used in all calibrations of JPCP and CRCP and appeared to provide reasonable results.

- Ultimate shrinkage at 40 percent relative humidity – the ultimate shrinkage may be estimated using the procedures presented in PART 2, Chapter 2 for any of the three levels of input.
- Reversible shrinkage – percent of ultimate drying shrinkage that is reversible upon rewetting. Use 0.5 unless more accurate information is available.
- Curing method – curing compound or wet curing (affects ultimate shrinkage).

Table 3.4.1. Zero-Stress Temperatures based on PCC cement content and mean monthly ambient temperature during construction (equation 3.4.1).

Mean Monthly Temperature	H	Cement Content lbs/cy			
		400	500	600	700
40	0.1533	52*	56	59	62
50	0.1963	66	70	74	78
60	0.2333	79	84	88	93
70	0.2643	91	97	102	107
80	0.2893	103	109	115	121
90	0.3083	115	121	127	134
100	0.3213	126	132	139	145

*Mean PCC temperature in degrees F.

Strength and Stiffness Properties

The long-term strength gain of PCC, and corresponding change in PCC stiffness, are considered in this Guide. The PCC strength and stiffness inputs consist of the following:

- Modulus of rupture (flexural strength), MR.
- Static modulus of elasticity, E_{PCC}.
- Compressive strength, f'_c.
- Split tensile strength (as measured by the indirect tensile strength test), f_t.

Depending on the input level, different amount of information is required as follows:

- Level 1—Laboratory values of MR, f'_c, f_t, and E_c at 7, 14, 28, and 90 days determined using appropriate testing procedures. The ratio of 20-yr to 28-day strength is also required. A best-fit regression line is fit through these data points to interpolate or

extrapolate strength and stiffness at various ages during incremental damage calculation (see details in PART 2, Chapter 2).
- Level 2—Laboratory-determined values of compressive strength (f'_c) at 7, 14, 28, and 90 days and the 20-yr to 28-day strength ratio. The strength at each damage increment is determined using a best-fit regression line fit through these data points, and the remaining strength parameters (MR, f_t, and E_c) are estimated using well established strength-to-strength and strength-to-stiffness correlations (see PART 2, Chapter 2 for details).
- Level 3—Estimated 28-day compressive strength or modulus of rupture from historical data or other information. The PCC strength over time is estimated using the default strength model, and the other inputs are calculated based on the projected strength using the appropriate correlations (see PART 2, Chapter 2 for details). The PCC elastic modulus can also be entered at level 3 if desired

The processed input for PCC strength and modulus properties is the monthly strength and modulus values for the entire design period.

<u>Asphalt-Stabilized Base Layer</u>

No sub-layering is done within the asphalt-stabilized base layer for rigid design and analysis purposes within the Design Guide software. The materials inputs required for this layer are grouped under two broad categories – general materials inputs and inputs required to construct E^* master curve. These are discussed below. More detailed guidance on these inputs is provided in PART 2, Chapter 2.

General Layer Property Inputs

- Layer thickness.
- Poisson's ratio.
- Thermal conductivity – the quantity of heat that flows normally across a surface of unit area per unit of time of temperature gradient normal to the surface. The typical value for asphalt-stabilized base material is 0.67 BTU/hr-ft-°F.
- Heat capacity – the heat required to raise the temperature of a unit mass of material by a unit temperature. A typical value for asphalt-stabilized base is 0.23 BTU/lb-°F.
- Total unit weight – typical range for dense-graded hot-mix asphalt is 134 to 148 lb/ft^3.

Inputs Required to Construct E Master Curve*

The primary material property of interest for asphalt stabilized layers is its dynamic modulus, E^*. For Level 1 input, the dynamic modulus, E*, is determined in the laboratory using standard test protocols (see PART 2, Chapter 2 for details) for various frequencies and rates of loading. A master curve of E* versus reduced time is then derived from this data that defines the behavior of this layer under loading and at various climatic conditions. For input Levels 2 and 3, the dynamic modulus prediction equation presented in PART 2, Chapter 2 is used to construct the master curve from the following information:

- Asphalt mixture properties

- Percent retained on ¾ in sieve – a typical value is 5 to 16 % for dense graded and 30% for permeable.
- Percent retained on 3/8 in sieve – a typical value is 27 to 49 % for dense graded and 70% for permeable.
- Percent retained on #4 sieve – a typical value is 38 to 61 % for dense graded and 95% for permeable.
- Percent passing the #200 sieve – a typical value is 3 to 8% for dense graded and 1% for permeable.

- Asphalt binder – Level 1 input is generally not needed for rigid design.
  - For input Level 2 – specify PG grade or Viscosity grade.
  - For input Level 3 – specify PG grade, Viscosity grade, or Penetration Grade.
- Asphalt general
  - Volumetric effective binder content (percent).
  - Air voids (percent).
  - Reference temperature for master curve development (70 °F typical).

More detailed discussion on the determination of dynamic modulus using the prediction equation presented in PART 2, Chapter 2.

<u>Chemically Stabilized Layers</u>

No sub-layering is done for any cementitious stabilized base layers. The following inputs are required to define a cementitious stabilized layer:

- Mean modulus of elasticity of the layer – this value is assumed to remain constant over the design period. The typical values for this input vary widely depending on material type and stabilizer content. Mean backcalculated values from all LTPP sites for two major types of chemically-stabilized bases are as follows:
  - Cement stabilized aggregate – mean modulus is 900,000 psi; range is 494,000 to 2,195,00 psi.
  - Lean concrete – mean modulus is 2,099,000 psi; range is from 275,000 to 3,046,000 psi.
- Unit weight of the material.
- Poisson's ratio.
- Thermal conductivity – a typical value for chemically stabilized base is 1.0 BTU/hr-ft-°F.
- Heat capacity – a typical value for chemically stabilized base is 0.28 BTU/lb-°F.

<u>Unbound Base/Subbase/Subgrade</u>

The major inputs required for unbound base/subbase and subgrade layers are:

- Layer thickness (only for base and subbase layers) – for subgrade layers if the lime modified or compacted subgrades need to be considered separately from the natural subgrade, they can be defined as a structural layer.
- Layer resilient modulus.
- Poisson's ratio.

- Coefficient of lateral earth pressure, K_o – a typical value for unbound compacted materials is 0.5.

The layer moduli for unbound layers and subgrade can be estimated at two levels—Level 2 and Level 3. For rigid pavement analysis, Level 1 inputs are not available (see PART 2, Chapter 2). Level 2 requires testing of a soil sample using some test such as CBR or R-value and then estimating the layer resilient modulus using a prediction equation. Level 3 requires estimation using a correlation from soil classification such as AASHTO or UCS. A guide for selecting an appropriate Level 3 resilient modulus is provided in PART 2, Chapter 2. Note that whenever a granular subgrade exists, the recommended resilient modulus is fairly high and if this subgrade layer is not truly infinite in depth, will result in overestimation of the subgrade support and a very high backcalculated k value (see section titled "Computation of Effective k-value"). If the stiffer granular layer is relatively thin (e.g., less than 5 to 10 ft) then a reduction in the selected subgrade resilient modulus is warranted.

The designer also has the choice of including or not including seasonal analysis for the unbound base materials and soils. PART 2, Chapters 2 and 3 present a more detailed discussion on these inputs.

Seasonal Analysis

PART 2, Chapter 3 should be consulted for a more comprehensive coverage of the materials inputs required for climatic analysis.

The following options are available for Level 2:

1. Enter a representative design resilient modulus (at the optimum moisture content) or other allowable soil strength/stiffness parameters (CBR, R-value, AASHTO structural layer coefficient, or PI and gradation) and use the EICM module linked to the Design Guide software to estimate seasonal variations based on changing moisture and temperature profiles through the pavement structure. The additional inputs for EICM include plasticity index, percent passing No. 4 and No. 200 sieves, and the effective grain size corresponding to 60 percent passing by weight (D_{60}) for the layer under consideration. Using these inputs, EICM estimates the unit weight, the specific gravity of solids, saturated hydraulic conductivity of the pavement layer, optimum gravimetric moisture content, degree of layer saturation, and the soil water characteristic curve parameters. These computed quantities can be substituted with direct inputs.
2. In lieu of using EICM, the seasonal moduli, CBR, R-value, or other values may be entered directly. For direct input, 12 laboratory-estimated pavement resilient moduli (or other allowable soil tests) are required.
3. Finally at input Level 2, seasonal variation in modulus of unbound materials may be ignored. In this case, a representative design modulus value (or other test value) is required.

For Level 3, the required input is the layer resilient modulus at optimum water content, and the EICM will do the seasonal adjustment. If seasonal analysis is not desired, a single resilient modulus is entered that the designer wishes to hold constant throughout the entire year (no moisture content is entered).

Sublayering of Unbound Layers and Subgrade

The original pavement structure defined by the user usually has four to six layers. However, the Design Guide software may internally subdivide the pavement structure into 12 to 15 sub-layers for the modeling of temperature and moisture variations. Only the unbound base layers thicker than 6 in and unbound subbase layer thicker than 8 in are sub-layered. For the base layer (first unbound layer), the first sub-layer is always 2 in. The remaining thickness of the base layer and any subbase layers that are sub-layered are divided into sub-layers with a minimum thickness of 4 in. For compacted and natural subgrades, the minimum sub-layer thickness is 12 in. A pavement structure is sub-layered only to a depth of 8 feet from the surface. Any remaining subgrade is treated as an infinite layer. If bedrock is present, the remaining subgrade is treated as one layer beyond 8 feet. Bedrock is not sub-layered and is always treated as an infinite layer.

The maximum number of layers that can be analyzed by the analysis module is 20. This refers to the total number of sub-layers within the pavement structure, including any sub-layering done internally by the program. Note that the Design Guide software requires that an unbound material be designated as a "granular base" or "subgrade." If a pavement structure is input that includes one or more thick layers of unbound base material the sub-layering performed by the software may result in more than 20 layers which cannot be analyzed by the program. A message to this effect will appear on the screen and the user will have to modify the layering system. This can be done easily by reducing the thickness of the unbound base material and adding an identical material as a subgrade layer which is sub-divided into thicker sub-layers (e.g., an A-1-a granular base of 60 in could be transformed into a 24 in A-1-a base layer and 36 in A-1-a subgrade layer). Note that there can be as many "subgrade" layers as desired.

<u>Bedrock</u>

The presence of bedrock within 10 ft of the pavement surface influences the structural response of pavement layers. The inputs for this layer include the following:

- Unit weight.
- Poisson's ratio.
- Layer modulus.

Input Levels 1 and 2 do not apply for bedrock. Typical modulus values for bedrock in various conditions (e.g., solid, or highly fractured and weathered) are provided in PART 2, Chapter 2.

<u>Conversion of Layer Resilient Moduli to an Effective Dynamic Modulus of Subgrade Reaction</u>

The subgrade and unbound pavement layers are characterized using resilient modulus in this Guide for all pavement types. For rigid pavement design, the subgrade k-value needed for the structural analysis is obtained through a conversion process, which transforms the actual pavement structure into an equivalent structure that consists of the PCC slab, base, and an effective dynamic k-value, as shown in figure 3.4.14.

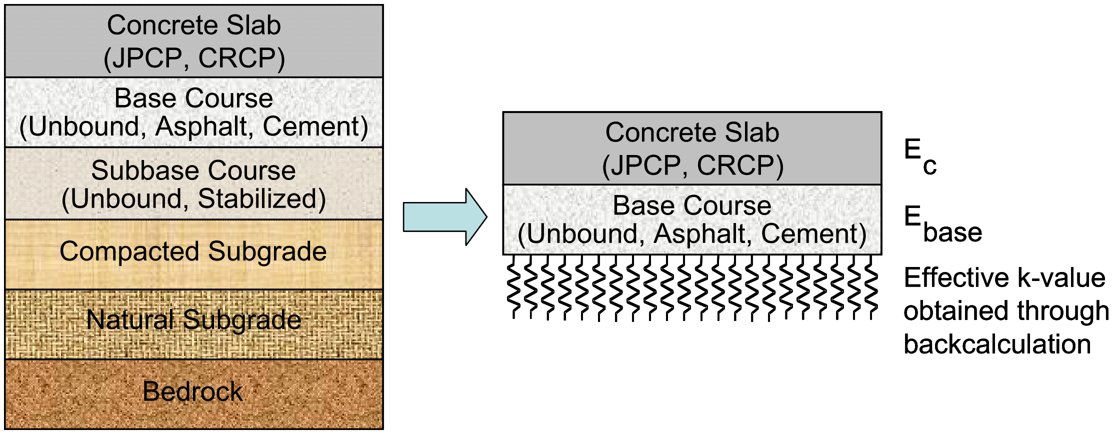

Figure 3.4.14. Structural model for rigid pavement structural response computations.

This approach ensures that all pavement designs are accomplished using the same input for subgrade and other pavement layers. The "E-to-k" conversion is performed internally in the Design Guide software as a part of input processing.

Computation of Effective Dynamic k-Value

The effective dynamic k-value is obtained by first determining the deflection profile of the PCC surface using an elastic layer program (JULEA), modeling all layers specified for the design. The subgrade resilient modulus is adjusted to reflect the lower deviator stresses that typically exist under a concrete slab and base course as compared to the deviator stress used in laboratory resilient modulus testing. Next, the computed deflection profile is used to backcalculate the effective dynamic k-value. Thus, the effective dynamic k-value is a computed value, not a direct input to the design procedure (except in rehabilitation).

The effective k-value used in this Guide is a dynamic k-value, which should be distinguished from the traditional static k-values used in previous design procedures. The procedure to obtain the effective dynamic k-value for each time increment (month) is outlined in the following steps:

1. Assign layer parameters (E and Poisson's ratio) in a manner consistent with flexible pavement design (PART 3, Chapter 3).
2. Using the elastic layer program JULEA, simulate a 9,000-lb Falling Weight Deflectometer (FWD) load with the plate radius 5.9 in and compute PCC surface deflections at 0, 8, 12, 18, 24, 36, and 60 in from the center of the load plate.
3. Adjust the subgrade resilient modulus to account for the lowered deviator stress level beneath a PCC slab and base.
4. Using the elastic layer program JULEA, again simulate a 9,000-lb FWD load with the plate radius equal to 5.9 in, and with the recalculated subgrade resilient modulus and subbase moduli.
5. Calculate PCC surface deflections at 0, 8, 12, 18, 24, 36, and 60 in from the center of the load plate.
6. Use the Best Fit method *(12)* to compute the dynamic modulus of subgrade reaction using the PCC surface deflections.

The “effective” dynamic k-value represents the compressibility of all layers beneath the PCC slab and base course. For example, if the pavement is constructed in a region with bedrock close to the surface (less than 10 ft), then the bedrock is entered as a stiff layer (high elastic modulus) beneath the subgrade soil layer. The PCC surface deflections calculated using JULEA reflects the presence of the bedrock layer; consequently, the presence of the bedrock layer is reflected in the calculated effective dynamic k-value.

The effective dynamic k-value of the subgrade is calculated for each month of the year and utilized directly to compute critical stresses and deflections in the incremental damage accumulation over the design life of the pavement. Factors such as water table depth, depth to bedrock, and frost penetration depth (frozen material) can significantly affect effective dynamic k-value. All of these factors are considered in the EICM.

3.4.3.8 Pavement Design Features

Various design features have significant effect on performance of both JPCP and CRCP. Examples of these include joint spacing and edge support (tied PCC shoulder or widened slab) for JPCP and steel content and base type for CRCP. The inputs associated with these design features are discussed in this section; additional details of pavement design features are provided in section 3.4.4 for JPCP and in section 3.4.5 for CRCP.

Permanent Curl/Warp Effective Temperature Difference

The magnitude of permanent curl/warp (section 3.4.3.5) is a sensitive factor that affects all rigid pavement performance. Some of the factors that affect the permanent effective permanent curl/warp include the following:

- Climate (air temperature, solar radiation, relative humidity, wind speed) during PCC placement.
- Construction time and curing procedure (morning construction with intense solar radiation adding to heat of hydration, nighttime construction with no solar radiation, type of curing compound, and wet curing).
- PCC mix properties including cement type, water-cement ratio, water content, cement quantity, and aggregate type.
- Creep of the PCC slab from self weight and edge constraints.
- Base type and properties.

The slab curvature after construction can be highly variable even along a given project, and a combination of adverse factors (e.g., a high shrinkage PCC mix, excessive temperature gradient at the time of PCC hardening, and poor curing) can lead to extremely high permanent curl/warp, resulting in early top down cracking. However, the available calibration results indicate that the average values of long-term effective permanent curl/warp is fairly uniform, with no obvious bias based on climate or design factors, including slab thickness and base type. The recommended value for permanent curl/warp is -10 °F (obtained through optimization) for all new and reconstructed rigid pavements for all climatic regions. This is an equivalent linear temperature difference from top to bottom of the slab. Appendix KK provides additional discussion of permanent curl/warp.

Various design situations may occur where an increase or decrease in this parameter may be warranted. For example, nighttime construction should result in a lower value due to no solar radiation at night. Another example identified during calibration of the JPCP cracking model indicated that when a significant amount of erosion occurs beneath a non-doweled transverse joint and loss of support occurs, an increased top down stress results. This often caused a transverse crack near the transverse joint on the leave side. Use of an increased value for permanent curl/warp (such as -15 °F) helps to account for this critical situation and predicts more accurately the amount of cracking that develops over time. Note that this situation could better be handled through use of dowel bars and a more non-erodible base course. Nevertheless, it is recommended that the default value be used unless local calibration can be conducted to more clearly define varying conditions at construction.

JPCP Design Features

Joint Spacing

The joint spacing is a critical JPCP design factor that affects structural and functional performance of JPCP, as well as construction and maintenance cost. The stresses in JPCP increase rapidly with increasing joint spacing. To a lesser degree, joint faulting also increases with increasing joint spacing. Joint spacing must be selected within the context of design features such as slab thickness, slab width, PCC materials properties, base type, and subgrade stiffness. A particular joint spacing may be adequate for a given set of design features, but inadequate for another. The interaction between slab thickness and joint spacing is shown in figure 3.4.15.

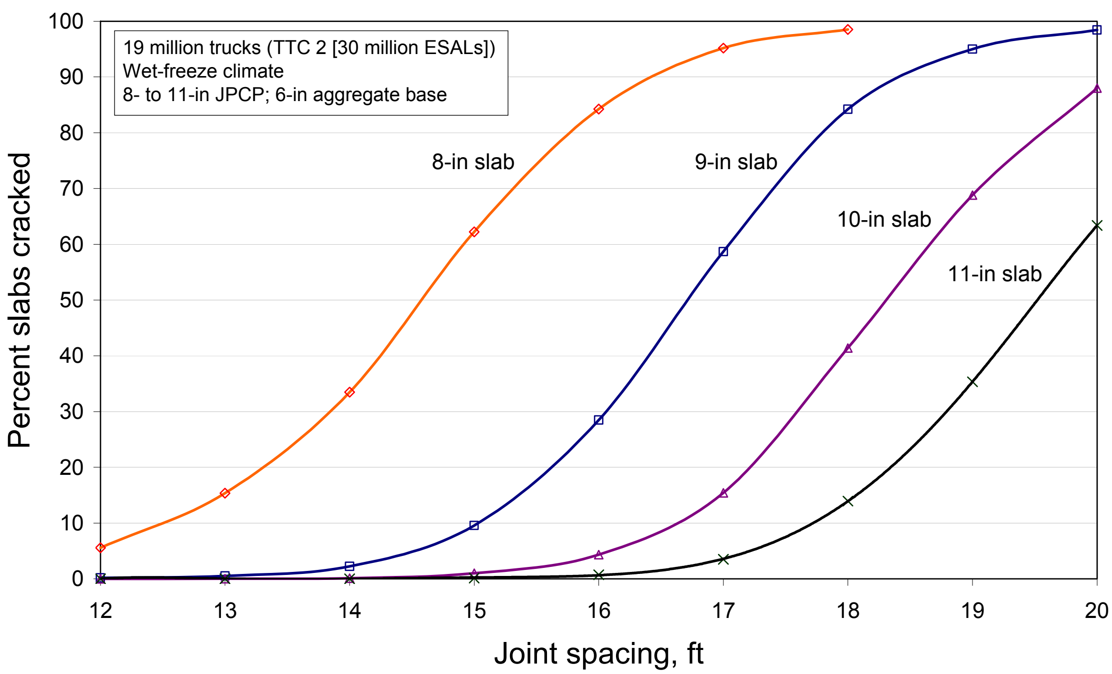

Figure 3.4.15. Sensitivity of JPCP transverse cracking to slab thickness and joint spacing.

In general, a short joint spacing (e.g., 15 ft) is recommended; however, there is no need to make joint spacing less than 12 ft, since the minimum lane width is 12 ft. If random joint spacing is used, the average joint spacing may be used for the evaluation of faulting performance, but for transverse cracking the long and short panels should be evaluated separately. For example, if 12-13-19-18 ft joint spacing pattern is used, the 12- and 13-ft panels should grouped and analyzed using 13 ft joint spacing, and the 18- and 19-ft panels should be grouped and analyzed using 19 ft joint spacing. The average cracking from the two designs is the expected cracking in the random jointed section. The Design Guide software uses the average joint spacing for faulting analysis and the maximum joint spacing for cracking analysis when random joint spacing is entered.

Dowel Diameter and Dowel Spacing

For doweled pavements, dowel diameter and dowel spacing are critical design inputs. The larger the dowel diameter, the lower the concrete bearing stress and joint faulting. JPCP joint faulting is highly sensitive to dowel diameter. The sensitivity of JPCP joint faulting to dowel diameter is shown in figure 3.4.16. Dowel spacing is simply the spacing between dowels. Typical dowel spacing is 12 in. Typically, as the required slab thickness increases (due to heavier traffic to control slab cracking), an increase in dowel diameter is required to control joint faulting. Note that increasing slab thickness without a corresponding increase in dowel diameter may result in a small increase in predicted joint faulting due to a reduction in effective area of the bar relative to slab thickness.

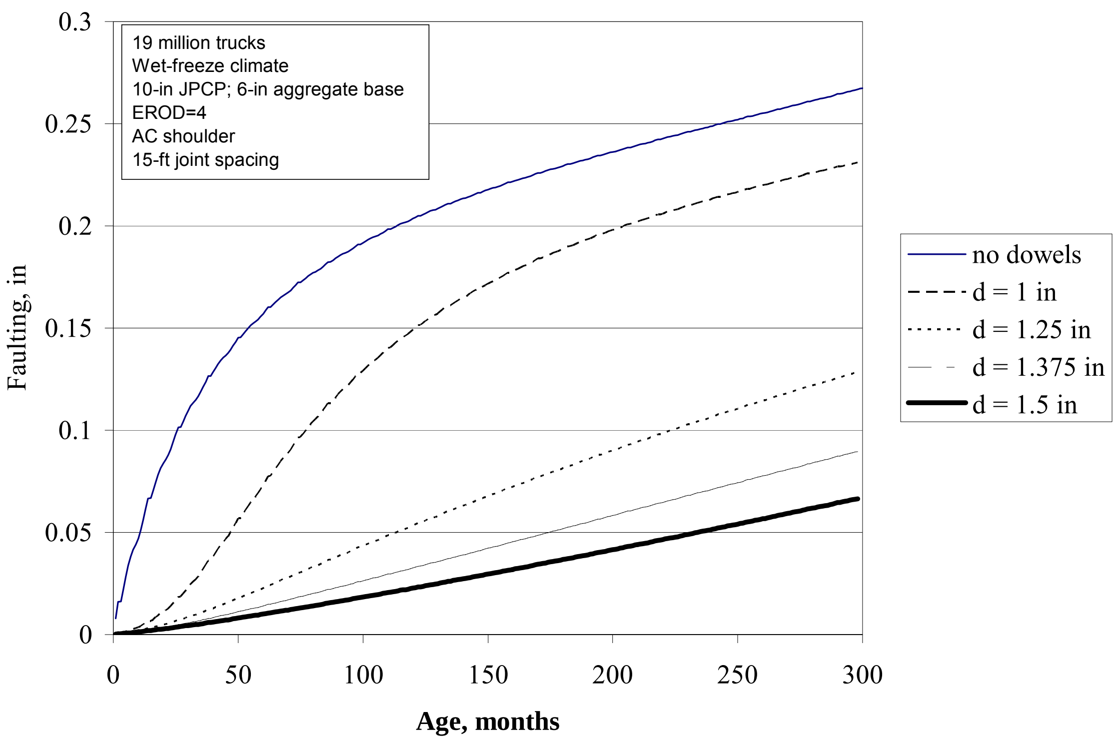

Figure 3.4.16. Sensitivity of JPCP joint faulting to dowel diameter.

Sealant Type

Sealant type is an input to the empirical model used to predict spalling. Spalling is used in smoothness predictions, but it is not considered directly as a measure of performance in this Guide. The sealant options are liquid, silicone, and preformed.

Edge Support

Tied PCC shoulders and widened slabs can significantly improve JPCP performance by reducing critical deflections and stresses along the edge. The shoulder type also affects the amount of moisture infiltration into the pavement structure as discussed in section 3.4.3.6. The effects of moisture infiltration are considered in the determination of seasonal moduli values of unbound layers. The structural effects of the edge support features are directly considered in the design process, as illustrated in figure 3.4.17 for cracking and 3.4.18 for faulting. The design inputs for these design features are as follows:

- Tied PCC Shoulder – for tied concrete shoulders the long-term LTE between the lane and shoulder must to be provided. The LTE is defined as the ratio of deflections of the unloaded and loaded slabs. The higher the LTE, the greater the support provided by the shoulder to reduce critical responses of the mainline slabs. Typical long-term deflection LTE are:
    - 50 to 70 percent for monolithically constructed and tied PCC shoulder.
    - 30 to 50 percent for separately constructed tied PCC shoulder.
    - Untied concrete shoulders or other shoulder types do not provide significant support; therefore, a low LTE value should be used (e.g., 10 percent due to the support from extended base course).
- Widened Slab – widened slabs improve JPCP performance by effectively moving the mean wheelpath well away from the pavement edges where the critical loadings occur. The design input for widened slab is the slab width which can range from 12 to 14 ft.

Base Erodibility

The potential for base or subbase erosion (layer directly beneath the PCC layer) has a significant impact on the initiation and propagation of pavement distress. Different base types are classified based on long-term erodibility behavior as follows:

- Class 1 – Extremely erosion resistant materials.
- Class 2 – Very erosion resistant materials.
- Class 3 – Erosion resistant materials.
- Class 4 – Fairly erodible materials.
- Class 5 – Very erodible materials.

Rigorous definitions of the material types that qualify under these various categories are provided in PART 2, Chapter 2. The design input is the erodibility class.

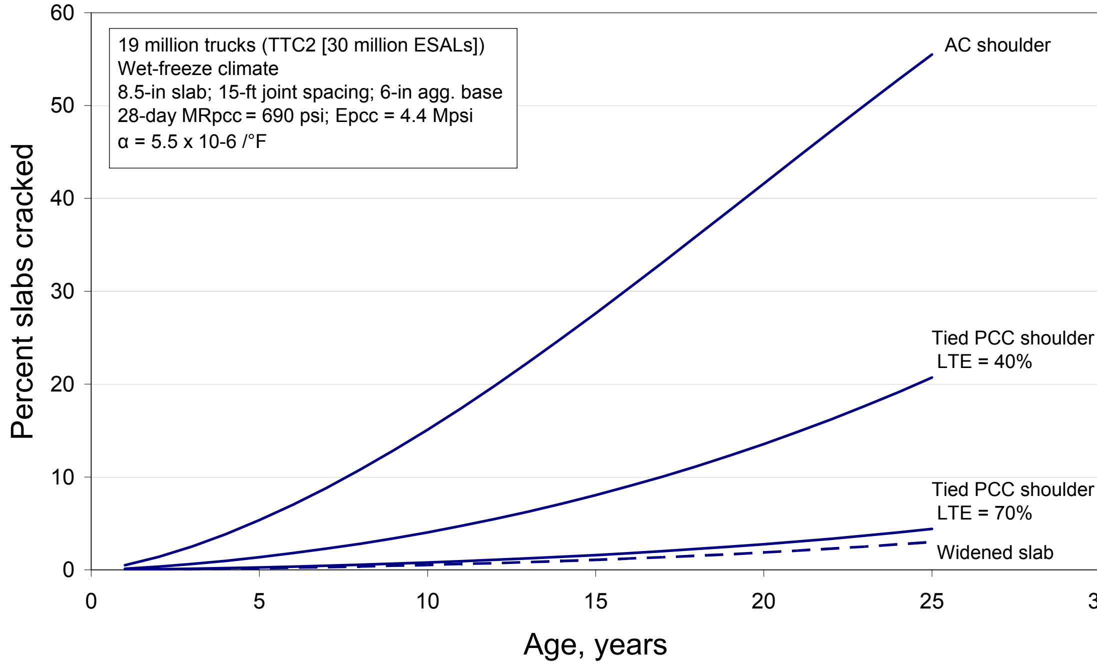

Figure 3.4.17. Effects of edge support on JPCP transverse cracking.

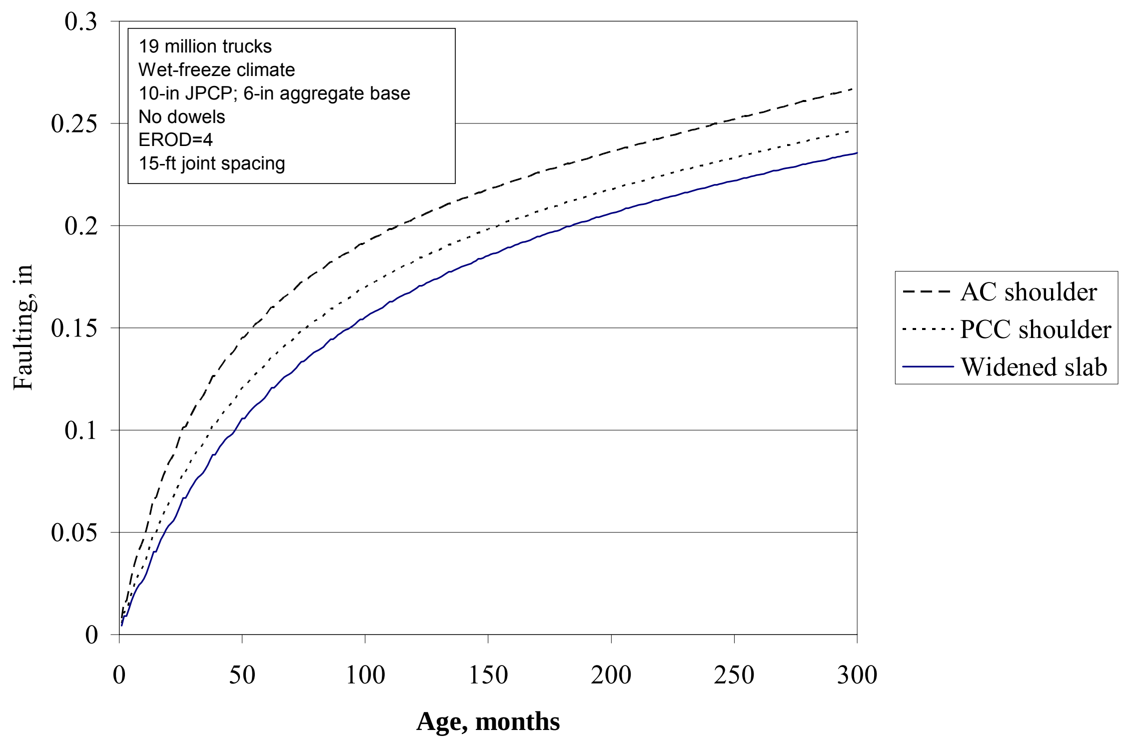

Figure 3.4.18. Effects of edge support on nondoweled JPCP transverse joint faulting.

PCC–Base Interface

The interface between a stabilized base and PCC slab is modeled either completely bonded or unbonded for JPCP design. The structural contribution of a stabilized base is significant, if the base is fully bonded to the slab. Stabilized bases (especially asphalt-stabilized bases) are often bonded to the slab, and the deflection testing conducted at slab interior typically shows a bonded response. However, the effects of environmental and traffic loading tend to weaken this bond over time around the edges, and the bonded-interface assumption over the entire design period may be unconservative.

The JPCP design procedure includes the modeling of the changes in the interface bond condition over time. This is accomplished by specifying the pavement age at which the debonding occurs. Up to the debonding age, the slab-base interface is assumed fully bonded; after the debonding age, the interface is assumed fully unbonded. The design input is the pavement age at debonding, in months. In general, specifying the debonding age greater than 5 years (60 months) is not recommended and was not used in calibration.

<u>CRCP Design Features</u>

Steel Design

Longitudinal steel is an important design parameter that controls the opening of the transverse cracks. Crack width (at steel level) is extremely important and should be controlled (or limited) directly in design to be less than 0.02 in at steel level. The LTE of the transverse cracks should be greater than 95 percent. The steel design is also critical from the standpoint of its effect on crack spacing. Field studies have shown that increased steel content results in fewer punchouts and increased smoothness, even though the crack spacing typically decreases significantly (for the same design and construction conditions) (see figure 3.4.19). The inputs related to steel design include the following:

- Percent steel – steel content expressed as a percentage of steel cross sectional area of the PCC cross section. Steel percentages of 0.60 to 0.70 have provided suitable cracking patterns and past performance of CRCP. However, a higher steel percentage (e.g., 0.70 to 1.00) may be desirable for roadways subjected to high volumes of heavy vehicles with long design lives to maintain crack width less than 0.02 in and crack LTE greater than 95 percent. The typical effect of steel percentage on punchout development is shown in figure 3.4.19 for a given project.
- Bar diameter – diameter of the reinforcing bar (typically ⅝ to ¾ is used successfully).
- Steel depth – depth from pavement surface to the center of reinforcing steel. A minimum steel depth of 3.5 in and a maximum of mid-depth are recommended. Studies have shown that placing the reinforcement closer to the surface results in much tighter cracks and fewer punchouts. (26) This effect is reflected in the Design Guide prediction.

The effect of transverse reinforcement on CRCP crack patterns is not directly considered in this Guide. Transverse reinforcement is normally provided to facilitate placement of longitudinal steel on chairs.

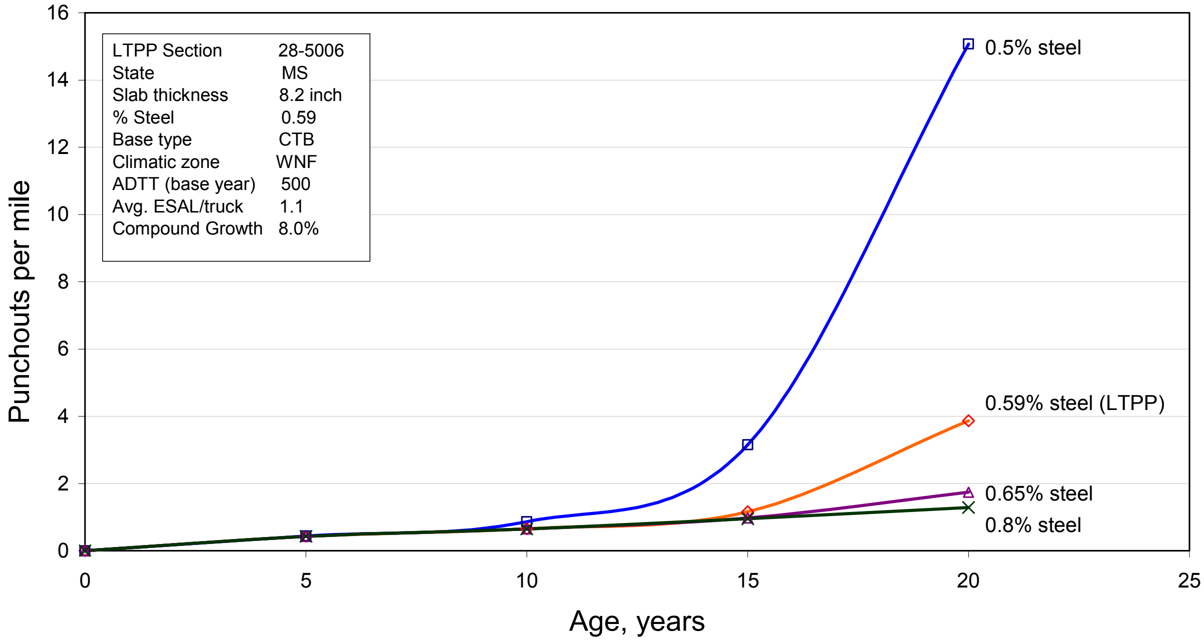

Figure 3.4.19. Illustration of effect of CRCP reinforcement percentage on punchout development.

Base Properties

The base type and material characteristics are critical features that affect the crack spacing and thus crack width, slab support, erosion (loss of support), punchouts, and smoothness, as well as CRCP construction costs. These factors can strongly influence the performance of CRCP. The base properties are characterized using the following inputs:

- Base modulus and thickness – the modulus and thickness of a treated base add significantly to the structural capacity of the CRCP slab.
- Base erodibility – the base erodibility is defined by the base type and classified into the following categories:
    - Class 1 – Extremely erosion resistant materials.
    - Class 2 – Very erosion resistant materials.
    - Class 3 – Erosion resistant materials.
    - Class 4 – Fairly erodible materials.
    - Class 5 – Very erodible materials.
- Descriptions of the material types that qualify under these various categories are provided in PART 2, Chapter 2. The design input is the erodibility class.
- Base/Slab friction coefficient – the coefficient of friction of base material. Typical values for different types of base that were used in calibration are summarized in table 3.4.2 (note the mean values obtained from all of the calibration sections that were required to match field crack spacing). More detailed information on base/slab friction coefficient is given in Appendix LL. It is recommended to use the mean friction coefficient for design unless local calibration shows differently.

Table 3.4.2. Typical values of base/slab friction coefficient recommended for design.

Subbase/Base type	Friction Coefficient (low – mean – high)
Fine grained soil	0.5 – 1.1 – 2
Sand*	0.5 – 0.8 – 1
Aggregate	0.5 – 2.5 – 4.0
Lime-stabilized clay*	3 – 4.1 – 5.3
ATB	2.5 – 7.5 – 15
CTB	3.5 – 8.9 – 13
Soil cement	6.0 – 7.9 – 23
LCB	3.0 – 8.5 – 20
LCB not cured*	> 36 (higher than LCB cured)

* Base type did not exist or not considered in calibration sections.

Crack Spacing, Crack Width, and Crack LTE

Crack spacing is a critical factor affecting crack width, which is the dominant factor governing the performance of CRCP. Crack width computed by the Design Guide software is at steel depth, not surface (which is wider). Crack width increases over time and could be used as a key design criterion. Through proper selection of steel content, PCC mixture parameters, and base type and friction, the designer can obtain acceptable mean crack width that is less than 0.02 in. The mean crack spacing can be specified either directly, or estimated using a model incorporated in the Design Guide software based on design inputs. Calculations for crack opening are based on mean crack spacing. The maximum recommended mean crack spacing is 6 ft, however, crack width and LTE are the key design criteria.

Shoulder Type

A CRCP can be designed with either tied PCC or AC. A typical shoulder design for CRCP traffic lanes is either a JPCP (placed after the mainline traffic lanes) without dowels or an asphalt concrete (AC) shoulder. Field data shows that tied-PCC shoulders can provide a significant reduction in CRCP punchouts if the load transfer across the lane-shoulder joint is adequate. The tied shoulder reduces deflection at the CRCP edge. Key design aspects include the tie between the shoulder and the traffic lane, the erodibility of the underlying base materials of the shoulder, the use of the shoulder for regular traffic for emergencies, to increase capacity, and for parking. The design input is the shoulder type.

3.4.4 JPCP DESIGN CONSIDERATIONS

The JPCP performance depends on numerous factors, and the design solutions are by no means unique. The design goals can be achieved using any number of combinations of design features. Various design features may also be used to improve pavement performance and reduce the risk of poor performance. For example, a stabilized base and an aggregate subbase may be used where weak or variable subgrade conditions are a concern to improve both strength and uniformity of foundation support. A stabilized base is also more resistant to erosion, which may be an important quality to reduce the risk of poor faulting performance when designing for high volumes of heavy trucks. For long design periods (e.g., 50 yr), subsurface drainage may be important to ensure adequate long-term material performance. A careful consideration of the design conditions and available options is important to obtain optimal design. This section provides a discussion of the factors that should be considered in the design of JPCP.

3.4.4.1 Slab Thickness

This is one of the most critical design features from the standpoint of both performance and cost (*5*). In general, as the slab thickness increases, critical bending stresses and deflections decrease, with consequent reduction in cracking and faulting. Field and analytical studies have shown that with increasing slab thickness, slab cracking decreases greatly and joint faulting decreases slightly. Slab thickness is the most dominant factor that affects cracking performance of JPCP. However, various other design factors also affect JPCP cracking, including joint spacing, edge support, PCC properties (strength, coefficient of thermal expansion, shrinkage, and elastic modulus), and base type. Therefore, slab thickness must be selected within the context of those design features and climate. A slab thickness that is adequate for a given set of design features may be totally inadequate for another set of design features. The goal is to select the minimum thickness that provides acceptable levels of transverse cracking, joint faulting, and smoothness (IRI) over the design period at the desired level of reliability.

3.4.4.2 Slab Width

Typically, slab width has been synonymous with lane width (usually 12 ft). Several States and other countries have utilized wider slabs (typically 2 ft wider), keeping the lane width the same, to improve performance. Field and analytical studies have shown that the wider slabs greatly improves the cracking and faulting performance of JPCP by keeping the truck axles well away from the free edge and corners where they can cause critical stresses and deflections (*2, 5*). The drastic reduction or elimination of free-edge loading conditions results in substantial reduction in the maximum stresses and deflections that occur under typical service conditions, which leads to less cracking and faulting. However, some sections with widened slabs have shown increased tendency to develop longitudinal cracking in the wheelpath, such cracking is not addressed in this Guide. Therefore, the widened slab design should not be used without full consideration of other design features.

3.4.4.3 PCC Materials

Arguably, the most important PCC material property is the durability. All design analyses in this guide are performed assuming that the material will perform well throughout the design period. The predicted pavement performance is valid only if durability problems such as D-cracking or alkali-silica reactivity (ASR) do not develop to cause premature failures. Thus, measures must be taken to ensure adequate material performance to achieve the design goals. These measures include PCC mix components, as well as providing subsurface drainage. The material durability is especially important when a long design period is selected (e.g., 50 years). Additional discussion of PCC durability issues is provided in PART 2, Chapter 2.

The PCC material properties directly considered in this Guide include flexural strength, modulus of elasticity, drying shrinkage, coefficient of thermal expansion, thermal conductivity, and heat capacity. JPCP performance can be quite sensitive to many of these parameters. For example, the highly significant effects of PCC flexural strength on cracking are well known. The coefficient of thermal expansion is also a highly sensitive factor affecting curling stresses and joint opening in JPCP. The amount of shrinkage also affects both cracking and faulting of JPCP.

In general, PCC elastic modulus increases with increasing flexural strength for any given PCC mixture. An increase in strength leads to lower fatigue damage; however, since the modulus of elasticity also increases, the bending stress will increase. Thus, the reduction in fatigue damage is not as dramatic as commonly believed when PCC strength is increased. In addition, a higher strength PCC obtained through increased cement content results in a higher shrinkage of the hardened mixture and higher α_{PCC} (39). Higher shrinkage and α_{PCC} leads to greater warping and curling, which tends to increase top-down stresses.

Although the PCC modulus for any given mix is correlated to strength, the PCC modulus for different mixes can be quite variable, depending on aggregate type. The effects of PCC modulus on stress are quite significant. Thus, for a given strength PCC, the mix with a lower modulus will provide significantly better cracking performance. However, a lower modulus leads to greater deflections, which can be deleterious to faulting performance, although the most dominant factor affecting faulting is dowel diameter.

The following is a summary of the effects of various PCC properties on JPCP performance:

- PCC strength – higher the better for all JPCP performance, but a higher strength for a given material is accompanied by higher modulus, which tends to moderate the beneficial effect. Also, if achieved by higher cement content, the increased shrinkage and α_{PCC} will result in higher curling and warping.
- PCC modulus – the lower the better for cracking, but a lower modulus can be deleterious to faulting performance.
- Shrinkage – the lower the better for all JPCP performance.
- Coefficient of thermal expansion – the lower the better for all JPCP performance.

Most of the PCC properties are dictated by the local materials, and the designer may have very little control over the mix properties other than the strength. However, it is possible to optimize the PCC mix for pavement performance, and the mix optimization may be practical on some projects. Some of the PCC properties affect material cost as well as pavement performance.

3.4.4.4 Transverse Joint Spacing

The joint spacing affects both transverse cracking and construction cost of the JPCP. To a lesser degree, it also affects joint faulting. Field studies have shown that the longer the joint spacing, the greater the potential for transverse cracking. Joint spacing must be selected within the context of design features such as slab thickness, slab width, PCC materials properties, and base type. A specific joint spacing may be adequate for a given set of other design features, but inadequate for another set of design features. The goal is to select the maximum joint spacing that provides an acceptable level of transverse cracking and smoothness over the design life at the desired level of reliability. The direct consideration of top-down cracking has made joint spacing even more critical. Truck axle spacing (particularly between the steering axle and the drive axle) has been shown to greatly affect the bending stress at the top of the slab when all of these axles fit within a given slab, which can lead to serious top-down transverse or diagonal cracking. In general, a short joint spacing (e.g., 15 ft) is recommended; however, there is no need to make joint spacing less than 12 ft, since the lane width is 12 ft.

3.4.4.5 Transverse Joint LTE

The load transfer across transverse joints is the most critical factor controlling JPCP joint faulting and, therefore, smoothness (*5, 13*). Load transfer also affects top-down cracking of JPCP. Field studies have shown that the use of mechanical devices (dowels) greatly decreases the potential for transverse joint faulting. The dowel diameter is an important factor affecting JPCP faulting. Small-diameter (1 in or less) dowels are relatively ineffective in preventing joint faulting, while large-diameter (e.g., 1.5 in) dowels are highly effective. A stabilized base (asphalt or cement) also increases the joint load transfer.

Joint faulting is the most critical factor in controlling smoothness of JPCP. The JPCP design factors that affect joint faulting include dowel diameter, base type, edge support (tied PCC shoulder or widened slab), and slab thickness. PCC mix properties (including shrinkage, thermal coefficient, and elastic modulus) and climate also affect joint faulting. However, dowel diameter is by far the most dominant factor affecting transverse joint faulting. Adequate LTE must be provided across transverse joints to ensure acceptable level of faulting and smoothness over the design life at the desired level of reliability.

3.4.4.6 Transverse Joint Sawcut Depth

The sawcut depth is important to ensure proper formation of transverse joints. It is desirable to keep the sawcut depth to a minimum that will still provide a high degree of assurance that the joints will form properly to avoid random cracking. Conventional practice has been to saw transverse joints to a depth of 25 percent of the slab thickness. This depth has worked well in most cases, but a deeper cut should be considered where a permeable or stabilized base is used. The penetration of PCC into a permeable base or the initial bonding of the PCC slabs to a stabilized base results in a greater effective slab thickness, requiring a deeper sawcut to ensure proper joint formation. For these designs, a sawcut depth of one-third the slab thickness is recommended. For cement stabilized base and lean concrete bases, notching of the base (1/3 of its depth) at the planned locations of transverse joints in the PCC is also recommended to minimize the potential for random cracking.

3.4.4.7 Longitudinal Joint Load Transfer and Ties

The longitudinal joint load transfer across between traffic lanes and with tied PCC shoulder affects the bending stresses and deflections in PCC slabs. Consequently, the load transfer across longitudinal joints affects the transverse cracking and joint faulting. In addition to improving LTE across the longitudinal joints, the tie bar system also prevents lane separation. Lane separation can lead to greater infiltration of water into the pavement structure, as well as becoming a safety concern.

An adequate tie bar system is critical to ensuring the effectiveness of the longitudinal construction joints. Studies showed that No. 5 bars (30-in long) spaced at 30-in intervals provide adequate performance for most moderate- to heavy-traffic roadways (*14*). In areas frequently crossed by heavy trucks (e.g., acceleration/deceleration lanes, truck climbing lanes, and high-volume merge areas), the use of larger diameter bars and closer tie bar spacing should be considered.

3.4.4.8 Longitudinal Joint Sawcut Depth

The sawcut depth is important to ensure proper formation of longitudinal joints. It is desirable to keep the sawcut depth to a minimum that will still provide a high degree of assurance that the joints will form properly to avoid random cracking. In general, longitudinal joints need to be cut deeper (than transverse joints) to ensure proper formation of joints, especially at the lane-shoulder joints, because of lower restraint and curling stresses. The restraint and curling stresses help the weakened plane created by the sawcut to crack through, forming the joints. A sawcut depth of one-third the slab thickness is recommended for longitudinal joints.

3.4.4.9 Base

Several base types are available for use under JPCP, including dense-graded aggregate base (unstabilized), cement-treated base, asphalt-treated base, lean concrete base, recycled PCC base, and permeable bases. The base type has been shown to affect joint faulting, smoothness, and slab cracking (*15, 16*). The structural contribution of a stiff stabilized base can be very significant if the base is bonded to the slab. However, the main purpose of providing a base course in JPCP is to provide uniform support and resist erosion, which are critical to avoid localized failures and faulting. For structural capacity, several other design factors (e.g., slab thickness, PCC strength, and edge support) have more direct and far greater impact than a stabilized base. On the other hand, the functions provided by a base course cannot be substituted with additional structural capacity.

The joint faulting is significantly less in JPCP provided with a stabilized base; however, reflection cracking has been a concern for cement-treated and lean concrete bases. In the past, attempts had been made to debond a cement-stabilized or lean concrete base from the slab. In general, however, composite action between pavement layers is beneficial. The cement-stabilized or lean concrete base can be notched (1/3 of the base thickness) at the planned locations of joints in the PCC layer and bonded to the pavement slab as a more positive means of addressing reflection cracking concern and also realize the benefits of bond between the base and the slab (*2, 17, 18*). The notched and bonded base also provides good uniform cracking of the joints. The bond between the base and the slab, however, may not be counted on to last more than about 4 years (*18*).

The base type should be selected in consideration of site factors, (including climate and subgrade), traffic level, other pavement design features, and cost. A uniform, erosion-resistant base is more important for pavements subjected to a high volume of heavy vehicles, especially in wet or wet-freeze areas. The amount of stabilizer has a very significant effect on the erodibility of the base. Thus, the amount of stabilizer must be carefully selected to match the design life, climatic, traffic, and other design conditions.

3.4.4.10 Subbase

The use of a subbase beneath the base course depends on several factors, including the type and stiffness of the subgrade, the type of base course (unbound or stabilized base), and the use of an open-graded drainage layer. Field studies have shown that on JPCP constructed on a stabilized base, the erosion can take place beneath the stabilized base. For such designs, providing a granular subbase is important to minimize the potential for erosion and loss of support beneath the stabilized base. Several agencies specify such a granular layer beneath a stabilized base course. An aggregate subbase may also be used as a measure to protect the aggregate base against contamination by fines on very soft, fine-grained subgrade. Beneath a permeable base, the use of a dense-graded aggregate subbase meeting the gradation requirements for a filter layer is essential to prevent infiltration of fines into the open-graded drainage layer (*19*).

3.4.4.11 Subsurface Drainage

The current state of the art is such that conclusive remarks regarding the effectiveness of pavement subsurface drainage or the need for subsurface drainage are not possible. The effectiveness of subsurface drainage had been confounded with construction problems (e.g., damages to edge drains; contamination of permeable base), poor maintenance, and poor stability of some of the permeable base materials used. Without good subsurface drainage, the protection against pumping and erosion must be accomplished through a combination of several design features, including base, subbase, and shoulder, and the use of features such as doweled transverse joints and widened slabs. The experience with these design features indicates that a JPCP can be designed to provide adequate functional and structural performance without subsurface drainage; however, good subsurface drainage may be very important to achieve good long-term material performance. When pavement sections have included well designed, constructed, and maintained subsurface drainage systems, they have improved rigid pavement performance (*20*).

D-cracking had been a major cause of premature failures of rigid pavements, especially in wet-freeze areas. Studies indicate that good subsurface drainage may be important in mitigating D-cracking and other PCC material problems (*2, 21*). Long-term material performance is more critical for longer design periods, and subsurface drainage is a design feature that can significantly enhance material performance.

Various subsurface drainage options are available for JPCP, including daylighting, edgedrains, and permeable base. So-called “permeable shoulder,” a design where permeable base is provided only beneath the shoulder, has also been shown an effective subsurface drainage solution for rigid pavements (*18, 21*). The subsurface drainage should be used only if it will be maintained. See PART 3, Chapter 1 for detailed guidelines on subsurface drainage design.

3.4.4.12 Shoulder Design

Shoulder design affects the construction cost and pavement performance. The factors for consideration in selecting shoulder type and width include the use of the shoulder for detour traffic during pavement rehabilitation and for emergency uses. The shoulder may also be designed to be used as an extra lane during peak traffic hours. A monolithically constructed tied PCC shoulder is effective in improving structural capacity of JPCP. The use of tied PCC shoulders also reduces the potential for pumping and erosion, because the concrete-to-concrete lane-shoulder joint can be sealed more effectively and deflections at the joints are lower.

3.4.4.13 Subgrade Improvement

The improvement of the top of a soft subgrade provides greater support and uniformity to the pavement and aids construction. Subgrade improvement can be accomplished by stabilizing the upper portion or the placement of a thick granular layer. The effects of subgrade improvements are considered in the design procedure in terms of increased modulus, which affects slab deflection and stresses to some extent. Another benefit of an improved subgrade may be the reduced potential for erosion at the top of the subgrade. The subgrade improvement can also play a role in producing a smoother as-built pavement. PART 2, Chapter 1, discusses subgrade improvement techniques in more detail.

3.4.5 JPCP DESIGN PROCEDURE

This section presents a step-by-step description of the calculation procedures for the distress prediction and the ultimate selection of the design. As stated earlier, pavement design according to this Guide is an iterative process. The designer must first establish the performance criteria and select a trial design with the features appropriate for the design goals. The trial design is then analyzed for its performance. If the performance criteria are not met at the desired level of reliability, the design is adjusted until each of the selected performance criteria are satisfied. These procedures are described in this section, along with a discussion of sensitivity of each performance indicator to various input parameters and the approach for modifying the trial design to satisfy the design goals.

3.4.5.1 JPCP Performance Criteria

JPCP design is based on three performance measures: transverse cracking, faulting, and smoothness. The designer may select some or all three performance criteria. For each selected performance measure, the designer must select the desired performance level at the end of design life (e.g., percent slab cracking, amount of faulting, and IRI) and reliability level. Both the performance level and design reliability should be established considering functional class of the roadway. See section 3.4.3.3 of this chapter for discussion on performance criteria. PART 1, Chapter 1 presents some general recommendations on design reliability levels based on functional class but these should be evaluated and adjusted by highway agencies using this Guide.

3.4.5.2 Trial Design

The trial design should be selected considering the factors described in section 3.4.4 of this chapter. The local experience with pavement designs for various design conditions may be the most valuable resource in selecting trial design. The design catalog developed under NCHRP Project 1-32 (*19*) may also be helpful in selecting trial design. A typical trial section includes the following features:

- PCC strength – typical design strength. Note that the design input is the expected average strength, not the minimum required strength.
- Trial slab thickness – depends on traffic level, PCC properties, and climate. Suggested initial trial thicknesses for JPCP without edge supports (tied PCC shoulder or widened slab) are:
    - Low traffic (2-way average daily traffic [ADTT] < 1000) – 8 in or less.
    - Moderate traffic (2-way ADTT up to 3000) – 9 to 10 in.
    - Heavy traffic (2-way ADTT > 3000) – 10 in or more.

  A thicker slab is needed in dry-nonfreeze areas than in wet or wet-freeze areas. The trial thickness may be reduced by 1 in for JPCP with edge support.
- Joint spacing – in general, excessive joint spacing is not recommended. For typical traffic streams, 15-ft joint spacing works well. Consult sections 3.4.3.7 and 3.4.4.4 for guidelines.
- Base and subbase – Consult sections 3.4.4.9 and 3.4.4.10 for guidelines.
- Edge support – monolithically constructed tied PCC shoulders and widened slab designs are effective in reducing critical deflections and stresses. Consult section 3.4.4.12 for guidelines.

3.4.5.3 Performance Prediction—Transverse Cracking

For JPCP transverse cracking, both bottom-up and top-down modes of cracking are considered. Under typical service conditions, the potential for either mode of cracking is present in all slabs. Any given slab may crack either from bottom-up or top-down, but not both. Therefore, the predicted bottom-up and top-down cracking are not particularly meaningful by themselves, and combined cracking must be determined, excluding the possibility of both modes of cracking occurring on the same slab.

<u>Cracking Model</u>

The percentage of slabs with transverse cracks in a given traffic lane is used as the measure of transverse cracking and is predicted using the following model for both bottom-up and top-down cracking:

$$CRK = \frac{1}{1 + FD^{-1.68}} \qquad (3.4.2)$$

where,

CRK	=	predicted amount of bottom-up or top-down cracking (fraction).
FD	=	fatigue damage calculated using the procedure described in this section.

Model Statistics:

R^2	=	0.68
N	=	521 observations
SEE	=	5.4 percent

The total amount of cracking is determined as follows:

$$TCRACK = \left(CRK_{Bottom-up} + CRK_{Top-down} - CRK_{Bottom-up} \cdot CRK_{Top-down}\right) \cdot 100\% \qquad (3.4.3)$$

where,

TCRACK	=	total cracking (percent).
$CRK_{Bottop-up}$	=	predicted amount of bottom-up cracking (fraction).
$CRK_{Top-down}$	=	predicted amount of top-down cracking (fraction).

Equation 3.4.3 assumes that a slab may crack from either bottom-up or top-down, but not both.

The JPCP transverse cracking model was calibrated based on performance of 196 field sections located in 24 States. The calibration sections consist of LTPP GPS-3 and SPS-2 sections and 36 sections from the FHWA study *Performance of Concrete Pavements* (*2*). Time-series data were available for many of the sections, making the total number of field cracking observations 522. The cracking predictions given by equation 3.4.2 are shown in figure 3.4.20. Figure 3.4.21 shows predicted cracking versus age for an example case. These predictions are valid only when the fatigue damage is calculated according to the procedure described in this section.

<u>Structural Response Modeling</u>

The following factors affect the magnitude of bending stresses in PCC slabs:

- Slab thickness.
- PCC modulus of elasticity.
- PCC Poisson's ratio.
- PCC unit weight.
- PCC coefficient of thermal expansion and shrinkage.
- Base thickness.
- Base modulus of elasticity.
- Base unit weight (for bonded interface between PCC slab and base).
- Interface condition between the PCC slab and base.
- Joint spacing.
- Subgrade stiffness.
- Lane-shoulder joint LTE.

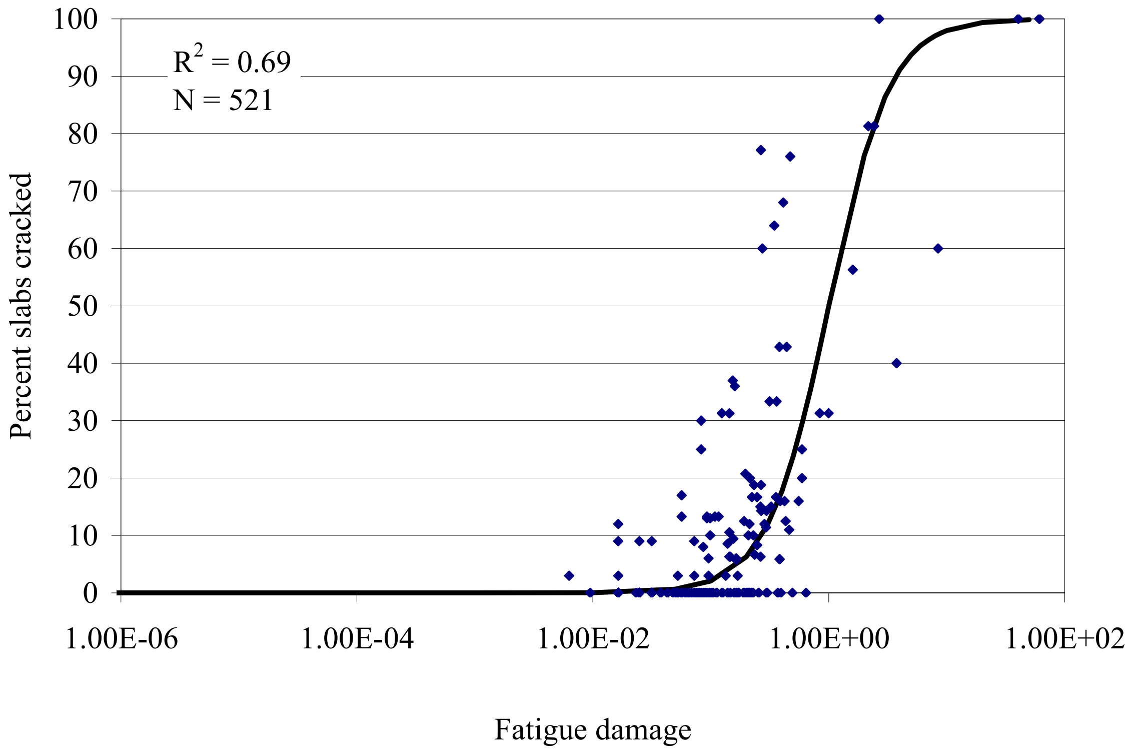

Figure 3.4.20. JPCP cracking model shown with the field data.

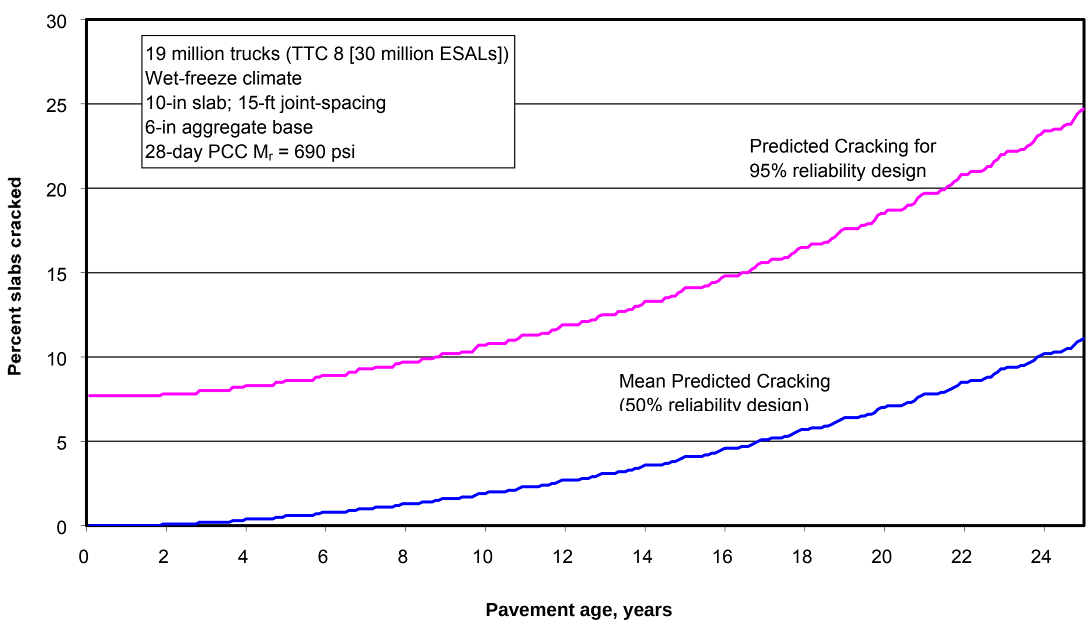

Figure 3.4.21. Example JPCP cracking predictions given by the cracking model.

- Longitudinal joint lane-to-lane LTE (for widened slab pavement).
- Temperature distribution through the slab thickness.
- Moisture distribution through the slab thickness.
- Magnitude of effective permanent curl/warp.
- Load configuration
    - Bottom-up cracking – axle type (single, tandem, tridem, and quad axles).
    - Top-down cracking – short, medium, and long wheelbase.
- Axle weight.
- Wheel tire pressure and wheel aspect ratio (length-to-width ratio).
- Axle position (distance from the critical slab edge).

While many of the parameters above remain constant throughout the design period (e.g., slab thickness and joint spacing), others vary seasonally, monthly, hourly, or with pavement age. For accurate fatigue analysis results, all cases that produce significantly different stresses must be evaluated separately. The fatigue damage increments defined in this Guide were determined to account for those cases as follows:

- Pavement age – accounts for the changes in PCC modulus and strength with age and the changes in interface bond condition between a stabilized base and PCC slab.
- Month – accounts for monthly variations in base stiffness, foundation stiffness (including the effects of moisture and temperature on the subbase layers incorporated in the effective k-value), and the effects of monthly variation in relative humidity on slab warping due to differential shrinkage.
- Load configuration
    - Single, tandem, tridem, and quad axles for bottom-up cracking.
    - Short, medium, and long wheelbase for top-down cracking.
- Load level
    - Single axles – 3,000 to 41,000 lb in 1,000-lb increments.
    - Tandem axles – 6,000 to 82,000 lb in 2,000-lb increments.
    - Tridem axles – 12,000 to 102,000 lb in 3,000-lb increments.
    - Quad axles – 12,000 to 102,000 lb in 3,000-lb increments.

  For top-down cracking, single-tandem axle combination is assumed with a fixed 12,000-lb load for the single axle. The load levels for the tandem axles of the single-tandem combination are assumed to be the same as the standard tandems.
- Temperature – the effects of actual temperature gradient (including the effects of nonlinear temperature distribution), permanent curl/warp, and monthly variation in warping expressed as the effective temperature difference (top minus bottom).
    - Bottom-up – 0 °F to the maximum value that occurs in the section in 2 °F steps.
    - Top-down – 0 °F to the minimum (most negative) value that occurs in the section in 2 °F steps.
- Load position – the procedure developed to account for the effects of traffic wander calls for calculating the damage at the critical damage location caused by the loads placed at six specific lateral offsets as follows:
    - Bottom-up cracking – outside edge of the axle loads placed 0.5555, 2.640, 5.360, 7.445, 10.536, and 17.464 in from the pavement edge. In the longitudinal

direction, the axle is centered on the slab to produce the maximum stress at each lateral offset.

- Top-down cracking – outside edge of the axle loads placed 1.666, 7.920, 16.080, 22.334, 27.381, and 36.619 in from the pavement edge. In the longitudinal direction, one of the axles of the tandem (front or rear) is placed close to the transverse joint at the approach end of the slab and the single axle is placed close to the transverse joint at the opposite end of the slab (as shown in figure 3.4.6) to produce the maximum stress at each lateral offset. The load position for maximum top-down stress depends on slab size and wheelbase.

The above combinations results in about 1 million cases per design year, for which the stresses must be calculated. However, the effects of changes in any one parameter on stress is a smooth function, and interpolation techniques can be used to greatly reduce the actual number of cases that must be analyzed using a structural model capable of producing accurate stress results (e.g., a finite element analysis program). For example, the load increments for single axles alone are 40 cases. However, the stresses at different load levels can be determined accurately using the results for a limited number of cases (e.g., 3,000 lb, 12,000 lb, 21,000 lb, 30,000 lb, and 40,000 lb) through interpolation. When such techniques are applied to all parameters, the actual number of cases that must be analyzed using a sophisticated structural model reduces to about 20,000 cases per design year (about 500,000 cases for a 25-yr design).

The structural model used to determine stress must be capable of accurately predicting stress considering the following:

- Temperature and wheel loads – the model must be capable of handling general nonlinear temperature distribution in the PCC layer and multiple wheel loads.
- Loss of support due to slab curling (separation of PCC slab from foundation).
- The effects of base course – the model must be able to consider bonded and unbonded cases.
- Slab-to-slab interaction in a multiple slab system and load transfer across both transverse and longitudinal joints.

In general, a finite element analysis program is required. The stress calculations in the Design Guide software is accomplished using neural networks developed based on a large number of finite element analysis runs made using ISLAB2000. The ranges of input parameters covered in the neural networks are shown in table 3.4.3 for bottom-up stresses and in table 3.4.4 for top-down stresses. These ranges represent practical limits for each parameter. The radius of relative stiffness listed in tables 3.4.3 and 3.4.4 is a composite parameter that represents the relative stiffness of the PCC slab with respect to foundation and is given by the following equation (*12*):

$$\ell = \sqrt[4]{\frac{E_{PCC} h_e^3}{12(1-\mu_{PCC}^2)k}} \qquad (3.4.4)$$

where,

E_{PCC} = elastic modulus of PCC, psi.

Table 3.4.3. Ranges of input parameters of the neural network for computing critical stresses at the bottom of PCC slab.

Input Parameter	**Minimum Value**	**Maximum Value**
Radius of relative stiffness [a]	22.5 in	80 in
Joint spacing	12 ft	30 ft [b]
Transverse joint LTE	0%	95%
Shoulder LTE	0%	90%
Axle offset from the slab edge	0 in	36 in
Wheel aspect (width-to-length) ratio	10	0.5
Temperature difference (top – bottom)	0 °F	> 40 °F [c]
Axle weight, single axle	0 lb	45,000 lb
Axle weight, tandem axle	0 lb	90,000 lb
Axle weight, tridem axle	0 lb	135,000 lb
Axle weight, quad axle	0 lb	135,000 lb
Tandem and tridem axle spacing	40 in	70 in

[a] The radius of relative stiffness of highway pavements typically fall between 22.5 and 80 in. Analyses based on plate theory become increasingly inaccurate for the radius of relative stiffness values beyond the limit shown above.

[b] For typical highway pavements the bottom-up stress reaches the maximum value at joint spacing less than 30 ft. The results for 30-ft slab are given for the actual joint spacing greater than 30 ft. In general, long joint spacing (20 ft or greater) is not recommended because of excessive curling stress.

[c] Depends on PCC coefficient of thermal expansion, k-value, PCC unit weight, PCC thickness, and radius of relative stiffness.

Table 3.4.4. Ranges of input parameters of the neural network for computing critical stresses at the top of PCC slab.

Input Parameter	**Minimum Value**	**Maximum Value**
Radius of relative stiffness [a]	22.5 in	80 in
Joint spacing	12 ft	20 ft [b]
Transverse joint LTE	50% if nondoweled 85% if doweled	
Shoulder LTE	0%	90%
Axle offset from the slab edge	0 in	36 in
Wheel aspect (width-to-length) ratio	10	0.5
Temperature difference (top – bottom)	0 °F	< -80 °F [c]
Wheelbase	12 ft	20 ft
Axle weight, single axle	Fixed at 12,000 lb	
Axle weight, tandem axle	0 lb	135,000 lb
Tandem axle spacing	40 in	70 in

[a] The radius of relative stiffness of highway pavements typically fall between 22.5 and 80 in. Analyses based on plate theory become increasingly inaccurate for the radius of relative stiffness values beyond the limit shown above.

[b] For typical highway pavements, the top-down stress is close to the maximum value when the joint spacing reaches 20 ft. The results for 20-ft slabs are given for the actual joint spacing greater than 20 ft. In general, long joint spacing (e.g., 20 ft or greater) is not recommended because of excessive curling stress.

[c] Depends on PCC coefficient of thermal expansion, k-value, PCC unit weight, PCC thickness, and radius of relative stiffness.

h_e	=	effective slab thickness, in.
μ_{PCC}	=	PCC Poisson's ratio.
k	=	dynamic modulus of subgrade reaction (k-value), psi/in.

<u>Cracking Prediction Procedure</u>

The calibrated JPCP transverse cracking prediction model is valid only if the fatigue damage is calculated following the procedures outlined in this section. Presented in this section is the step-by-step procedure for predicting JPCP transverse cracking. The steps involved include the following:

1. Tabulate input data – summarize all inputs needed for predicting JPCP cracking.
2. Process traffic data – the processed traffic data needs to be further processed to determine equivalent number of single, tandem, and tridem axles produced by each passing of tandem, tridem, and quad axles.
3. Process pavement temperature profile data – the hourly pavement temperature profiles generated using EICM (nonlinear distribution) need to be converted to distribution of equivalent linear temperature differences by calendar month.
4. Process monthly relative humidity data – the effects of seasonal changes in moisture conditions on differential shrinkage is considered in terms of monthly deviations in slab warping, expressed in terms of effective temperature difference.
5. Calculate stress – calculate stress corresponding to each load configuration (axle type for bottom-up and axle spacing for top-down), load level, load position, and temperature difference for each month within the design period.
6. Calculate fatigue damage – calculate damage for each damage increment and sum to determine total bottom-up and top-down damage.
7. Determine the amount of slab cracking using equations 3.4.2 and 3.4.3.

Assumptions

The following were assumed in the fatigue analysis:

- Linear damage accumulation – the procedure is based on Miner's hypothesis (*22*).
- The pavement structure is modeled as a two-layered system consisting of slab and base with either a bonded or unbonded interface. The effects of subbase layers, as well as the shear contribution of the base layer, are accounted for through the use of effective dynamic modulus of subgrade reaction.
- Lateral traffic wander is modeled as a normal distribution using mean wheelpath and standard deviation.
- The stresses in JPCP at the pavement edge do not immediately drop off to an insignificant level when the wheel is partially located at the pavement edge. The effects of wheels placed *x* inches outside of the pavement edge is assumed equal to those placed *x* inches inside of the pavement edge. Thus, the probability of traffic wheel being -*x* in and +*x* in from the pavement edge are added together for damage calculation, as illustrated in figure 3.4.22.

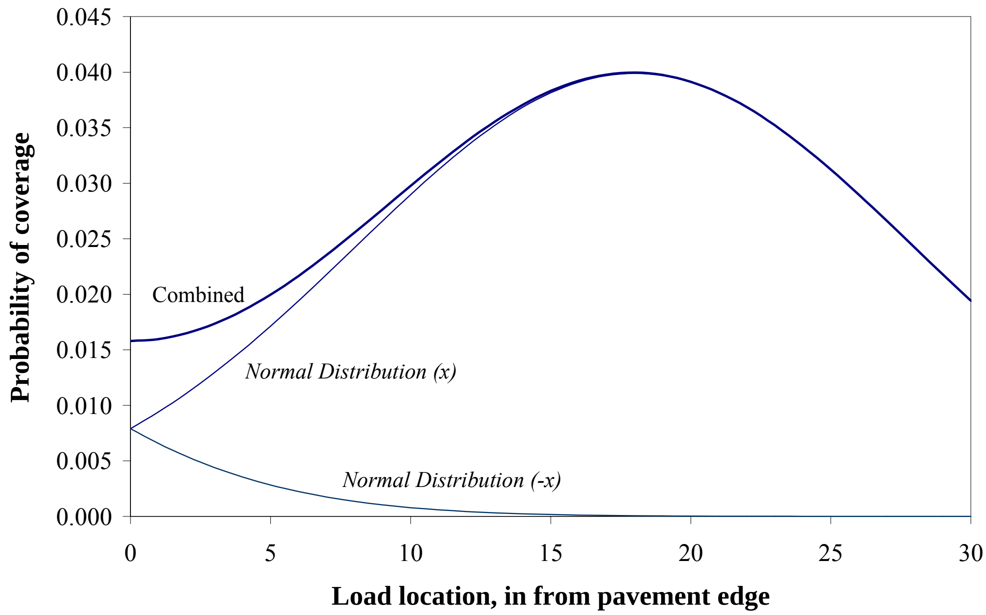

Figure 3.4.22. Illustration of probability of coverage including the effects of the axle load being partially off of the pavement.

- The use of widened slab design is assumed to change the critical damage location for fatigue damage from the lane-shoulder edge to the longitudinal lane-to-lane joint edge. Therefore, the effects of widened slabs (in terms of fatigue cracking) are similar to those of tied PCC shoulder, except that there is a further benefit of the mean wheelpath being further from the critical edge, which effectively reduces the number of critical load applications. If the mean wheelpath is measured from the paint stripe at the lane-shoulder edge to the outer edge of the wheel, the effective mean wheelpath for widened slab design is as follows:

$$x^* = LW - AW - x \tag{3.4.5}$$

where,

x^*	=	effective mean wheelpath, in.
LW	=	lane width, in. Typical lane width is 12 ft (144 in).
AW	=	axle width measured from the outer edge to outer edge of axle, in. Typical axle width is 8.5 ft (102 in).
x	=	mean wheelpath measured from the paint stripe to the outer edge of tire, in.

For example, if the mean wheelpath for widened slab design is 18 in (measured from the paint stripe to the outer edge of outermost tire closest to the paint stripe) and axle width is 8.5 ft (102 in), the effective mean wheelpath is 24 in.

- Base Poisson's ratio is equal to PCC Poisson's ratio.
- Base coefficient of thermal expansion is equal to PCC coefficient of thermal expansion.
- Temperature distribution through the base layer is constant.

Step 1: Tabulate input data

Tabulate all input required for JPCP cracking prediction. The required parameters are summarized in table 3.4.5. In addition to the inputs listed in this table, the processed inputs from Steps 2, 3, and 4 below are needed for the fatigue analysis of JPCP.

Step 2: Process traffic data.

The traffic inputs are first processed to determine the expected number of single, tandem, tridem, and quad axles in each month within the design period. This procedure is described in detail in PART 2, Chapter 4. For bottom-up damage, each passing of an axle may cause one or more occurrences of critical loading. Each passing of an axle is converted to an equivalent number of single, tandem, or tridem axles for bottom-up damage computation for different axle types as shown in figure 3.4.23:

- One actual single axle is effectively equal to one application of a single axle of the same load (figure 3.4.23a).
- One actual tandem axle is effectively equal to two applications of a tandem axle of the same load at the positions shown in figure 3.4.23b.
- One actual tridem axle is effectively equal to one tridem axle of the same load and two tandem axles with two-thirds the total load (figure 3.4.23c).

One actual quad axle is effectively equal to two tridem axles with three-fourths the total load and two tandem axles with half the total load (figure 3.4.23d).

For top-down cracking, the number of loadings by short, medium, and long wheel base trucks (or axle combinations) is determined by multiplying the total number of trucks by the percentages of short, medium, and long wheel base trucks. For both bottom-up and top-down cracking, the hourly traffic is calculated by multiplying the monthly load applications by the hourly truck traffic distribution factors.

Step 3: Process temperature profile data

The EICM produces temperatures at 11 evenly spaced points through the thickness of the PCC layer. For calculation expediency, each temperature profile is converted to equivalent linear temperature difference (top minus bottom), and the frequency distribution of the equivalent linear temperature difference is determined for each calendar month as follows:

1. Establish a table of temperature difference verses corresponding stress in 2 °F increments with the following loads placed at the pavement edge:
    - Bottom-up stress – 18,000-lb single axle. The axle should be placed halfway between the transverse joints to produce the maximum stress.
    - Top-down stress – a single-tandem axle combination with 12,000 lb on the single axle and 34,000 lb on the tandem. Use the medium wheelbase, and position the axles to produce maximum stress. A critical loading condition for top down stress is illustrated in figure 3.4.6.

Table 3.4.5. Summary of input parameters for JPCP cracking prediction.

Input	Variation*	Source
Design life (yr)	Fixed	Direct design input
Month of project opening	Fixed	Direct design input
PCC age at opening (mo)	Fixed	Direct design input
PCC strength for each month (psi)	Design mo[1]	Result of PCC strength input processing (section 3.4.3.6 *Pavement Structure Input*)
PCC modulus for each month (psi)	Design mo[1]	
Joint Spacing (ft)	Fixed	Direct design input
Dowel diameter (in)	Fixed	Direct design input
Loss of bond age (mo)	Fixed	Direct design input
Lane-shoulder deflection LTE (%)	Fixed	Direct design input
Widened slab (yes/no)	Fixed	Direct design input
Poisson's ratio	Fixed	Direct design input
PCC unit weight (pcf)	Fixed	Direct design input
Coefficient of thermal expansion (/°F)	Fixed	Direct design input
Ultimate reversible shrinkage strain (10^{-6})	Fixed	Direct design input or calculated value based on PCC mix properties
Time to 50% ult. Shrinkage (days)	Fixed	Direct design input
Base thickness (in)	Fixed	Direct design input
Base unit weight (pcf)	Fixed	Direct design input
Monthly base modulus (psi)	Calendar mo[2]	Result of Seasonal Analysis (section 3.4.3.6 *Pavement Structure Input*)
Monthly effective dynamic subgrade k-value (psi/in)	Calendar mo[2]	Results of "E-to-k" conversion (section 3.4.3.6 *Pavement Structure Input*)
Permanent curl/warp (°F)	Fixed	Direct design input
Edge-to-edge (outside) axle width (ft)	Fixed	Direct design input
Lane width (ft)	Fixed	Direct design input
Mean wheelpath (in)	Fixed	Direct design input
Traffic wander standard deviation (in)	Fixed	Direct design input
Slab width (ft)	Fixed	Direct design input
Tire pressure (psi)	Fixed	Direct design input
Axle spacing (in)	Fixed	Direct design input
Dual wheel spacing (in)	Fixed	Direct design input
Tire width (in)	Fixed	Direct design input
Wheelbase – short, medium, and long (ft)	Fixed	Direct design input
% trucks at each wheelbase (%)	Fixed	Direct design input

[1] Design mo: parameters that vary with pavement age; [2] Calendar mo: parameters that vary seasonally.

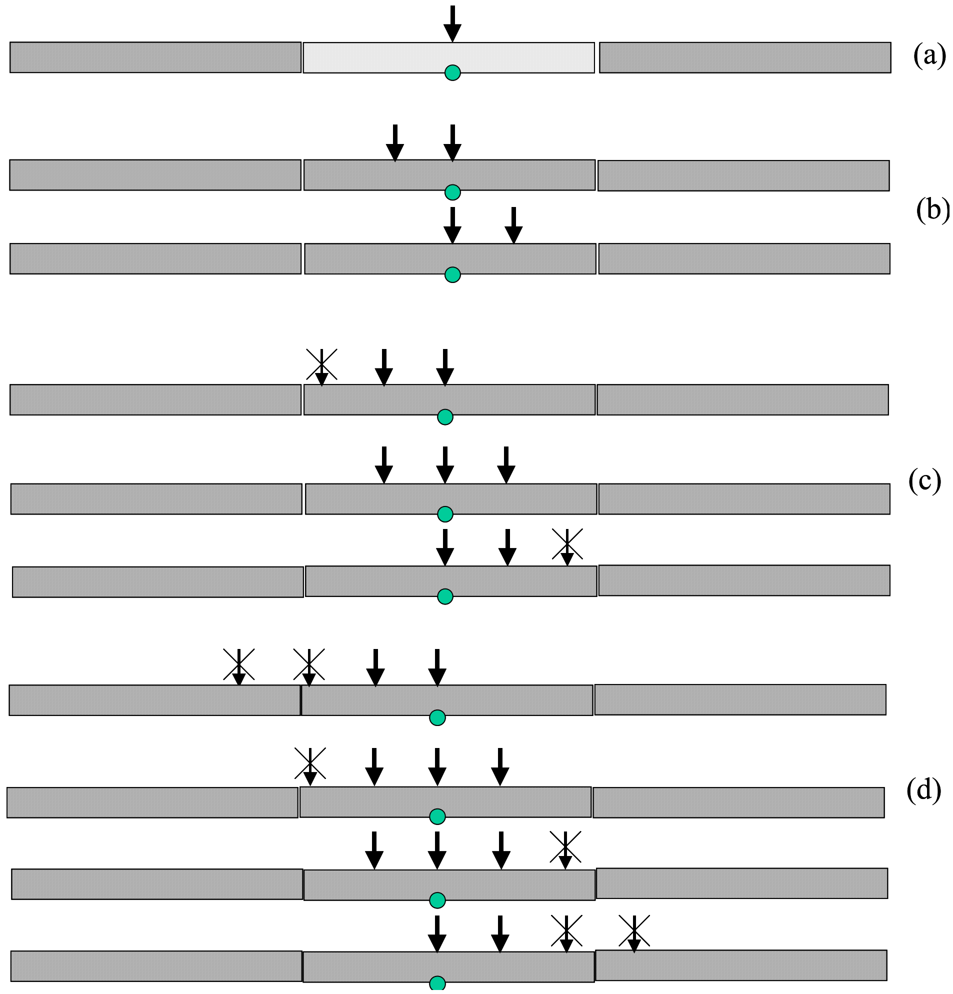

Figure 3.4.23. Accounting for different axle types in JPCP bottom-up cracking damage accumulation: (a) single, (b) tandem, (c) tridem, and (d) quad axles.

2. Determine the stress corresponding to the actual nonlinear temperature profile and the same wheel loads used in step 1 above (*23*). Prior to running stress analysis, the permanent curl/warp should be applied to each actual temperature profile so that the combined stress will be determined with the correct contact condition.
3. Look up the table created in step 1 to determine the equivalent linear temperature difference corresponding to each of the actual temperature case analyzed in step 2 based on stress equivalence.
4. Summarize the equivalent linear temperature difference by calendar month to obtain the frequency distribution of hourly temperature differences as follows:
   - Frequency distribution of positive temperature differences – all temperature profiles that produce a positive temperature difference (top warmer than bottom) is compiled together to determine the temperature frequency distribution for bottom-up cracking.
   - Frequency distribution of negative temperature differences – all temperature profiles that produce a negative temperature difference (top cooler than bottom) is compiled together to determine the temperature frequency distribution for top-down cracking.

The temperature-difference frequency distributions are determined for each month of the year to coordinate with the input variations that are considered on monthly basis (e.g., base stiffness, effective subgrade k-value, and moisture warping).

The equivalent linear temperature-difference frequency distributions are based on hourly temperature profiles; thus, the fatigue damage calculation, in effect, is performed on hourly basis. Additional details of the temperature linearization procedure are given in Appendix KK.

Step 4: Process monthly relative humidity data

Moisture warping is adjusted monthly based on atmospheric relative humidity. The effects of monthly variation in moisture warping are expressed in terms of equivalent temperature difference and are added to the equivalent linear temperature difference during stress calculations (41, 42).

$$ETG_{SHi} = \frac{3 \cdot (\varphi \cdot \varepsilon_{su}) \cdot (S_{hi} - S_{h\,ave}) \cdot h_s \cdot \left(\frac{h}{2} - \frac{h_s}{3}\right)}{\alpha \cdot h^2 \cdot 100} \qquad (3.4.6)$$

where,

ETG_{Shi}	=	temperature difference equivalent of the deviation of moisture warping in month *i* from the annual average, °F.
φ	=	reversible shrinkage factor, fraction of total shrinkage. Use 0.5 unless more accurate information is available.
ε_{su}	=	ultimate shrinkage (ε_{su} may be estimated based on PCC mix properties using the equation presented in PART 2, Chapter 2), x 10^{-6}:
S_{hi}	=	relative humidity factor for month *i*:

$$S_{hi} = 1.1 \cdot RH_a \quad \text{for } RH_a < 30\%$$
$$S_{hi} = 1.4 - 0.01 \cdot RH_a \quad \text{for } 30\% < RH_a < 80\% \qquad (3.4.6a)$$
$$S_{hi} = 3.0 - 0.03 \cdot RH_a \quad \text{for } RH_a \geq 80\%$$

RH_a	=	ambient average relative humidity, percent
Sh_{ave}	=	annual average relative humidity factor. Annual average of Shi.
h_s	=	depth of the shrinkage zone (typically 2 in).
h	=	PCC slab thickness, in.
α	=	PCC coefficient of thermal expansion, /°F.

The temperature-difference equivalent of the monthly deviations in moisture warping (ETG_{Shi}) given by equation 3.4.6 is based on ultimate shrinkage, which takes time to develop. The ETG_{Shi} at any time *t* days from placement is

$$ETG_{SHt} = S_t \cdot ETG_{SHi} \qquad (3.4.7)$$

where,

ETG_{Shi}	=	ETG_{Shi} at any time t days from PCC placement, °F.
ETG_{Shi}	=	temperature difference equivalent of the deviation of moisture warping in month *i* from the annual average, °F.

$$S_t = \frac{Age}{n + Age} \tag{3.4.8}$$

S_t	=	time factor for moisture-related slab warping.
Age	=	PCC age, days since placement.
n	=	time to develop 50% of ultimate shrinkage strain, days. Use 35 (the ACI Committee 209 recommended value), unless more accurate information is available (6).

Step 5: Calculate stress

Calculate stress for all cases that needs to be analyzed. The number of cases depends on the damage increment. For JPCP transverse cracking, the following increments are considered:

- Pavement age – by year.
- Season – by month.
- Load configuration – axle type for bottom-up cracking; wheelbase for top-down cracking.
- Load level – discrete load levels in 1,000 to 3,000 lb increments, depending on axle type.
- Temperature gradient – equivalent linear temperature difference from top to bottom in 2 °F increments.
- Lateral load position – 6 specific locations for both top-down and bottom-up cracking.

The damage increments and stress calculation were discussed earlier in this section.

Step 6: Calculate fatigue damage

As discussed earlier, all cases that produce significantly different stresses must be evaluated separately in the fatigue analysis (as a separate damage increment) to obtain accurate results. The general expression for fatigue damage accumulations considering all critical factors for JPCP transverse cracking is as follows:

$$FD = \sum \frac{n_{i,j,k,l,m,n}}{N_{i,j,k,l,m,n}} \tag{3.4.9}$$

where,

FD	=	total fatigue damage (top-down or bottom-up).
$n_{i,j,k,\ldots}$	=	applied number of load applications at condition *i, j, k, l, m, n*.
$N_{i,j,k,\ldots}$	=	allowable number of load applications at condition *i, j, k, l, m, n*.
i	=	age (accounts for change in PCC modulus of rupture, layer bond condition, deterioration of shoulder LTE).
j	=	month (accounts for change in base and effective dynamic modulus of subgrade reaction).
k	=	axle type (single, tandem, and tridem for bottom-up cracking; short, medium, and long wheelbase for top-down cracking).
l	=	load level (incremental load for each axle type).
m	=	temperature difference.

n = traffic path.

The damage increments were discussed previously in this section.

The applied number of load applications ($n_{i,j,k,l,m,n}$) is the actual number of axle type k of load level l that passed through traffic path n under each condition (age, season, and temperature difference). The allowable number of load applications is the number of load cycles at which fatigue failure is expected (corresponding to 50 percent slab cracking) and is a function of the applied stress and PCC strength. The allowable number of load applications is determined using the following fatigue model:

$$\log\left(N_{i,j,k,l,m,n}\right) = C_1 \cdot \left(\frac{MR_i}{\sigma_{i,j,k,l,m,n}}\right)^{C_2} + 0.4371 \qquad (3.4.10)$$

where,

- $N_{i,j,k,\ldots}$ = allowable number of load applications at condition i, j, k, l, m, n
- MR_i = PCC modulus of rupture at age i, psi
- $\sigma_{i,j,k,\ldots}$ = applied stress at condition i, j, k, l, m, n
- C_1 = calibration constant = 2.0
- C_2 = calibration constant = 1.22

The fatigue damage calculation is a simple process of summing damage from each damage increment, except that a numerical integration scheme is used to accurately determine the effects of traffic wander. The fatigue damage at the critical damage location caused by an axle load placed at any random distance away from the pavement edge (point j) is given by the following:

$$FD^*_{ij} = P\left(COV_j\right) \cdot FD_{ij} \qquad (3.4.11)$$

where,

- $FD^*_{ij.}$ = fatigue damage at location i (critical damage location) due to the fraction of total applied traffic passing through point j.
- $P(COV_j)$ = probability of traffic passing through point j.
- $FD_{ij.}$ = fatigue damage at location i (critical damage location) due to the traffic load passing through point j.

The probability of coverage is determined assuming normal distribution.

$$NORMDIST = \frac{1}{SD_{traf}\sqrt{2\pi}} e^{-\frac{1}{2}\left(\frac{x-\mu}{\sigma}\right)^2} \qquad (3.4.12)$$

where,

- $NORMDIST$ = normal distribution density function.
- x = wheel location – distance from pavement edge (or outside of the paint stripe for widened slab) to the outer edge of outermost wheel, in.

μ	=	mean wheel location, in.
SD_{traf}	=	traffic wander standard deviation, in.

The fatigue damage contribution due to traffic passes at different distances from the pavement edge is illustrated in figure 3.4.24. The total fatigue damage due to all traffic passes is obtained by summing damage caused by traffic passing through all traffic paths. This is simply the area under the curve shown in figure 3.4.24. The area under the curves can be calculated in thin strips (approximating the area for each strip as a trapezoid), but more accurate results can be obtained more efficiently using numerical integration methods. For both the JPCP cracking model and the CRCP punchout model, the Gauss integration method is used. Using the Gauss numerical integration scheme outlined below is equivalent to analyzing stresses using infinitesimally small load position increments. In this method, the value of the function evaluated at prescribed locations and the associated weighting factors are used to determine the area under polynomial functions as follows:

$$\int_a^b f(x)\,dx = A \cdot \sum_{i=0}^{n} f(x_i) \cdot w(x_i) \tag{3.4.13}$$

where,

$f(x)$	=	function being integrated.
A	=	scaling factor, width of traffic channel that produces significant fatigue damage (20 in for bottom-up cracking; 40 in for top-down cracking).
$f(x_i)$	=	function value at normalized location x_i (-1 to 1) (equation 3.4.9).
$w(x_i)$	=	weighting factor for the function value at normalized location x_i (-1 to 1).

The Gauss integration method integrates polynomials of order 2n-1 exactly, where n is the number of evaluation points used. For both the JPCP cracking model and the CRCP punchout model, the integration is performed in two pieces, because the relative fatigue damage contribution curves (e.g., figure 3.4.24) can have a very high gradient near the pavement edge but are typically very flat at distances away from the edge. A single polynomial function does a poor job of fitting curves that contains both a region of very high gradient and a flat portion. Therefore, 4-point Gauss integration is used for outer strip, and 2-point Gauss integration is used for the interior portion. The specified evaluation points and weighting factors for 2- and 4-point Gauss integration are as follows:

- 2-point Gauss integration:
  - Evaluation point: $\pm\frac{1}{\sqrt{3}}$ Weighting factor: 1
- 4-point Gauss integration:
  - Evaluation point: $\pm\sqrt{\frac{3+2r}{7}}$ Weighting factor: $\frac{1}{2}-\frac{1}{6r}$
  - Evaluation point: $\pm\sqrt{\frac{3-2r}{7}}$ Weighting factor: $\frac{1}{2}+\frac{1}{6r}$
  - $r=\sqrt{1.2}$

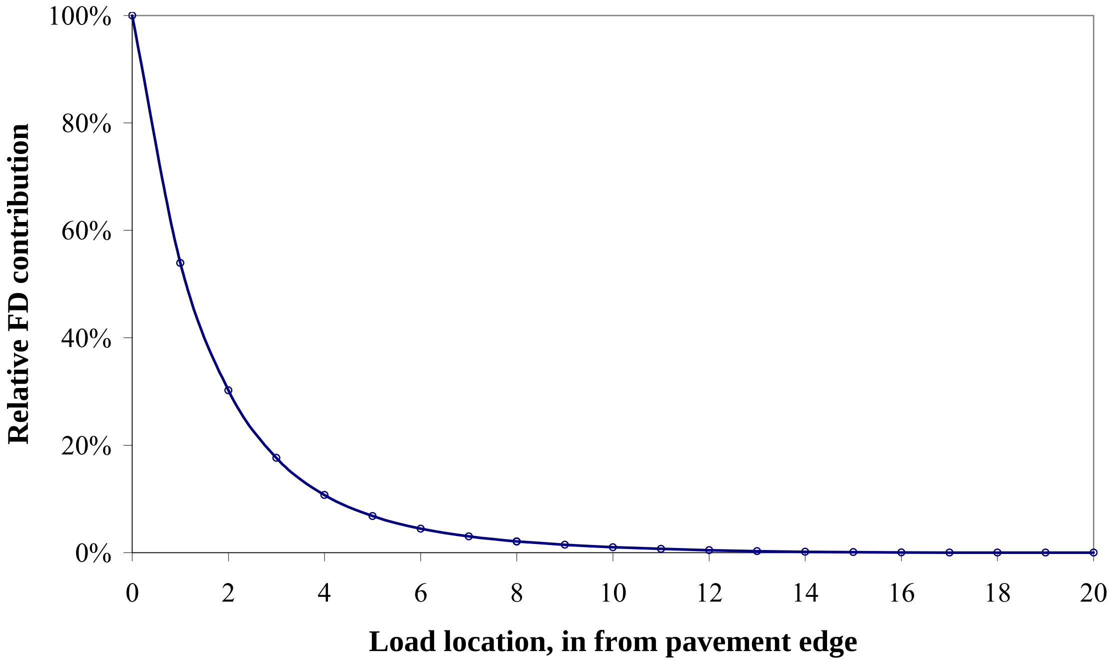

Figure 3.4.24. Illustration of fatigue damage contribution by traffic passes at various distances from the pavement edge.

For bottom-up cracking in JPCP, the following integration scheme was used:

- Total width of traffic path considered: 20 in.
- Outer 8-in strip: 4-point Gauss integration.
  - Gauss points: 0.5555, 2.640, 5.360, and 7.445 in from slab edge.
  - Weighting factors: 0.34785, 0.65215, 0.65215, and 0.34785, listed in the order of the Gauss points listed above.
- Remaining interior 12-in strip: 2-point Gauss integration.
  - Gauss points: 10.54, and 17.46 in from slab edge.
  - Weighting factors: 1.0 and 1.0.

For top-down cracking in JPCP, the following integration scheme was used:

- Total width of traffic path considered: 40 in.
- Outer 8-in strip: 4-point Gauss integration.
  - Gauss points: 1.666, 7.920, 16.080, and 22.334 in from slab edge.
  - Weighting factors: 0.34785, 0.65215, 0.65215, and 0.34785, instead in the order of the Gauss points listed above.
- Remaining interior 12-in strip: 2-point Gauss integration.
  - Gauss points: 27.381, and 36.619 in from slab edge.
  - Weighting factors: 1.0 and 1.0.

The stresses calculated for the six Gauss points under each pavement age, month, axle type, axle load, and temperature difference are used to calculate damage considering traffic wander under each combination of conditions. The process is repeated for the entire factorial of these parameters (pavement age, month, axle type, axle load, and temperature difference) and the calculated damage for each condition summed to determine the total damage. The same procedure is used for bottom-up and top-down damage calculation.

Cracking Reliability

The reliability design is obtained by determining the predicted cracking at the desired level of reliability as follows:

$$CRACK\_P = CRACK + STD_{CR} \bullet Z_P \qquad (3.4.14)$$

$$CRACK\_P \leq 100\ \%$$

where,

$CRACK\_P$ = predicted cracking at the reliability level P, percent of slabs.
$CRACK$ = predicted cracking based on mean inputs (corresponding to 50% reliability), percent of slabs.
STD_{CR} = standard deviation of cracking at the predicted level of mean cracking:

$$STD_{CR} = -0.00172\ \mathrm{CRACK}^2 + 0.3447\ \mathrm{CRACK} + 4.6772 \qquad (3.4.15)$$

Z_P = standard normal deviate (one-tailed distribution).

For example, if the predicted cracking based on mean inputs is 10 percent, the predicted cracking for 90 percent reliability design is obtained as follows:

$$STD_{CR} = -0.00172 \bullet 10^2 + 0.3447 \bullet 10 + 4.6772 = 8.0\ \%$$

$$Z_P = 1.28$$

$$CRACK\_P = 10 + 8.0 \bullet 1.28 = 20.2\ \%$$

Thus, if the design criteria are less than 10 percent slab cracking at 90 percent reliability, the structural capacity must be increased until *CRACK_P* is less than 10 percent. Equation 3.4.15 may be modified based on local calibration.

Figure 3.4.21 showed an example of predicted cracking over the design life based on mean input (50% reliability) and that for 95 percent reliability design. Figure 3.4.25 shows the required slab thickness at different levels of reliability of an example design. The reliability level corresponding to different slab thicknesses can also be obtained from this figure.

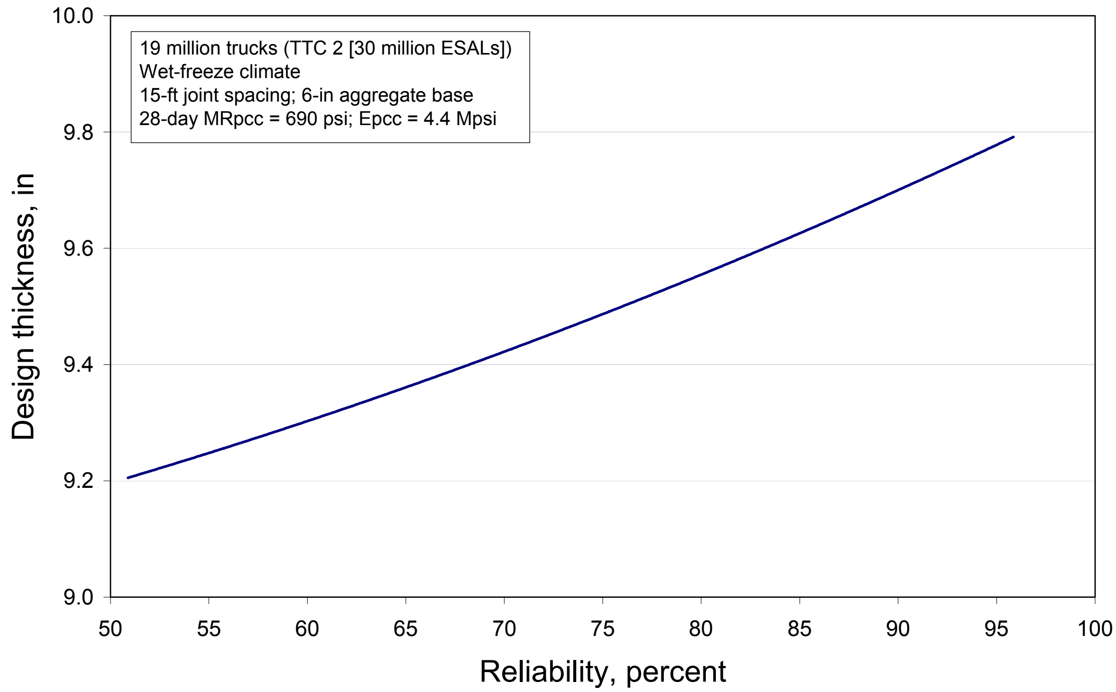

Figure 3.4.25. Required slab thickness at different reliability level for an example design.

Modification of JPCP Design to Reduce Transverse Cracking

If the predicted cracking is greater than the design requirements, the trial design must be modified to increase structural capacity. The same factors that affect bottom-up transverse cracking affect top-down cracking. However, different design parameters have a different impact on different performance measures. For example, slab thickness and PCC strength are both very dominant factors affecting JPCP cracking, but they have less profound effect on faulting and smoothness. On the other hand, widened slab has a very significant effect on both slab cracking and faulting (and consequently smoothness). Therefore, if all performance must be improved, the use of widened slab may be considered; whereas, if slab cracking is the only design deficiency, slab thickness or PCC strength may be increased to satisfy the design requirements.

The fatigue-related transverse cracking in JPCP is most effectively controlled by the following means:

- Increase slab thickness.
- Reduce joint spacing.
- Provide tied PCC shoulder.
- Use widened slab.
- Use a higher strength PCC mix (note, the PCC α_{PCC}, shrinkage, and elastic modulus may all vary).
- Use a stabilized base.

The slab thickness and joint spacing are very sensitive factors affecting cracking of JPCP. The sensitivity of JPCP cracking to slab thickness and joint spacing is shown in figure 3.4.15. The sensitivity of JPCP cracking to edge support features (widened slab and tied PCC shoulder) is shown in figure 3.4.26. The structural capacity provided by a tied PCC shoulder is equivalent to about 1 in of slab thickness. The increase in structural capacity due to widened slab is equivalent to about 1.5 in of slab thickness.

The effects of PCC modulus of rupture are shown in figure 3.4.27. In this figure, the ratio of PCC elastic modulus to that of modulus of rupture is assumed to remain constant (i.e., the PCC modulus changes proportionally with PCC strength). However, α_{PCC} and shrinkage were held constant (varying them would change the results presented). Figure 3.4.28 shows the effects of base type. The base type has a more pronounced effect on faulting.

The iterative process of determining the required slab thickness is illustrated in figure 3.4.29. The results obtained for different trial slab thicknesses can be plotted to determine the required slab thickness. In practice, the slab thickness would be rounded up to the next practical unit (the nearest 0.5 in).

3.4.5.4 Performance Prediction—Faulting

Transverse joint faulting is the differential elevation across the joint measured approximately 1 ft from the slab edge (longitudinal joint for a conventional lane width), or from the rightmost lane paint stripe for a widened slab.

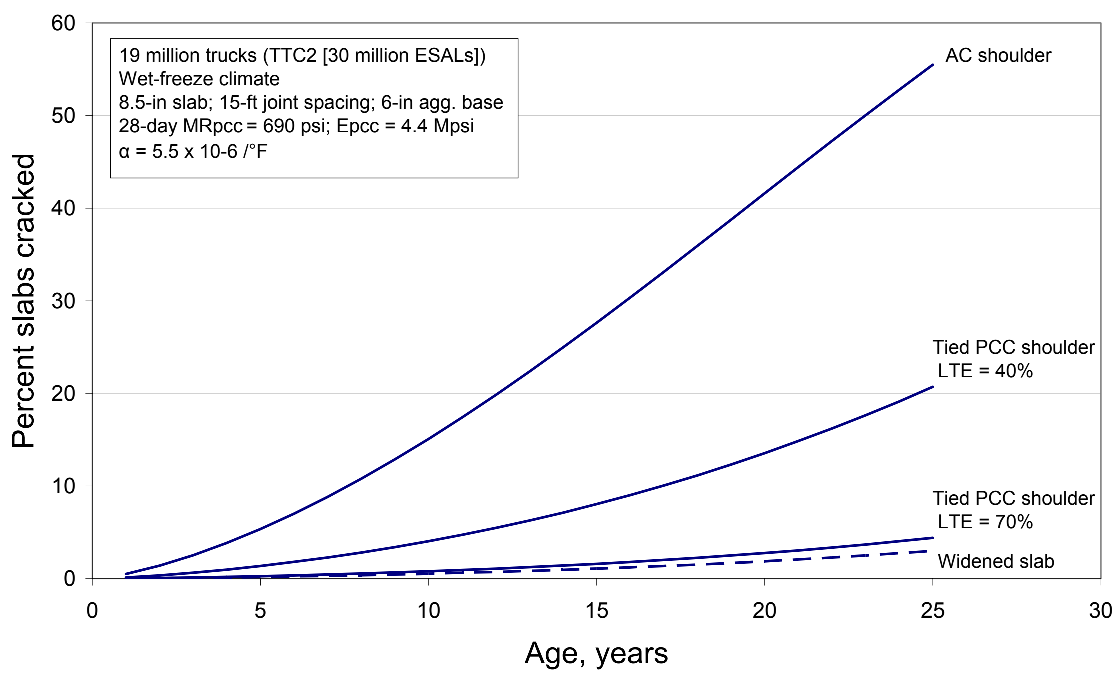

Figure 3.4.26. Effects of edge support features on JPCP transverse cracking.

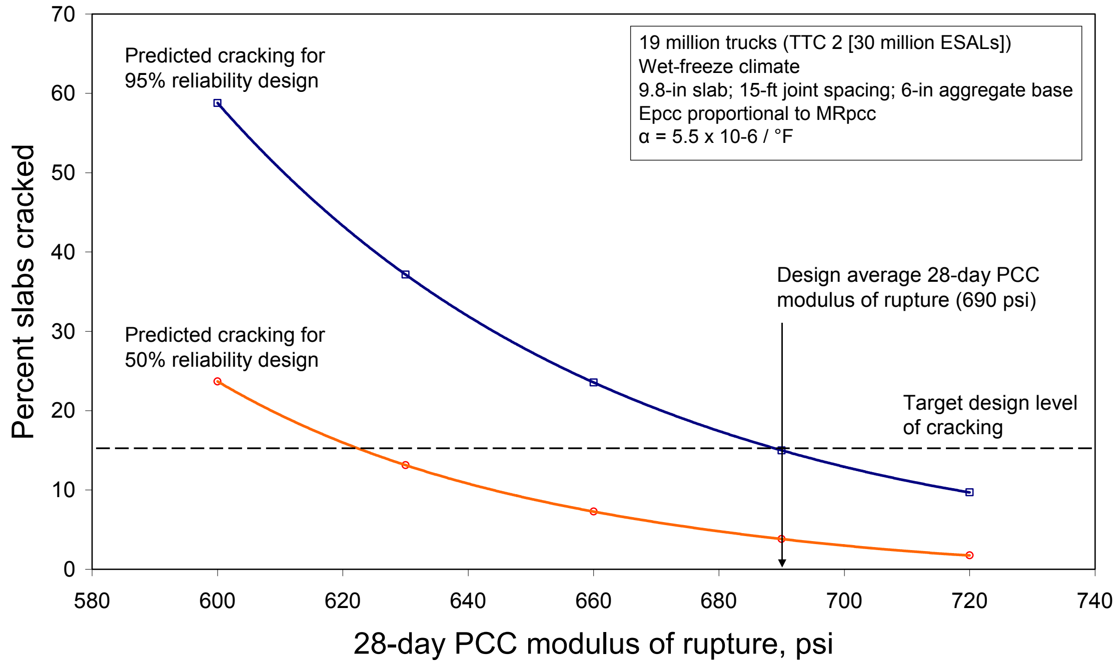

Figure 3.4.27. Sensitivity of JPCP transverse cracking to PCC strength, holding the ratio of PCC elastic modulus to PCC strength constant (note, the α_{PCC} and shrinkage may vary with strength if cement content was increased).

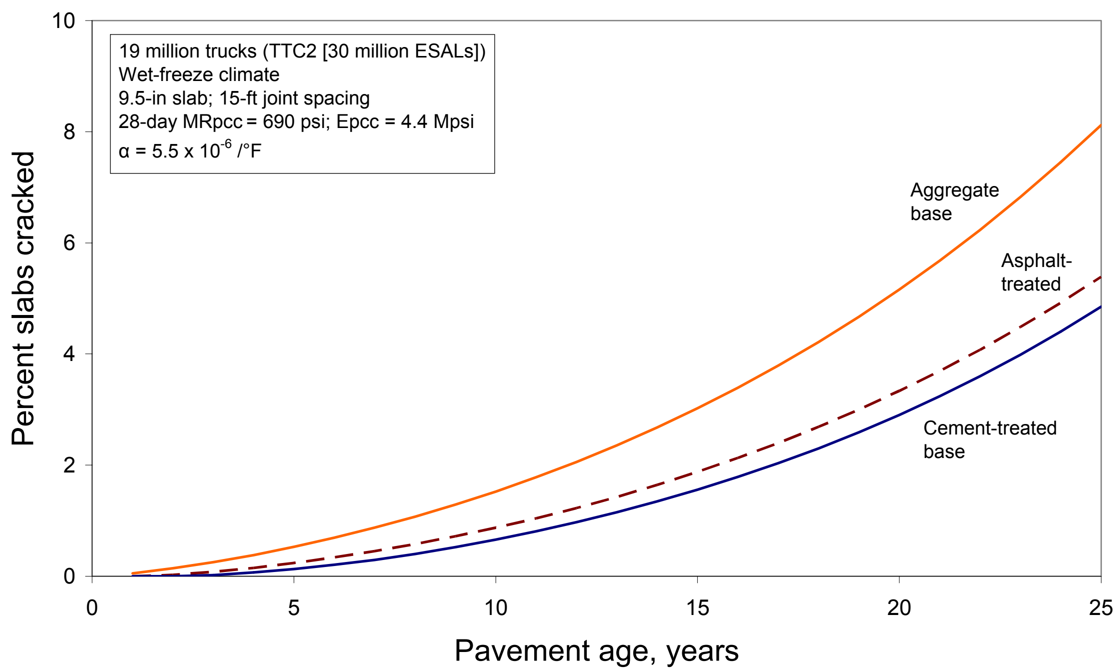

Figure 3.4.28. Effects of base type on JPCP transverse cracking.

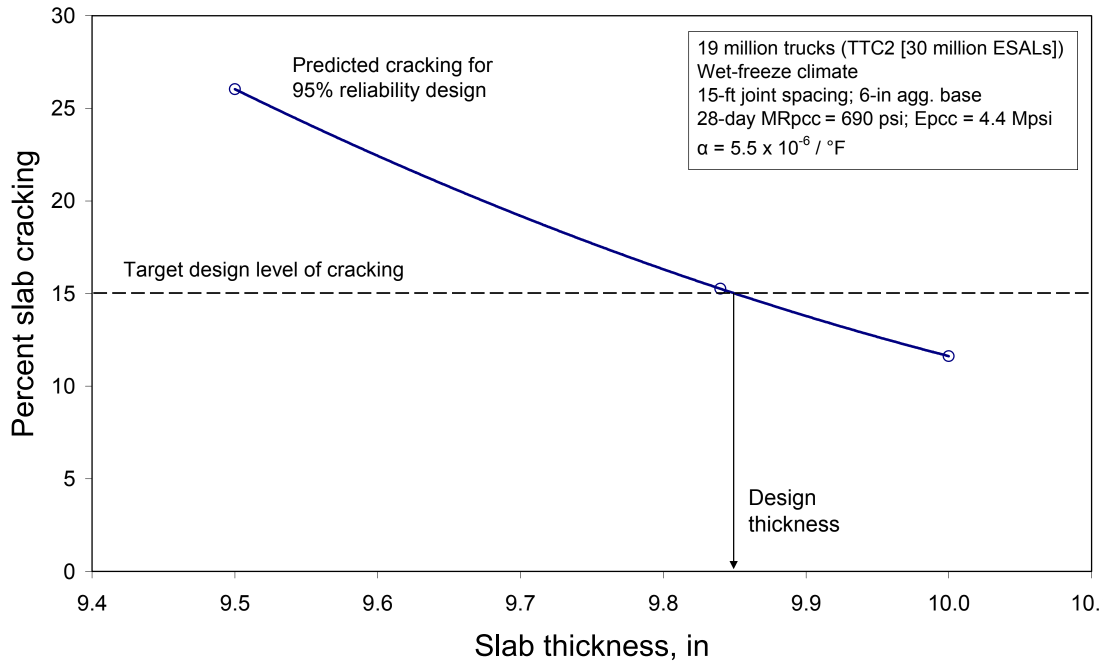

Figure 3.4.29. Iterative process of determining the required slab thickness.

Since joint faulting varies significantly from joint to joint, the mean faulting of all transverse joints in a pavement section is the parameter predicted by the model. Faulting is an important deterioration mechanism of JPCP because of its impact on ride quality. Joint faulting also has a major impact on the life cycle costs of a pavement in terms of increased costs due to early rehabilitation and on vehicle operating costs as faulting becomes severe.

Transverse joint faulting is the result of a combination of:

- Repeated applications of moving heavy axle loads.
- Poor load transfer across the joint.
- Free moisture beneath the PCC slab.
- Erosion of the supporting base/subbase, subgrade, or shoulder base material.
- Upward curling of the slab.

Erosion of underlying materials occurs when excess moisture is ejected from beneath the leave slab (i.e., the slab that the wheel loads are on after it crosses a given transverse joint) corner as a wheel load moves over the slab corner. The moisture that is ejected carries base, shoulder, and/or subgrade fines with it, typically resulting in a void beneath the leave slab corner. Most importantly, there also occurs an increasing deposition of this material back under the approach slab (i.e., the slab that the wheel loads are on just prior to crossing a given transverse joint) lifting up this slab. Due to the increasing build-up of material beneath the approach slab corner and the loss of support under the leave slab corner, faulting and corner cracking can develop (*2, 4, 5, 13, 15, 16*). The following factors have been shown to affect transverse joint faulting:

- Presence of dowels and dowel diameter.
- PCC slab thickness.
- Joint spacing.
- Use of stabilized base layers and the strength and durability of the materials.
- Subgrade type.
- Placement of vehicle loads near unsupported pavement edges.
- Poor slab edge support (e.g., lack of widened paving lanes, tied PCC shoulders, or edge beams).
- Precipitation.
- Subsurface drainage, including an open-graded base course.
- Freezing index/number of freeze-thaw cycles.
- Slab curling and warping, including permanent curling and warping.
- Large size and type of aggregates in the PCC (not accounted for in this procedure but should be controlled by specifications).
- Joint opening (zero-stress PCC temperature minus actual slab temperature plus PCC shrinkage)

<u>Faulting Model</u>

The mean transverse joint faulting is predicted using an incremental approach. A faulting increment is determined each month and the current faulting level affects the magnitude of increment. The faulting at each month is determined as a sum of faulting increments from all previous months in the pavement life since the traffic opening using the following model:

$$Fault_m = \sum_{i=1}^{m} \Delta Fault_i \tag{3.4.16}$$

$$\Delta Fault_i = C_{34} * (FAULTMAX_{i-1} - Fault_{i-1})^2 * DE_i \tag{3.4.17}$$

$$FAULTMAX_i = FAULTMAX_0 + C_7 * \sum_{j=1}^{m} DE_j * Log(1 + C_5 * 5.0^{EROD})^{C_6} \tag{3.4.18}$$

$$FAULTMAX_0 = C_{12} * \delta_{\text{curling}} * \left[Log(1 + C_5 * 5.0^{EROD}) * Log\left(\frac{P_{200} * WetDays}{p_s}\right) \right]^{C_6} \tag{3.4.19}$$

where,

$Fault_m$	=	mean joint faulting at the end of month m, in.
$\Delta Fault_i$	=	incremental change (monthly) in mean transverse joint faulting during month *i*, in.
$FAULTMAX_i$	=	maximum mean transverse joint faulting for month *i*, in.
$FAULTMAX_0$	=	initial maximum mean transverse joint faulting, in.
$EROD$	=	base/subbase erodibility factor.
DE_i	=	differential deformation energy accumulated during month *i*.
$EROD$	=	base/subbase erodibility factor (see PART 2, Chapter 2).
$\delta_{curling}$	=	maximum mean monthly slab corner upward deflection PCC due to temperature curling and moisture warping.
P_S	=	overburden on subgrade, lb.

P_{200} = percent subgrade material passing #200 sieve.
$WetDays$ = average annual number of wet days (greater than 0.1 in rainfall).

C_1 through C_8 and C_{12}, C_{34} are national calibration constants:

$$C_{12} = C_1 + C_2 * FR^{0.25} \quad (3.4.20)$$
$$C_{34} = C_3 + C_4 * FR^{0.25} \quad (3.4.21)$$

C_1 =	1.29	C_5 =	250
C_2 =	1.1	C_6 =	0.4
C_3 =	0.001725	C_7 =	1.2
C_4 =	0.0008		

FR = base freezing index defined as percentage of time the top base temperature is below freezing (32 °F) temperature.

Model Statistics:
R^2 = 0.71
SEE = 0.029 inches
N = 564 observations

The JPCP transverse joint faulting model given in equation 3.4.16 is a result of calibration based on performance of 248 field sections located in 22 States and is applicable for both doweled and undoweled JPCP. The calibration sections consist of 138 LTPP GPS-3 and SPS-2 sections and 110 sections from the FHWA study, *Performance of Concrete Pavements* (*2*). More than one-third of the sections (86 sections) were non-doweled. The dowel diameter in the remaining sections varies from 1 in to 1.5 in.

Structural Response Modeling for Faulting

Critical truck axle loading includes a single, tandem, tridem, or quad axle located close to the approach slab corner, as shown in figure 3.4.7. The closer the load is to the longitudinal lane-shoulder joint, the greater the slab corner deflection. The approach corner deflects depending on the slab joint design (load transfer of transverse and longitudinal joint), base course stiffness, and subgrade stiffness. Faulting progresses non-linearly over time. The differential corner deflection (difference between the loaded and non-loaded side of the joint) is a critical factor that affects faulting. The differential corner deflection as a function of a joint LTE and corner deflection. LTE across the transverse joint is modeled and varies with time (seasonal variation and long-term deterioration). The LTE at the mainline shoulder joint is assumed constant with time. The following factors affecting the magnitude of deflections at the corners of the PCC slab are directly considered by the Design Guide procedure:

- PCC thickness.
- PCC modulus of elasticity.
- PCC Poisson's ratio.

- PCC unit weight.
- PCC coefficient of thermal expansion.
- PCC ultimate shrinkage
- Base thickness.
- Base modulus of elasticity.
- Interface condition between the PCC slab and base (assumed to be unbonded).
- Joint spacing.
- Subgrade stiffness (dynamic modulus of subgrade reaction).
- LTE with shoulder.
- LTE at the transverse joints.
- Difference in top and bottom PCC slab surface temperature (mean monthly nighttime values plus PCC permanent curl/warp plus warping due to seasonal variation in PCC surface shrinkage).
- Variation in PCC relative humidity (seasonal and through PCC slab thickness).
- Axle type (single, tandem, or tridem).
- Axle weight.
- Axle position (distance from the critical slab edge) – set equal to wheel path minus 0.6 standard deviation of traffic wander in from lane paint stripe but not greater than 24 in.

Note 1. Since an unbonded interface is assumed between the PCC slab and the base, base unit weight is set equal to 0. This reflects that no normal tension exists between the PCC slab and the base at the unbonded interface and, therefore, the base cannot load the PCC slab.
Note 2. The coefficient of thermal expansion of the base layer is assumed equal to the PCC coefficient of thermal expansion.
Note 3. Deflection LTE of the longitudinal lane-lane joint is assumed equal to 70 percent.

While many of the parameters above remain constant throughout the design period (e.g., slab thickness and joint spacing), others vary seasonally, monthly, hourly, or with pavement age. For accurate faulting analysis results, all cases that produce significantly different deflections must be evaluated separately. The faulting damage increment defined in this Guide was determined equal to one month to account for those cases as follows:

- Pavement age – accounts for the changes in PCC modulus with age and the changes in interface bond condition between a stabilized base and PCC slab.
- Month – accounts for monthly variations in base stiffness, foundation stiffness (including the effects of moisture and temperature on the subbase layers incorporated in the effective k-value), and the effects of monthly variation in relative humidity on slab warping due to differential shrinkage.
- Load level
  - Single axles – 3,000 to 41,000 lb in 1,000-lb increments.
  - Tandem axles – 6,000 to 82,000 lb in 2,000-lb increments.
  - Tridem axles – 12,000 to 102,000 lb in 3,000-lb increments.
  - Quad axles – 12,000 to 102,000 lb in 3,000-lb increments.
- Temperature – the effects of mean monthly nighttime temperature gradient, permanent curl/warp, and monthly variation in warping expressed as the effective temperature difference (top minus bottom).

The structural model used to determine deflection must be capable of accurately predicting deflection considering the following:

- Temperature and wheel loads – the model must be capable of handling the effects of PCC slab curling and multiple wheel loading
- Separation from the PCC slab from underlying layers.
- The effects of base course – the model must be able to consider the effect of an unbonded case.
- Multiple slabs and load transfer across both transverse and longitudinal joints.

In general, a finite element analysis program is required. The deflection calculations in the Design Guide software is accomplished using neural networks developed based on a large number of finite element analysis runs made using ISLAB2000. The neural networks were developed using the results of thousands of ISLAB2000 runs. These neural networks directly incorporate all factors listed above and closely match ISLAB2000 deflections for a wide range of input parameters, as shown in table 3.4.6.

Table 3.4.6. Ranges of input parameters for the neural networks computing corner deflections for JPCP faulting analysis.

Input Parameter	**Minimum Value**	**Maximum Value**
Radius of relative stiffness [a]	22.5 in	80 in
Joint spacing	12 ft	30 ft [b]
Transverse joint LTE	0%	95%
Shoulder LTE	0%	90%
Axle offset from the slab edge	0 in	36 in
Temperature difference (top – bottom)	0 °F	> 55 °F [c]
Axle weight, single axle	0 lb	45,000 lb
Axle weight, tandem axle	0 lb	90,000 lb
Axle weight, tridem axle	0 lb	135,000 lb
Axle weight, quad axle	0 lb	135,000 lb
Tandem and tridem axle spacing	40 in	70 in

[a] The radius of relative stiffness of highway pavements typically fall between 22.5 and 80 in. Analyses based on plate theory become increasingly inaccurate for the radius of relative stiffness values beyond the limit shown above.

[b] The results for 30-ft slab are given for the actual joint spacing greater than 30 ft. In general, long joint spacing (20 ft or greater) is not recommended because of excessive curling deflection.

[c] Depends on PCC coefficient of thermal expansion, k-value, PCC unit weight, PCC thickness, and radius of relative stiffness.

Faulting Prediction Procedure

Presented in this section is the step-by-step procedure for predicting JPCP transverse joint faulting. The steps involved include the following:

1. Tabulate input data – summarize all inputs needed for predicting JPCP transverse joint faulting.
2. Process traffic data – the processed traffic data needs to be further processed to determine equivalent number of single, tandem, and tridem axles produced by each passing of tandem, tridem, and quad axles.
3. Process pavement temperature profile data – the hourly pavement temperature profiles generated using EICM (nonlinear distribution) need to be converted to effective nighttime differences by calendar month.
4. Process monthly relative humidity data – the effects of seasonal changes in moisture conditions on differential shrinkage is considered in terms of monthly deviations in slab warping, expressed in terms equivalent temperature differential.
5. Calculate initial maximum faulting.
6. Evaluate joint LTE.
7. Calculate current maximum faulting.
8. Determine critical pavement responses for the increment.
9. Evaluate loss of shear capacity and dowel damage.
10. Calculate faulting increment.
11. Calculate cumulative faulting.

Assumptions

The following were assumed in the fatigue analysis:

- Incremental damage accumulation – the faulting increment depend of damage accumulated during the design increment and the current level of faulting.
- The pavement structure is modeled as a two-layered system consisting of slab and base with unbonded interface. The effects of subbase layers, as well as the shear contribution of the base layer, are accounted for through the use of effective dynamic modulus of subgrade reaction.
- Lateral traffic wander is modeled as normal distribution using mean wheelpath and standard deviation. The effective load wheelpath is determined suing the following equation:

$$x^* = x - 2/3 * SD_{traf} + LW - SW \qquad (3.4.22)$$

where,

x^*	=	effective mean wheelpath, in.
LW	=	lane width, in. Typical lane width is 12 ft (144 in).
SW	=	slab width, in.
x	=	mean wheelpath measured from the paint stripe to the outer edge of tire, in.
SD_{traf}	=	standard deviation of the traffic wander, in.

If the calculated effective wheelpath from equation 3.4.22 is greater than 24 in then the effective wheelpath equal to 24 in is used in the analysis.

- Base Poisson's ratio is equal to PCC Poisson's ratio.
- Base coefficient of thermal expansion is equal to PCC coefficient of thermal expansion.
- Temperature distribution through the base layer is constant.
- Effective nighttime lane-shoulder deflection load transfer efficiency is related to user's input for daytime condition as follows:

$$LTE^*_{sh} = 5 + LTE^*_{sh}/2 \tag{3.4.23}$$

where,

LTE^*_{sh} = effective nigh time lane-shoulder deflection load transfer efficiency, percent
LTE^*_{sh} = daytime lane-shoulder deflection load transfer efficiency, percent

Step 1: Tabulate input data

Tabulate all input required for JPCP transverse joint faulting prediction. The required parameters are summarized in table 3.4.7. In addition to the inputs listed in this table, the processed inputs from steps 2, 3, and 4 below are needed for the JPCP fatigue analysis.

Step 2: Process traffic data.

The traffic inputs are first processed to determine the expected number of single, tandem, tridem, and quad axles in each month within the design period. This procedure is described in detail in PART 2, Chapter 4. For faulting analysis, each passing of an axle may cause only one occurrence of critical loading:

- One actual single axle is effectively equal to one application of a single axle of the same load (figure 3.4.30a).
- One actual tandem axle is effectively equal to one application of a tandem axle of the same load (figure 3.4.30b).
- One actual tridem axle is effectively equal to one application of a tridem axle of the same load (figure 3.4.30c).
- One actual quad axle is effectively equal to one tridem axle with equal weight (figure 3.4.30d).

Since the maximum faulting development occurs during nighttime when the slab is curled upward and joints are opened, only axle load repetitions applied from 8 p.m. to 8 a.m. are accounted in the faulting analysis.

Step 3: Process monthly relative humidity data

Moisture warping is adjusted monthly based on atmospheric relative humidity. The effects of monthly variation in moisture warping are expressed in terms of equivalent temperature difference defined by equation 3.4.6, which is adjusted for PCC age using equation 3.4.8.

Table 3.4.7. Summary of input parameters for JPCP transverse joint faulting prediction.

Input	Variation*	Source
Design life (months)	Fixed	Direct design input
Month of project opening	Fixed	Direct design input
PCC age at opening (mo)	Fixed	Direct design input
PCC strength for each month (psi)	Design mo	Result of PCC strength input processing (section 3.4.3.6 *Pavement Structure Input*)
PCC modulus for each month (psi)	Design mo	
Joint Spacing (ft)	Fixed	Direct design input
Dowel diameter (in)	Fixed	Direct design input
Lane-shoulder deflection LTE (%)	Fixed	Direct design input
Widened slab (yes/no)	Fixed	Direct design input
Poisson's ratio	Fixed	Direct design input
PCC unit weight (pcf)	Fixed	Direct design input
Coefficient of thermal expansion (/°F)	Fixed	Direct design input
Ultimate shrinkage strain (10^{-6})	Fixed	Direct design input
Reversible shrinkage strain (10^{-6})	Fixed	Direct design input
Time to 50% ult. Shrinkage (days)	Fixed	Direct design input
Base thickness (in)	Fixed	Direct design input
Base unit weight (pcf)	Fixed	Direct design input
Monthly base modulus (psi)	Calendar mo	Result of Seasonal Analysis (section 3.4.3.6 *Pavement Structure Input*)
Base erodibility	Fixed	Direct design input
Monthly effective subgrade k-value (psi/in)	Calendar mo	Results of "E-to-k" conversion (section 3.4.3.6 *Pavement Structure Input*)
Permanent curl/warp (°F)	Fixed	Direct design input
PCC zero-stress temperature	Fixed	Direct design input or estimated from construction month and cement content
Lane width (ft)	Fixed	Direct design input
Mean wheelpath (in)	Fixed	Direct design input
Traffic wander standard deviation (in)	Fixed	Direct design input
Slab width (ft)	Fixed	Direct design input

* Design mo: parameters that vary with pavement age; Calendar mo: parameters that vary seasonally.

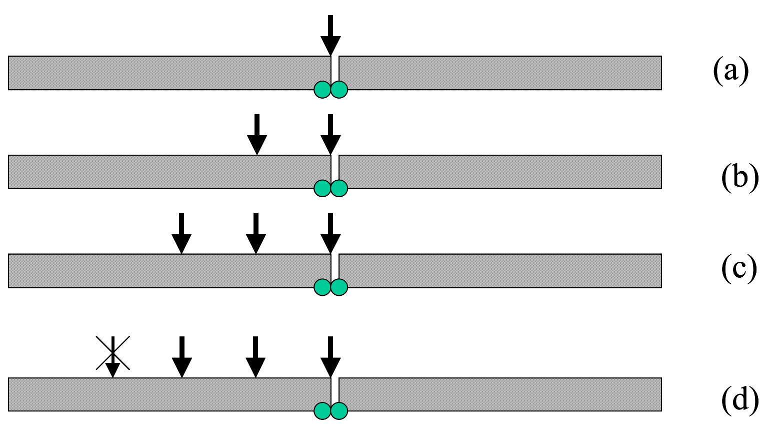

Figure 3.4.30. Accounting for different axle types in JPCP joint faulting damage accumulation: (a) single, (b) tandem, (c) tridem, and (d) quad axles.

The temperature-difference equivalent of the effects of variation in moisture warping at any PCC age is obtained using equation 3.4.7. Minimum monthly relative humidity and seasonal variation of relative humidity also affect joint opening (see step 6).

Step 4: Process temperature profile data

The EICM produces temperatures at 11 evenly spaced points through the thickness of the PCC layer for every hour using the available climatic data. For faulting analysis, the equivalent linear temperature difference for nighttime is determined for each calendar month as mean difference between top and bottom PCC surfaces occurred from 8 p.m. to 8 a.m. For each month of the year, the equivalent temperature gradient for the month is then determined as follows:

$$\Delta T_m = \Delta T_{t,m} - \Delta T_{b,m} + \Delta T_{sh,m} + \Delta T_{PCW} \tag{3.4.24}$$

where,

- ΔT_m = effective temperature differential for month m.
- $\Delta T_{t,m}$ = mean PCC top-surface nighttime temperature (from 8 p.m. to 8 a.m.) for month m.
- $\Delta T_{b,m}$ = mean PCC bottom-surface nighttime temperature (from 8 p.m. to 8 a.m.) for month m.
- $\Delta T_{sh,m}$ = equivalent temperature differential due to reversible shrinkage for month m for old concrete (i.e. shrinkage is fully developed).
- ΔT_{PCWt} = equivalent temperature differential due permanent curl/warp.

PCC temperature data are also used to find base freezing index parameter and LTE adjustment parameter. The base freezing index, FR, is defined as percentage of time during the year (both daytime and nighttime) for which PCC bottom temperature is below freezing (32^oF). This parameter is used in equations 3.4.20 and 3.4.21.

The LTE adjustment factor is determined for each calendar month. If the mean nighttime PCC temperature at the mid-depth is below freezing (32 °F) then joint LTE for that month is increased. That is done by assigning base LTE for that month equal to 90 percent.

Step 5: Determine maximum faulting

Using the effective temperature differential for each calendar month determined in step 4 and corresponding effective k-value and base modulus for the month, the corner deflections due to slab curling and shrinkage warping is determined for each month. The corner deflections can be determined using either a finite element analysis program or neural networks (the latter is implemented in the Design Guide software). The initial maximum faulting is determined using the calculated corner deflections and equation 3.4.19.

Step 6: Evaluate initial joint LTE.

To evaluate initial joint LTE, the LTE from aggregate interlock, dowels (if present), and base/subgrade are determined.

Aggregate interlock LTE. LTE depends on joint opening, which is determined for each increment (month) using the following equation:

$$jw = Max\left(12000 * L * \beta * (\alpha_{PCC} * (T_{constr} - T_{mean}) + \varepsilon_{sh,m}),\ 0\right) \qquad (3.4.25)$$

where,

jw	=	joint opening, mils (0.001 in).
L	=	joint spacing, ft.
β	=	friction coefficient between the base and the PCC; assumed equal 0. 0.65 for a stabilized base and 0.85 for a granular base.
α_{PCC}	=	PCC coefficient of thermal expansion, in/in/°F
T_{mean}	=	mean monthly nighttime mid depth temperature, °F
T_{constr}	=	PCC temperature at set, °F
$\varepsilon_{sh,m}$	=	PCC slab mean shrinkage strain

PCC shrinkage strain depends on PCC material properties, PCC relative humidity, and PCC age (see section 3.2.6). PCC moisture varies with PCC depth. Then mean shrinkage strain, $\varepsilon_{sh,m}$, is defined as follows:

$$\varepsilon_{sh,m} = \varepsilon_{sh,b} + \left(\varepsilon_{sh,t} - \varepsilon_{sh,b}\right) \cdot \frac{h_d}{h_{PCC}} \qquad (3.4.26)$$

where

$\varepsilon_{sh,m}$	=	mean shrinkage strain.
$\varepsilon_{sh,b}$	=	shrinkage strain at the bottom surface of the PCC slab.
$\varepsilon_{sh,t}$	=	shrinkage strain at the top surface of the PCC slab.
h_d	=	depth of a drier portion of the PCC slab set equal to 2 in.
h_{PCC}	=	PCC slab thickness, in.

Shrinkage strain at the top of the PCC slab is determined as follows:

$$\varepsilon_{sh,t} = \varepsilon_{su} S_t \left(S_{h\max} - \phi S_{hi}\right) \qquad (3.4.26a)$$

where,

ε_{su}	=	ultimate shrinkage (ε_{su} may be estimated based on PCC mix properties using the equation presented in PART 2, Chapter 2), x 10^{-6}:
S_{hi}	=	relative humidity factor for month *i* (equation 3.4.6a):
S_{hmax}	=	maximum average relative humidity factor. Maximum of S_{hi}.
S_t	=	time factor for moisture-related slab warping (equation 3.4.7).

Shrinkage strain at the bottom of the PCC slab is determined as follows:

$$\varepsilon_{sh,b} = \varepsilon_{su} S_t S_{hbot} \qquad (3.4.26b)$$

where,

ε_{su}	=	ultimate shrinkage (ε_{su} may be estimated based on PCC mix properties using the equation presented in PART 2, Chapter 2), x 10^{-6}:
S_{hbot}	=	relative humidity factor at the bottom of the PCC slab. Assumed to be equal to 90 percent

Initial (in the first increment) joint shear capacity is a function of joint opening and slab thickness only.

$$s_0 = 0.05 h_{PCC}\, e^{-0.032jw} \qquad (3.4.27)$$

where,

s_0	=	dimensionless aggregate joint shear capacity.
h_{PCC}	=	PCC slab thickness, in.
jw	=	joint opening

The aggregate joint stiffness is determined as a function of load shear capacity, S.

$$Log(J_{AGG}) = -28.4 * e^{-a^{-\left(\frac{S-e}{b}\right)}} \qquad (3.4.28)$$

where,

J_{AGG}	=	joint stiffness on the transverse joint for the current increment, *i*.
a	=	0.35.
b	=	0.38.
S	=	joint shear capacity equal to s_0 at the first time increment.

Load transfer efficiency due to aggregate interlock is determined using the following equation:

$$LTE_{AGG} = \frac{100}{1 + 0.012 J_{AGG}^{-0.849}} \qquad (3.4.29)$$

where,

LTE_{AGG}	=	load transfer efficiency on the transverse crack due to aggregate interlock.
J_{AGG}	=	transverse joint stiffness

Dowel LTE (if dowels are present). A non-dimensional stiffness of a joint due to dowel is determined as follows:

$$J_d = J_d^* + (J_0 - J_d^*)\exp(-DAM_{dowels}) \qquad (3.4.30)$$

where,

J_d	=	non-dimensional dowel stiffness.
J_0^*	=	initial dowel stiffness.
	=	120.*d^2/hpcc

J_d^* = critical dowel stiffness.

$$J_d^* = Min\left(118,\ Max\left(165 \cdot \frac{d^2}{h_{PCC}} - 19.8120,\ 0.4\right)\right) \tag{3.4.31}$$

d = dowel diameter, in (d is greater than 0.75 in) .
h_{PCC} = PCC thickness, in.
DAM_{dowels} = cumulative damage of a dowel joint depending on dowel bearing stresses and number of load repetitions. Initially is equal to 0.

Dowel component of LTE is determined as follows:

$$\mathrm{LTE}_{\mathrm{dowel}} = \frac{100}{1 + 0.012 J_d^{-0.849}} \tag{3.4.32}$$

Base/Subgrade LTE. $\mathrm{LTE}_{\mathrm{base}}$ can be determined from table 3.4.8 (these values are assumed in the Design Guide software). However, if the mean mid-depth PCC temperature for a given month is less than 32 °F then $\mathrm{LTE}_{\mathrm{base}}$ is set equal to 90 percent.

Table 3.4.8. Assumed effective base LTE for different base types.

Base Type	***LTE_{Base}***
Aggregate base	20%
ATB or CTB base	30%
LCB base	40%

After the contributions of the aggregate interlock, dowels, and base/subgrade are determined, the total initial joint load transfer efficiency is determined as follows:

$$LTE_{joint} = 100\left(1 - (1 - LTE_{dowel}/100)(1 - LTE_{agg}/100)(1 - LTE_{base}/100)\right) \tag{3.4.33}$$

where,

LTE_{joint} = total joint LTE, percent.
LTE_{dowel} = joint LTE if dowels are the only mechanism of load transfer, percent.
LTE_{base} = joint LTE if the base is the only mechanism of load transfer, percent.
LTE_{agg} = joint LTE if aggregate interlock is the only mechanism of load transfer, percent.

Step 7. Determine current maximum faulting.

Using equation 3.4.18, the maximum faulting is adjusted for the past traffic damage using past cumulative differential energy, i.e. differential energy accumulated form axle load applications for all month prior to the current month. Past cumulative differential energy is zero for the first month.

Step 8: Determine critical pavement responses for the increment.

For each increment, for each axle type and axle load, deflections at the loaded and unloaded corner of the slab are calculated using the neural networks. Using these deflections, the differential energy of subgrade deformation, DE, shear stress at the slab corner, τ, and (for doweled joints) maximum dowel bearing stress, σ_b are calculated:

$$DE = k/2\ (\delta^2_{loaded} - \delta^2_{unloaded}) \tag{3.4.34}$$

$$\tau = \frac{AGG * (\delta_{loaded} - \delta_{unloaded})}{h} \tag{3.4.35}$$

$$\sigma_b = \frac{D_d * (\delta_{loaded} - \delta_{unloaded})}{d * dsp} \tag{3.4.36}$$

where,

DE	=	differential energy, lb/in.
δ_{loaded}	=	loaded corner deflection, in.
$\delta_{lunloaded}$	=	unloaded corner deflection, in.
AGG	=	aggregate interlock stiffness factor.
k	=	coefficient of subgrade reaction, psi/in.
D_d	=	dowel stiffness factor = $J_d * k * l * dsp$.
d	=	dowel diameter, in.
dsp	=	dowel spacing, in.

Step 9: Evaluate loss of shear capacity and dowel damage.

The loss of shear capacity (Δs) due to repeated wheel load applications is characterized in terms of the width of the transverse joint based on a function derived from the analysis of load transfer test data developed by the Portland Cement Association (PCA). The following loss of shear occurs during the time increment (month):

$$\Delta s = \begin{cases} 0 & if \quad w < 0.001\,h \\ \sum_j \frac{0.005}{1.0 + (jw\ /h)^{-5.7}} \left(\frac{n_j}{10^6}\right)\left(\frac{\tau_j}{\tau_{ref}}\right) & if \quad jw < 3.8\,h \\ \sum_j \frac{0.068}{1.0 + 6.0 * (jw\ /h - 3)^{-1.98}} \left(\frac{n_j}{10^6}\right)\left(\frac{\tau_j}{\tau_{ref}}\right) & if \quad jw > 3.8h \end{cases} \tag{3.4.37}$$

where,

n_j	=	number of load applications for the current increment by load group *j*.
w	=	joint opening, mils (0.001 in).
h_{PCC}	=	PCC slab thickness, in.
τ_j	=	shear stress on the transverse crack from the response model for the load group *j*.

τ_{ref} = reference shear stress derived from the PCA test results.

$$\tau_{ref} = 111.1 * \exp(-\exp(0.9988 * \exp(-0.1089 \log J_{AGG}))) \qquad (3.4.38)$$

where,

J_{AGG} = joint stiffness on the transverse crack computed for the time increment.

The coefficients of this function may vary for different aggregate types, but preliminary test results indicate little difference in the shear wear-out behavior among mixes made with different coarse aggregate types.

The dowel damage, DAM_{dow} is determined as follows:

$$DAM_{dow} = C_8 \sum_j \left(\frac{n_j}{10^6} \right) \left(\frac{\tau_j}{f_c^{'}} \right) \qquad (3.4.39)$$

where,

DAM_{dow} = damage at dowel-concrete interface.
C_8 = coefficient equal to 400.
n_j = number of load applications for the current increment by load group *j*.
τ_j = shear stress on the transverse joint from the response model for the load group j.
f'_c = PCC compressive strength, psi.

Step 10. Calculate incremental faulting.

Using equation 3.4.17, determine faulting increment developed using the current month. The magnitude of the increment depends on the level of maximum faulting, level of faulting at the beginning of the month, and total differential energy, DE, accumulated for a month from all axle loads passed from 8 p.m. to 8 a.m.

Step 11. Calculate mean joint faulting at the end of the month.

Using equation 3.4.16, determine faulting at the end of the current month. Steps 6 through 11 should be repeated the number of months in the pavement design life times.

Faulting Reliability

JPCP pavements designed with the faulting model presented (equation 3.4.16 through 3.4.19) will have 50 percent design reliability. That is, they are just as likely to fail before the design life as after the design life. For design purposes a higher reliability than 50 percent may be specified. In these circumstances the predicted faulting must be adjusted upwards to provide the desired level of reliability. The equations used to adjust predicted mean faulting at any given level of reliability is presented below:

$$Fault_R = Fault_m + Z_R S_F \tag{3.4.40}$$

where,

$Fault_R$	=	predicted transverse joint faulting at reliability level R, in.
$Fault_m$	=	incremental change (monthly) in mean transverse joint faulting, in.
Z_R	=	standard normal deviate for the given reliability level R.
S_F	=	standard deviation corresponding to the predicted mean faulting level, in.

S_F is defined as follows:

$$S_F = \sqrt{0.03261 * Fault(t) + 0.00009799} \tag{3.4.41}$$

where

Fault(t)	=	predicted mean transverse joint faulting at any given time t.

Equation 3.4.41 may be modified based on local calibration.

Figure 3.4.31 shows that increase in reliability level leads to increases in predicted faulting. This mean that modification of design may be needed to increases reliability that the pavement will meet faulting performance criteria at the end of the design life. Figure 3.4.32 shows the effect of dowel diameter on the level of reliability that faulting will not exceed specified 0.15 in faulting limit.

Modification of JPCP Design to Reduce Joint Faulting

If the trial design produces a mean joint faulting that does not meet the performance criteria selected by the designer (within the desired reliability level), it can be modified to lower the faulting. As discussed under section 3.4.5.3, different design parameters have a different impact on different performance measures. When modifying pavement design to satisfy the design requirement, the effects of the design parameter on all applicable performance indicators should be considered. Some of the most effective ways of reducing faulting are listed below.

- **Include dowels or increase dowel diameter.** The use of properly sized dowels is the most reliable and cost-effective way to control joint faulting. A slight increase of diameter of the dowels (i.e., 0.25 in) will significantly increase joint shear stiffness and reduce the mean steel-to-PCC bearing stress and, thus, the joint faulting as shown in figure 3.4.16. Studies have shown that properly sized dowels with adequate consolidation will reduce faulting dramatically.

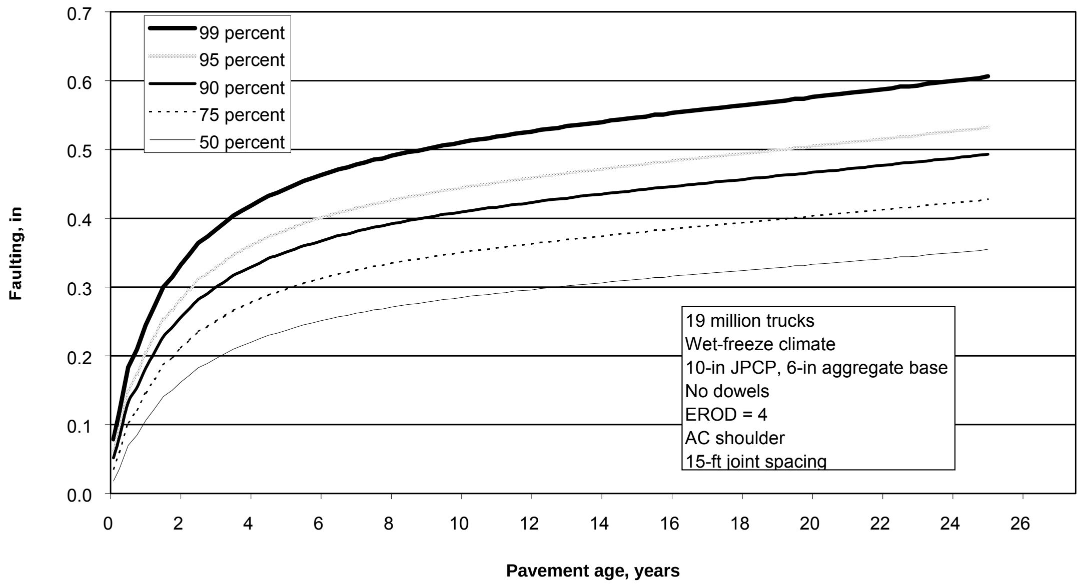

Figure 3.4.31. Predicted faulting for different reliability levels.

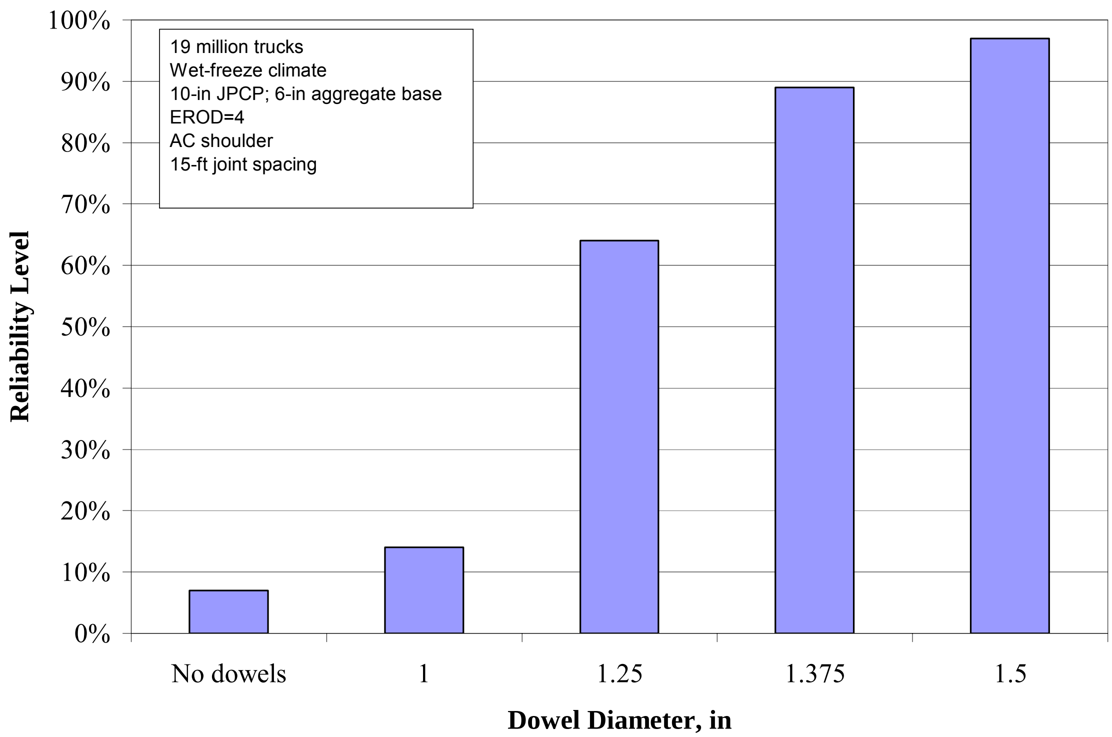

Figure 3.4.32. Effect of dowel diameter on reliability level that mean faulting will not exceed 0.15 in.

- **Stabilize the base course (if nonstabilized dense graded aggregate was specified) and provide open-graded base course.** The treating of nonstabilized aggregate base with adequate amounts of asphalt or cement will reduce the erosion potential of the base. Stabilized dense and open graded bases have lower erodibility than aggregate bases. See sections 3.4.4.9 and 3.4.4.10 for additional guidelines on the use of a stabilized base. Figures 3.4.33 and 3.4.34 show the effect of base erodibility on predicted faulting for non-doweled and doweled pavements, respectively. One can see that lower faulting is expected if less erodible bases are used particularly if dowels are not used.
- **Provide a PCC shoulder (if AC shoulder was specified).** A tied PCC shoulder (especially those constructed monolithically with the mainline) provides better edge and corner support than an AC shoulder and reduces the deflection of the slab and the potential for erosion and pumping, especially for non-doweled pavements. Figures 3.4.35 and 3.4.36 illustrate the effect of shoulder type on faulting in non-doweled and doweled pavements, respectively. The shoulder type also has a significant impact on slab cracking.
- **Widen the traffic lane slab by 2 ft.** Widening the slab effectively moves the wheel load away from the slab corner, greatly reducing the deflection of the slab and the potential for erosion and pumping. Studies have shown that slab widening can reduce faulting. Figures 3.4.37 and 3.4.38 illustrate that lower faulting is expected if widened slab is used for non-doweled and doweled pavements, respectively. Widened slab also has a significant impact on slab cracking.
- **Decrease joint spacing.** Generally speaking, shorter joint spacing results in smaller joint openings. Thus, aggregate interlock has a more useful effect on maintaining higher LTE. Figures 3.4.39 and 3.4.40 show that predicted mean joint faulting is smaller for shorter joint spacing. However, the effects of joint spacing on total faulting will be somewhat less due to increased number of joints.
- **Decrease permanent curl/warp.** Permanent curl/warp increases voids under PCC slab corners and increases corner deflections. Depending on curing conditions, permanent curl/warp may either increase or decrease from mean conditions corresponding to the equivalent temperature gradient -10 °F. Figures 3.4.41 and 3.4.42 show that decrease in effective permanent curl/warp temperature gradient decreases predicted mean joint faulting for non-doweled and doweled pavements, respectively.
- **Decrease PCC zero-stress temperature.** Paving in hot weather may result in a high PCC zero-stress temperature. That may lead to high joint opening, accelerated loss of aggregate shear capacity, and low load transfer efficiency. Figures 3.4.43 and 3.4.44 show that decrease in zero-stress temperature decreases mean joint faulting for non-doweled and doweled pavements, respectively.

3.4.5.5 Performance Prediction—Smoothness

Smoothness is the most important pavement characteristic as rated by the highway user. In this Guide, smoothness is defined by IRI. The mathematical definition of IRI is provided in PART 1, Chapter 1 of the Guide. Smoothness is the result of a combination of the initial as-constructed profile of the pavement and any change in the longitudinal profile over time and traffic.

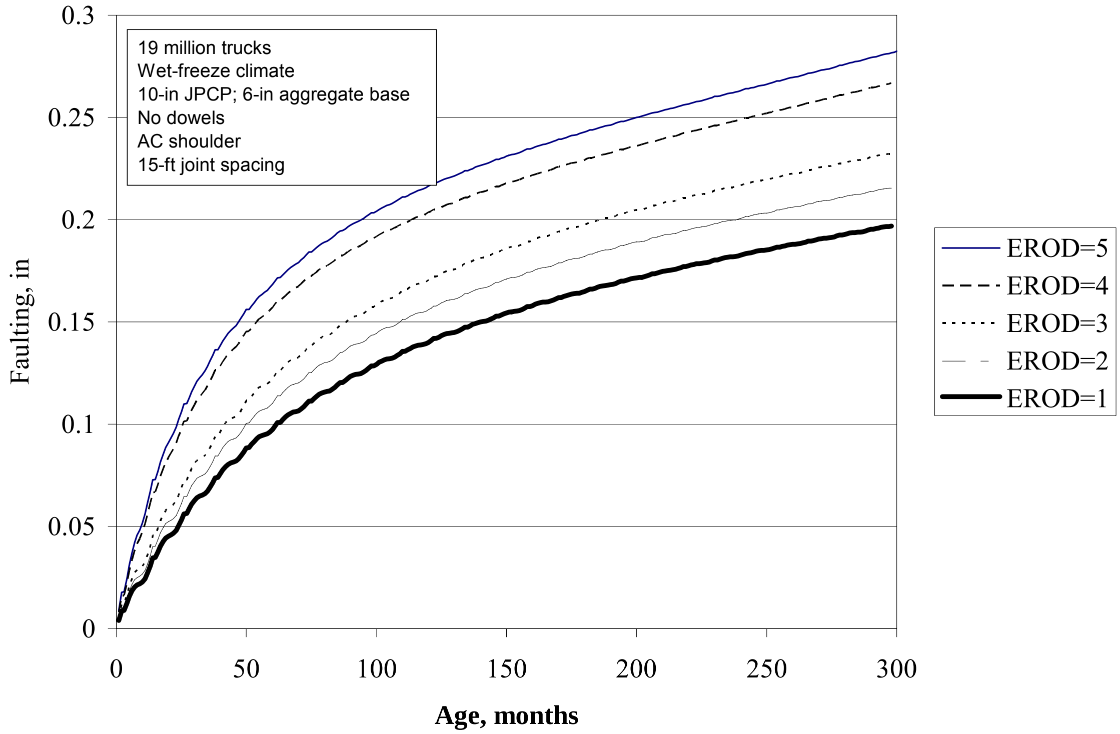

Figure 3.4.33. Effect of base erodibility on predicted faulting (50 percent reliability).

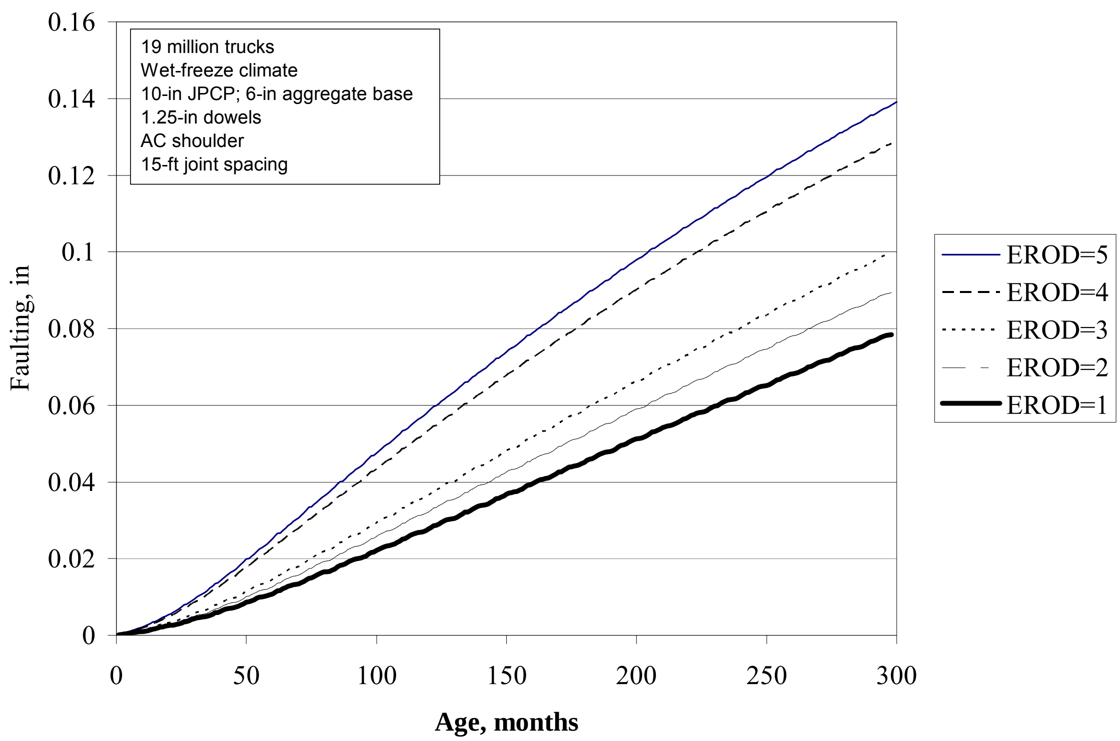

Figure 3.4.34. Effect of base erodibility on predicted faulting of doweled pavements (50 percent reliability).

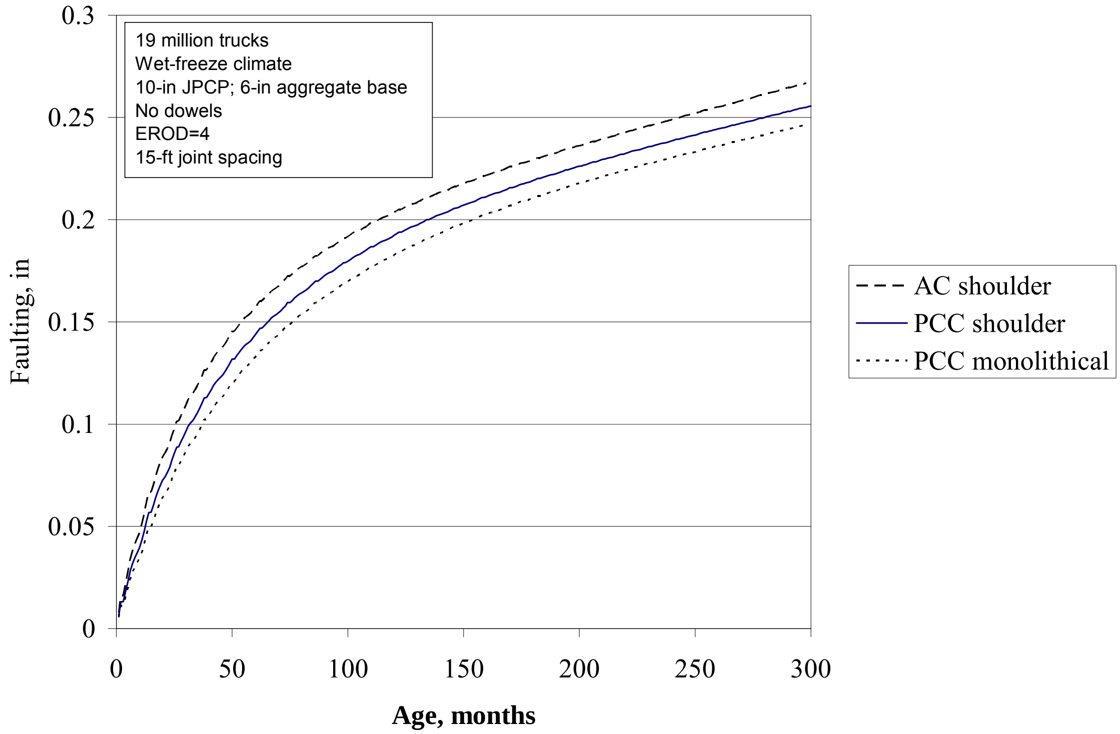

Figure 3.4.35. Effect of shoulder type on predicted faulting of non-doweled pavements (50 percent reliability).

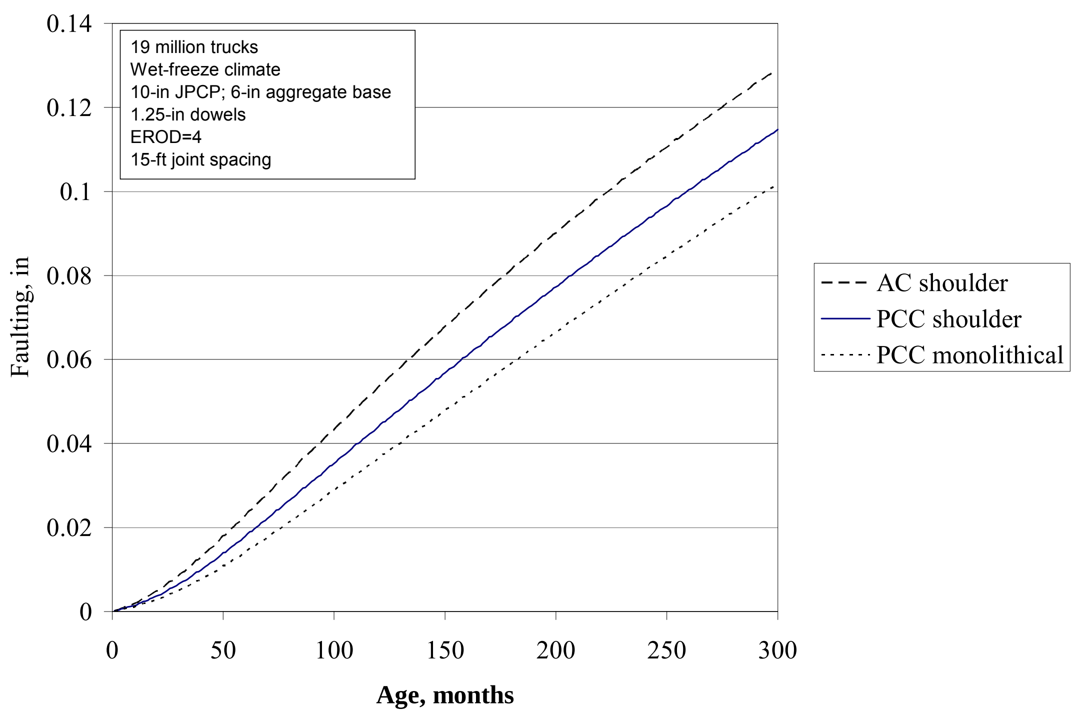

Figure 3.4.36. Effect of shoulder type on predicted faulting of doweled pavements (50 percent reliability).

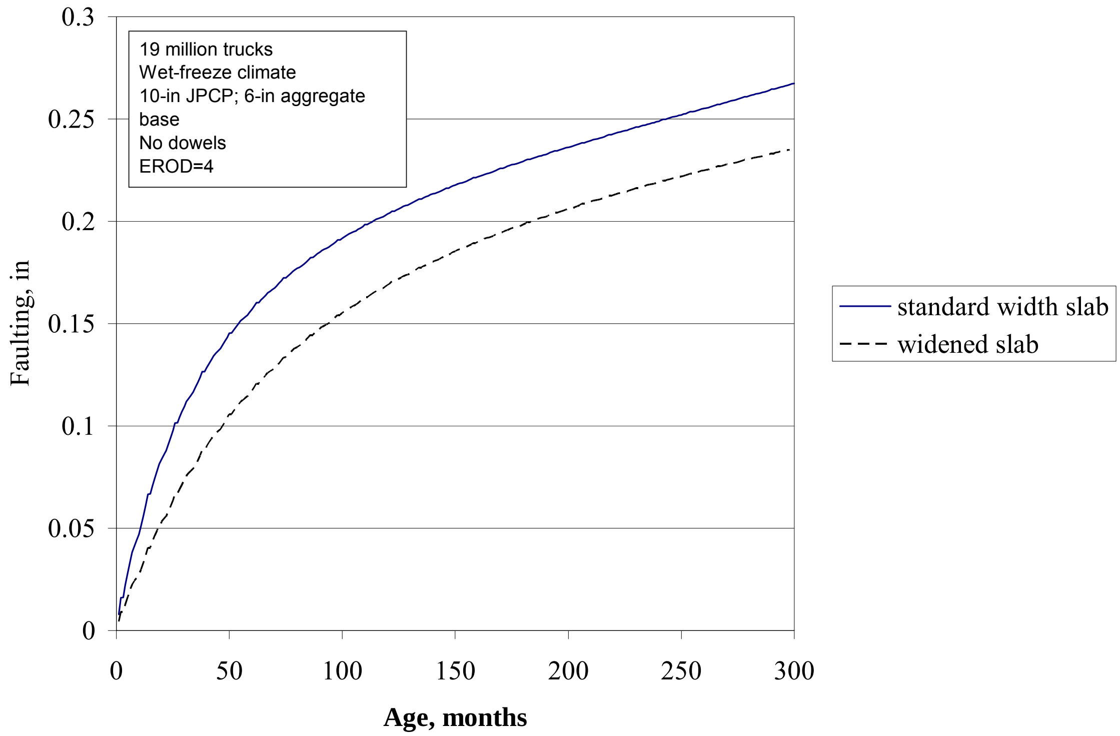

Figure 3.4.37. Effect of slab widening on predicted faulting in non-doweled pavements (50 percent reliability).

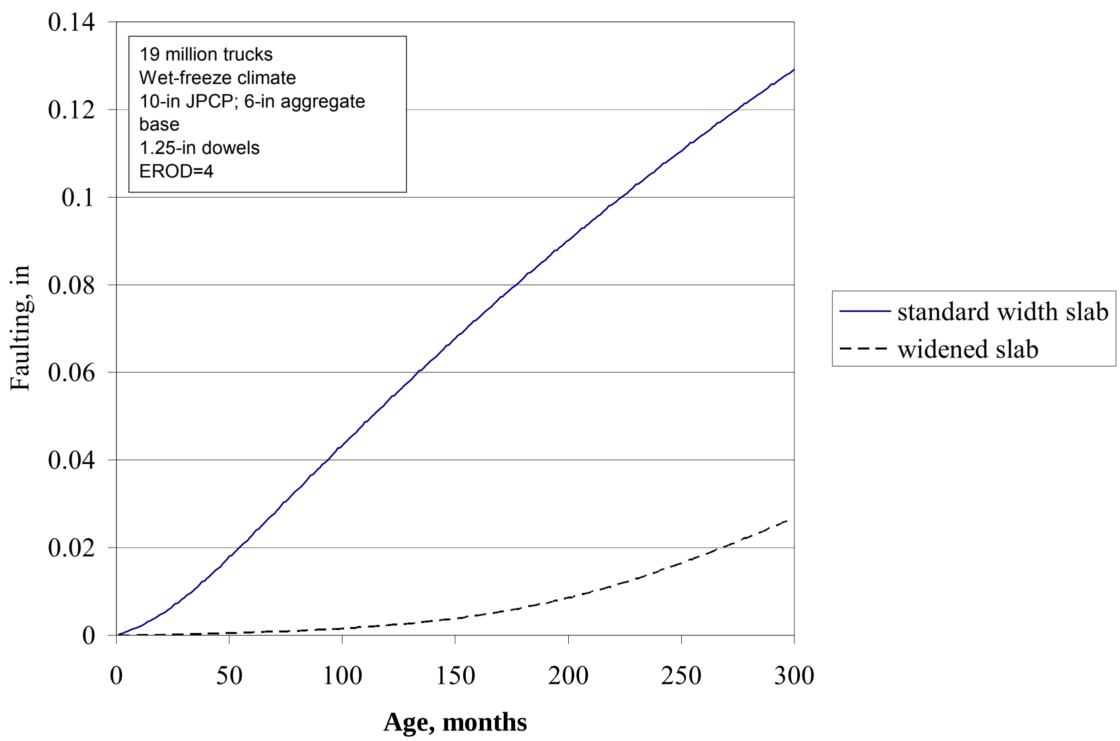

Figure 3.4.38. Effect of slab widening on predicted faulting in doweled pavements (50 percent reliability).

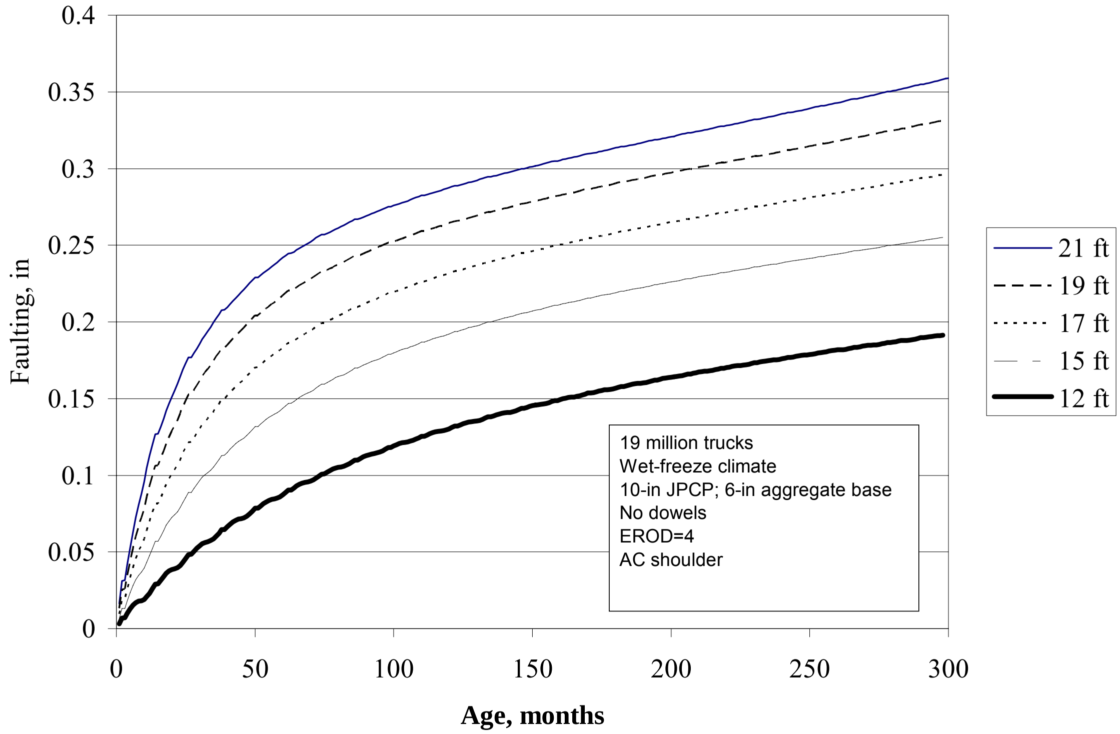

Figure 3.4.39. Effect of joint spacing on predicted faulting in non-doweled pavements (50 percent reliability).

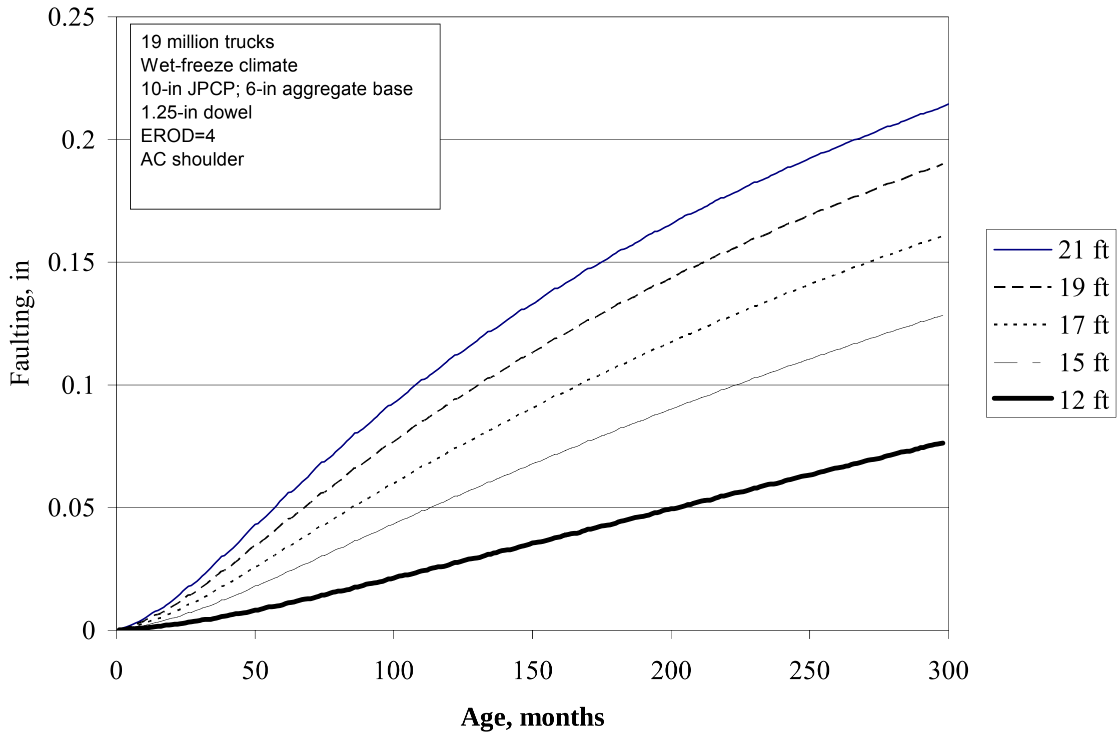

Figure 3.4.40 Effect of joint spacing on predicted faulting in doweled pavements (50 percent reliability).

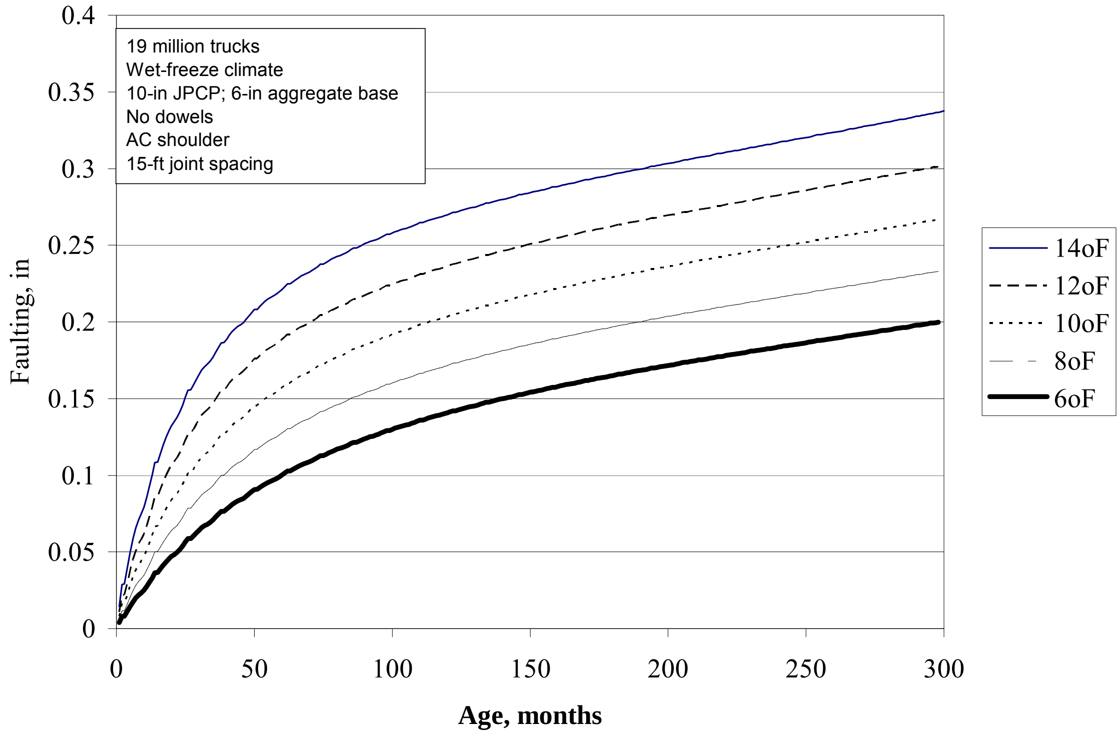

Figure 3.4.41. Effect of permanent curl/warp on predicted faulting in non-doweled pavements (50 percent reliability).

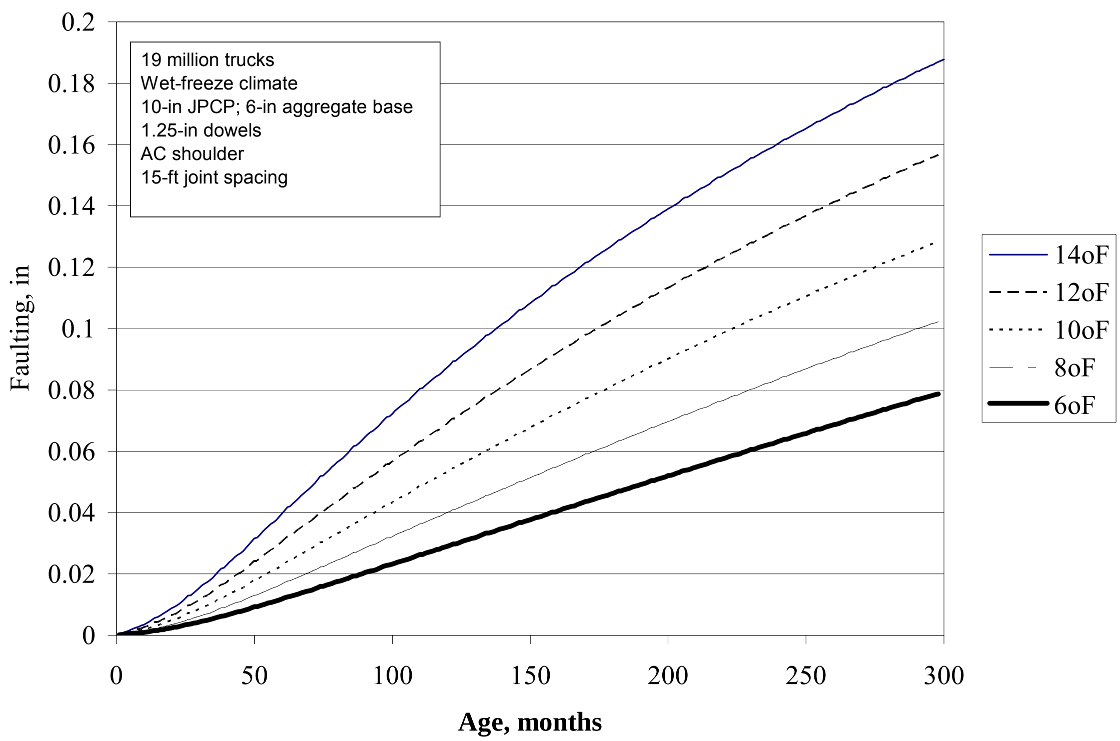

Figure 3.4.42. Effect of permanent curl/warp on predicted faulting in doweled pavements (50 percent reliability).

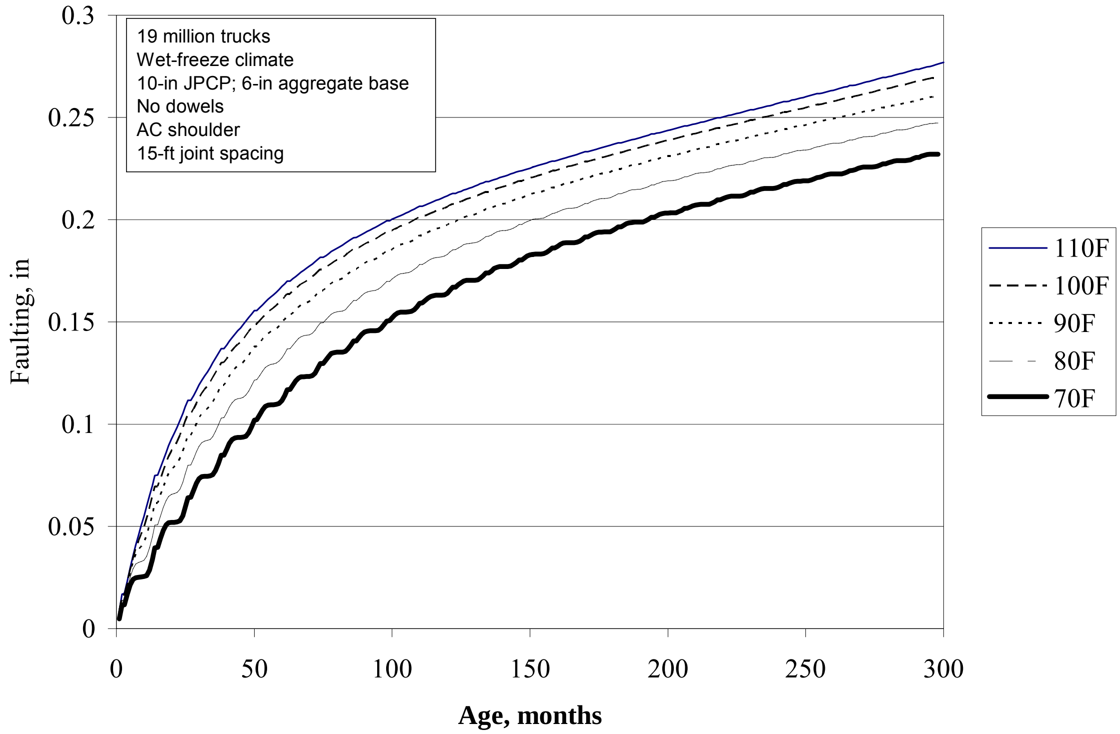

Figure 3.4.43. Effect of PCC zero-stress temperature on predicted faulting in non-doweled pavements (50 percent reliability).

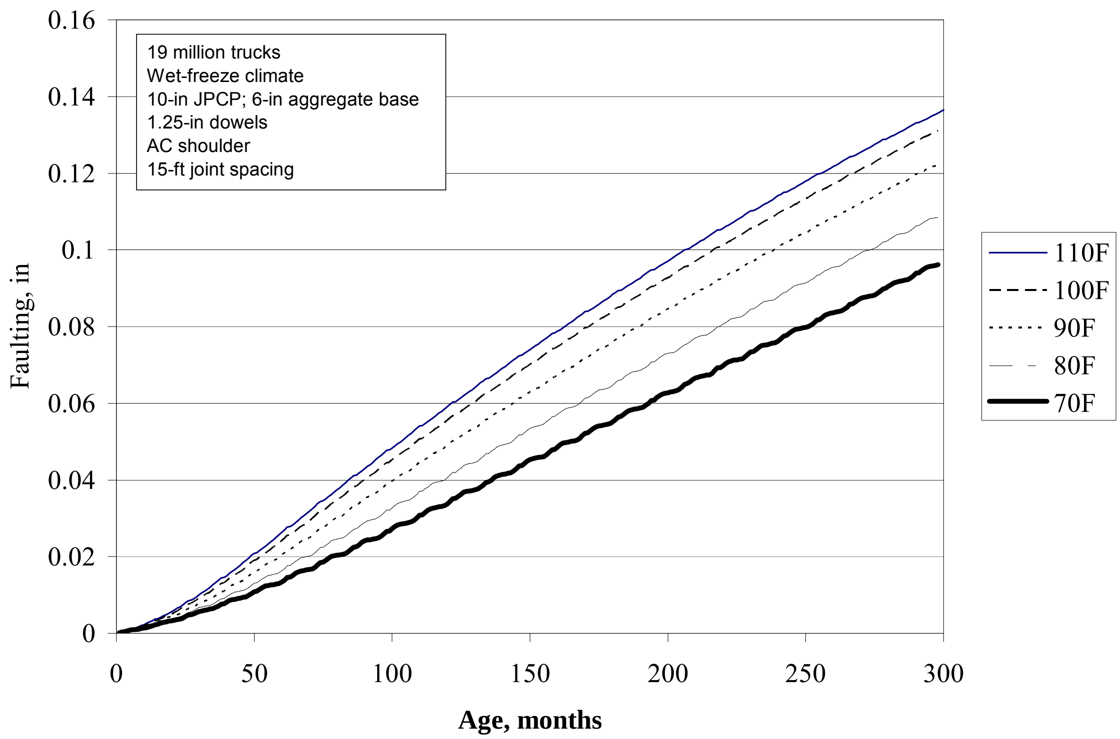

Figure 3.4.44. Effect of PCC zero-stress temperature on predicted faulting in doweled pavements (50 percent reliability).

Key distresses affecting the IRI for JPCP include transverse joint faulting and transverse cracking. The IRI model for JPCP also considers joint spalling, which is predicted using an empirical model.

IRI Model

The IRI model was calibrated and validated using LTPP and other field data to assure that it would produce valid results under a variety of climatic and field conditions. The following is the final calibrated model:

$$IRI = IRI_I + C1 * CRK + C2 * SPALL + C3 * TFAULT + C4 * SF \tag{3.4.42}$$

where,

IRI	=	predicted IRI, in/mi.
IRI_I	=	initial smoothness measured as IRI, in/mi.
CRK	=	percent slabs with transverse cracks (all severities).
$SPALL$	=	percentage of joints with spalling (medium and high severities).
$TFAULT$	=	total joint faulting cumulated per mi, in.
$C1$	=	0. 8203
$C2$	=	0.4417
$C3$	=	1.4929
$C4$	=	25.24
SF	=	site factor
	=	$AGE\ (1+0.5556*FI)\ (1+P_{200})*10^{-6}$

where,

AGE	=	pavement age, yr.
FI	=	freezing index, °F-days.
P_{200}	=	percent subgrade material passing No. 200 sieve.

Model Statistics:
R^2 = 0.60
SEE = 27.3 in/mile
N = 183

The transverse cracking and faulting are obtained using the models described in this Guide (section 3.4.5.3, *Transverse Cracking*; and section 3.4.5.4, *Joint Faulting*). The transverse joint spalling is determined using the following model calibrated using LTPP and other data (*24*):

$$\mathrm{SPALL} = \left[\frac{\mathrm{AGE}}{\mathrm{AGE} + 0.01}\right]\left[\frac{100}{1 + 1.005^{(-12*\mathrm{AGE} + \mathrm{SCF})}}\right] \tag{3.4.43}$$

where,

$SPALL$	=	percentage joints spalled (medium- and high-severities).
AGE	=	pavement age since construction, years.
SCF	=	scaling factor based on site-, design-, and climate-related variables:

$$SCF = -1400 + 350 \cdot AIR\% \cdot (0.5 + PREFORM) + 3.4\, f'c \cdot 0.4 - 0.2\,(FTCYC \cdot AGE) + 43\, h_{PCC} - 536\, WC\_Ratio \quad (3.4.44)$$

SCF	=	spalling prediction scaling factor used in equation 3.4.43.
$AIR\%$	=	PCC air content, percent.
AGE	=	time since construction, years
$PREFORM$	=	1 if preformed sealant is present; 0 if not.
$f'c$	=	PCC compressive strength, psi.
$FTCYC$	=	average annual number of freeze-thaw cycles.
h_{PCC}	=	PCC slab thickness, in.
WC_Ratio	=	PCC water/cement ratio.
Statistics:	R^2	= 78 percent, N = 179, SEE = 6.8 percent of joints

Reduced joint spalling is achieved with proper entrained air content and increased PCC strength in freeze areas. The IRI prediction model given in equation 3.4.42 is based on field performance of 183 LTPP pavement sections. An example prediction given by the IRI model is shown in figure 3.4.45.

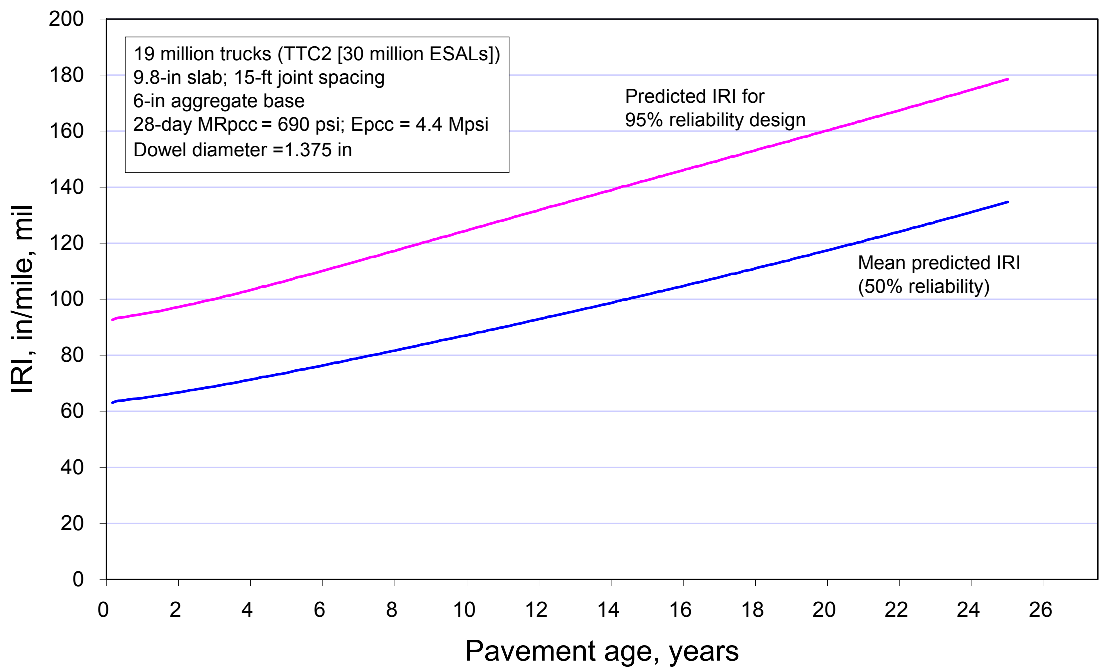

Figure 3.4.45. Predicted IRI over design life (initial IRI = 63 in/mi).

<u>IRI Prediction Procedure</u>

The IRI prediction is simple once the cracking and faulting predictions have been completed. The steps for predicting IRI are as follows:

Step1: Predict transverse cracking and faulting

- Follow the procedure for JPCP transverse cracking prediction (section 3.4.5.3) to obtain predicted cracking.
- Follow the procedure for JPCP joint faulting prediction (section 3.4.5.4) to obtain predicted faulting.

Step2: Predict joint spalling

Use the empirical model given in equation 3.4.43 to determine joint spalling.

Step3: Select initial IRI and predict IRI

The initial IRI depends on the project smoothness specifications. Typical values of initial IRI range from 50 to 100 in/mi. Select the initial IRI and use the IRI model given in equation 3.4.42 to predict IRI over the project life.

<u>IRI Reliability</u>

The reliability design is obtained by determining the predicted IRI at the desired level of reliability as follows:

$$IRI\_P = IRI + STD_{IRI} \bullet Z_P \tag{3.4.45}$$

$$IRI\_P \leq 100\ \%$$

where,

IRI_P	=	predicted IRI at the reliability level P, in/mi.
IRI	=	predicted IRI based on mean inputs (corresponding to 50% reliability), in/mi.
STD_{IRI}	=	standard deviation of IRI at the predicted level of mean IRI.
Z_P	=	standard normal deviate.

$$STD_{IRI} = \left(Var_{IRIi} + C1^2 \cdot Var_{CRK} + C2^2 \cdot Var_{Spall} + C3^2 \cdot Var_{Fault} + S_e^2\right)^{0.5} \tag{3.4.46}$$

where,

STD_{IRI}	=	standard deviation of IRI at the predicted level of mean IRI.
Var_{IRIi}	=	variance of initial IRI (obtained from LTPP) = 29.16, $(\text{in/mi})^2$.
Var_{CRK}	=	variance of cracking [equation 3.4.15], $(\text{percent slabs})^2$.
Var_{Spall}	=	variance of spalling (obtained from spalling model) = 46.24, $(\text{percent joints})^2$.
Var_{Fault}	=	variance of faulting [equation 3.4.41], $(\text{in/mi})^2$.
S_e^2	=	variance of overall model error = 745.3 $(\text{in/mi})^2$.

Modification of JPCP Design to Improve Smoothness

When the trial design produces an IRI that does not meet the performance criteria selected by the designer, the trial design can be modified to lower the IRI. The sensitivity of IRI to various input parameters is illustrated in figure 3.4.46. By far the most sensitive factor affecting JPCP smoothness is joint faulting and the most critical factor affecting joint faulting is dowel diameter. Figure 3.4.47 shows the sensitivity of JPCP smoothness to dowel diameter. The JPCP smoothness can be improved by building the pavement smooth, and limiting distresses, especially faulting. Some of the most effective ways to accomplish this are as follows:

- **Construct the pavement very smooth**. Smoothness specifications that offer significant incentives to build a smooth pavement are standard in many states. These specifications have had a dramatic effect, decreasing the mean IRI over a period of several years of implementation. Thus, it is well known now that a very smooth pavement can be constructed. This will provide the customer with a smoother pavement over a long period of time.
- **Include dowels or increase diameter of dowels**. The use of properly sized dowels is generally the most reliable and cost-effective way to control joint faulting. See section 3.4.5.4 for the discussion on the effects of dowels and dowel diameter on faulting.
- **Us a treated base** (if nonstabilized dense graded aggregate was specified). The treating of nonstabilized aggregate base with asphalt or cement will reduce the erosion potential of the base. Studies have show that properly treating the base course can reduce faulting by about 50 percent. The use of a treated base also leads to slight reduction in cracking. See section 3.4.5.3 for discussion of the effects of base type on cracking and section 3.4.5.4 for the effects on faulting.
- **Widen the traffic lane slab by 2 ft**. Studies have show that slab widening can reduce faulting by about 50 percent. Widening the slab effectively moves the wheel load away from the longitudinal free edge of the slab, thus, greatly reducing the critical bending stress and the potential for transverse cracking. See section 3.4.5.3 for discussion of the effects of slab widening on cracking and section 3.4.5.4 for the effects on faulting.
- **Decrease joint spacing**. Reducing joint spacing is an effective means of reducing cracking and faulting, which directly affect pavement smoothness. See section 3.4.5.3 for discussion of the effects of joint spacing on cracking and section 3.4.5.4 for the effects on faulting.
- **Increase slab thickness**. Slab thickness affects slab cracking very significantly and faulting to a lesser extent. At some thickness, however, a point of diminishing returns is reached and fatigue cracking can no longer occur. Thus, smoothness performance can be improved to an extent by increasing slab thickness (by reducing slab cracking), but those factors that more directly affects faulting have a greater impact. See section 3.4.5.3 for discussion of the effects of slab thickness on cracking and section 3.4.5.4 for the effects on faulting.
- **Ensure PCC has proper entrained air content**. PCC mixtures with proper levels of entrained air experience significantly less joint spalling in freeze areas.

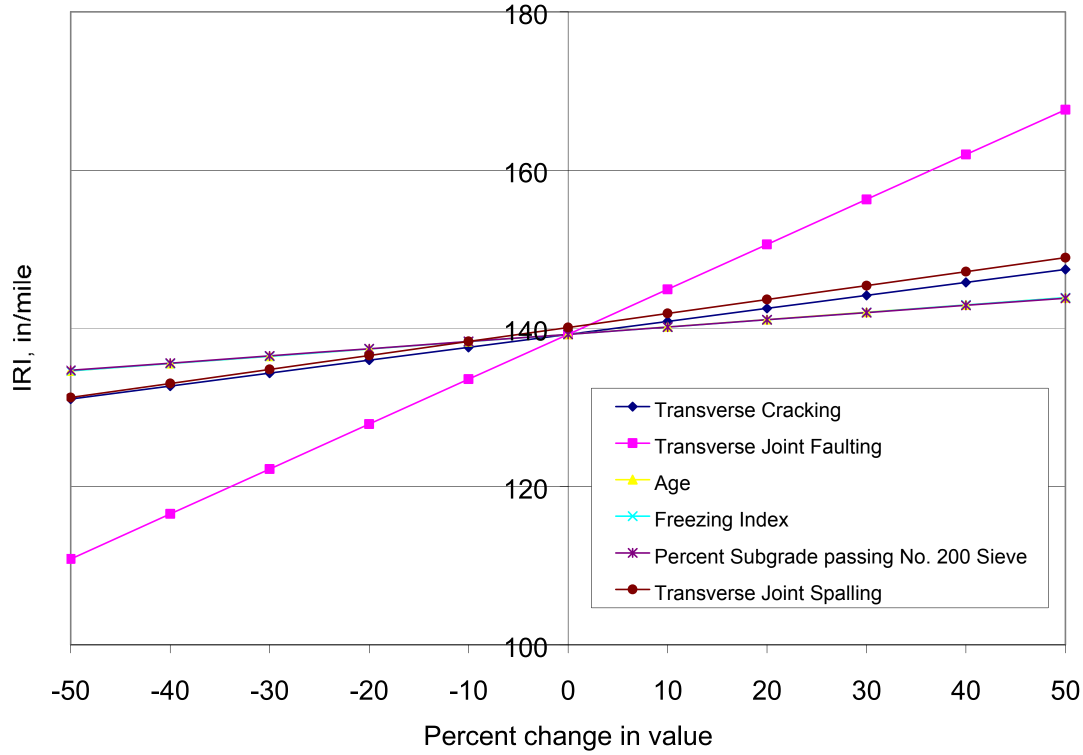

Figure 3.4.46. The effects of changes in key distresses and site variables on JPCP smoothness.

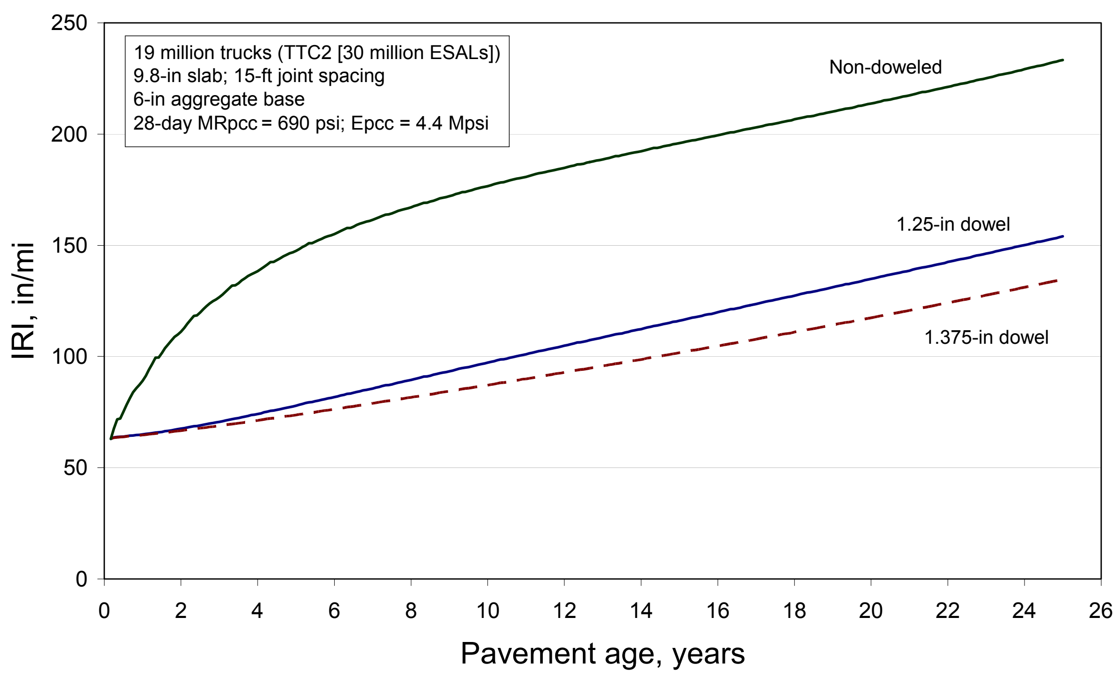

Figure 3.4.47. Effects of dowel diameter on JPCP smoothness.

3.4.6 CRCP DESIGN CONSIDERATIONS

CRCP performance depends on numerous factors, and the design solutions are by no means unique. The design goals can be achieved using any number of combinations of design features. Various design features may also be used to improve pavement performance and reduce the risk of poor performance. For example, increased reinforcement content will help assure tight cracks over the design period. A stabilized base and an aggregate subbase may be used where weak or variable subgrade conditions are a concern to improve both strength and uniformity of foundation support. A designed stabilized base is more resistant to erosion, which may be an important quality to reduce the risk of erosion along the edge when designing for high volumes of heavy trucks. For long design periods (e.g., 50 yr), subsurface drainage may be important to ensure adequate long-term material performance. A careful consideration of the design conditions and available options is important to obtain optimal design. This section provides a discussion of the factors that should be considered in the design of CRCP.

3.4.6.1 Slab Thickness

Slab thickness is an important CRCP design factor from the standpoint of both performance and slab stiffness. In general, as the slab thickness increases, the capacity to resist critical bending stresses increases, as does the slab's capability to transfer load across the transverse cracks. Consequently, as slab the thickness increases, punchouts decrease and smoothness increases (*25-28*).

Slab thickness must be selected within the context of other design features, including crack spacing, transverse crack width, percent steel reinforcement, PCC mixture properties, and base type and stiffness. Weather conditions at the time of construction must also be considered. In other words, depending upon the construction conditions, one slab thickness may be adequate for a given set of design features but not for another set of design features. The goal is to select the minimum thickness that provides acceptable levels of aggregate interlock wear-out, punchout development, and smoothness over the design period at the desired level of reliability.

3.4.6.2 Transverse Crack Width and Spacing

The width of the transverse crack is fundamental to many aspects of CRCP performance, as it plays a dominant role in controlling the degree of load transfer capacity provided at the transverse cracks and is used to determine the required design steel content. Smaller crack widths generally increase the capacity of the crack for transferring repeated shear stresses (caused by heavy axle loads) between adjacent slab segments. Wider cracks generally exhibit lower and lower LTE over time and traffic, which results in increased load-related critical tensile stresses at the top of the slab, followed by increased fatigue damage and eventually the development of longitudinal cracks and punchouts.

The mean seasonal (monthly) crack width along the project is directly considered in design and predicted using all mean inputs. Of course, crack widths vary widely along the project. At this time, variability is considered indirectly only through the calibration process. Obviously, those cracks that do break down over time tend to be those that are wider for whatever reasons and not the mean cracks. Crack width is also important in regions where deicing salts are used. In these areas, crack widths must be maintained very tight to minimize the possibility of corrosion of the reinforcement (e.g., < 0.02 in at steel depth which is calculated in this Guide). Field studies have shown that longer crack spacing increase the potential for wider opening of transverse cracks.

Crack spacing has been considered in CRCP design by attempting to limit it between a minimum and maximum value. This is extremely difficult to do because of the large effect that construction climate and other factors have on crack spacing. This procedure focuses more on crack width, as it is believed to be the more fundamental design criteria directly related to punchout development. Limiting mean crack widths to 0.02 in at the steel depth (or other values as selected by the designer) has been found to control the mean crack spacing to a reasonable level. The maximum recommended mean crack spacing is 6 ft. Through proper selection of steel percentage, PCC mixture parameters, and base type and friction, the designer can obtain acceptable mean crack width and mean crack spacing. This will minimize the loss of LTE as described in 3.4.6.6.

3.4.6.3 PCC Materials

The PCC material properties that must be considered in design and construction of CRCP include compressive strength, flexural strength, tensile strength, coefficient of thermal expansion, thermal diffusivity, the heat of hydration, modulus of elasticity, ultimate drying shrinkage, and aggregate type. PART 2, Chapter 2 discusses these inputs in great detail, with the exception of thermal diffusivity and heat of hydration, which are empirically incorporated into the CRCP design procedure.

The higher the compressive strength, the higher the modulus of elasticity for any given PCC mixture. As PCC strength increases, a greater fatigue life typically results. However, since the modulus of elasticity also increases with increased strength, the increase in fatigue life may not be as dramatic as commonly believed due to an increase in crack spacing ultimately leading to greater crack width and lower LTE.

One consequence of higher PCC strength is possibly a higher PCC zero-stress temperatures due to increased cement content. However, drying shrinkage often increases with cement content as well. The zero-stress temperature is related to the concrete placement temperature and the heat of hydration of the cement. The heat of hydration is a function of the solar radiation, cement composition and fineness, mineral admixtures (e.g., fly ash), and chemical admixtures (e.g., set-retarding or accelerating agents).

The coefficient of thermal expansion (α_{PCC}) of the coarse aggregate has a significant effect upon the spacing of cracks and crack width. The higher the α_{PCC} the longer the crack spacing and wider crack opening. The higher the CTE the higher the thermal curling stresses which contribute to punchouts. Increased PCC strength obtained by increased cement content would also increase the PCC α_{PCC} significantly.

The following is a summary of the effects of various PCC properties on CRCP performance:

- PCC strength – the higher the better for CRCP performance, but a higher strength obtained by higher cement content for a given material is accompanied by higher modulus, higher shrinkage, and higher α_{PCC} which tends to moderate the beneficial effect.
- PCC modulus – the lower the better for CRCP performance.
- Shrinkage – the lower the better for CRCP performance.
- Coefficient of thermal expansion – the lower the better for CRCP performance.

Most of the PCC properties are dictated by the local materials, and the designer may have very little control over the mix properties other than the strength. However, it is possible to optimize the PCC mix for pavement performance, and the mix optimization may be practical on some projects. Some of the PCC properties affect material cost as well as pavement performance.

3.4.6.4 Longitudinal Reinforcement

Longitudinal steel is an important design parameter because it is used to control the opening of the transverse cracks. It is also critical from the standpoint of its effect on crack spacing. Decreased crack spacing is associated with increased steel percentages (*26*-*28*). In the United States, steel percentages of 0.60 to 0.80 (mostly in colder climates) have provided suitable cracking patterns and performance in CRCP systems. Field studies have shown that increased steel content results in fewer punchouts and increased smoothness (*17, 26, 28, 29*). Thus, it is very important to consider the effect of steel content in design.

Steel content is determined with consideration of several other design features, including reinforcement bar size, slab thickness, maximum allowable crack width, PCC materials properties, base type and stiffness, and regional climatic characteristics. In other words, a specific percentage of steel may be adequate for a given set of design features and inadequate for another set of design features, particularly with respect to different coarse aggregate types. The goal is to select the steel content that provides an acceptable transverse crack width throughout the project and resistance to punchout development over the design life at the desired level of reliability. Variability in crack widths throughout a project needs to be considered in design, or localized cracks having exceptional widths will fail quickly under heavy traffic. These are often the initial cracks that form within a few days after construction.

3.4.6.5 Depth of Longitudinal Reinforcement

Most specifications require the reinforcement to be placed at (or just above) mid-depth in the slab. However, studies have shown that placing the reinforcement closer to the surface results in much tighter cracks and fewer punchouts due to shorter crack spacing (12*, 17, 26*). For example, Illinois places the steel 3.5 in below the surface of the slab, regardless of slab thickness, and this has lead to closer spaced cracks at the pavement surface. However, placing the steel too high can lead to construction problems. A minimum steel depth of 3.5 in and a maximum of mid-depth are recommended. This Guide does not consider the use of two-layers of reinforcement.

3.4.6.6 Transverse Crack LTE

The load transfer of transverse cracks is a critical factor in controlling the development of punchout-related longitudinal cracking. Field studies have shown that close transverse cracking patterns are associated with small crack widths that maintain a high resistance to wear-out of aggregate interlock. Maintaining load transfer of 95 percent or greater will maximize aggregate interlock over the design life of the pavement and limit the development of punchout distress.

Crack LTE can be controlled via a number of design features, including slab thickness, percent steel, crack width, crack spacing, PCC materials properties, coarse aggregate gradation, and base type and stiffness. The goal is to select the crack spacing and slab thickness that would provide a crack load transfer of 95 percent or greater. Maintenance of LTE above 95 percent would provide an acceptable level of punchout development and smoothness over the design life at the desired level of reliability.

3.4.6.7 Slab Width

Slab width has typically been synonymous with lane width (usually 12 ft). A few projects in the U.S. and in foreign countries have been constructed with wider slabs (typically 14 ft) to improve CRCP performance. Field and analytical studies have shown that the wider slab keeps truck axles away from the free edge, greatly reducing bending stresses at the top slab surface and deflections and most likely reducing the occurrence of edge punchouts (2*, 30*). This design procedure does not directly address CRCP with widened slabs. An indirect approach is to input an increased lateral offset of the truck tire to show fewer loads at the free edge of the CRCP. A maximum of 30 in is recommended due to the wheel becoming more critical at the lane to lane joint. Certainly, the design for conventional width slabs would be acceptable for widened slab CRCP. When the slab is widened, the mode of failure will change completely to where slab stresses at the bottom of the slab under the inner wheel may become excessively high leading to bottom-up punchout. Further research and development is required to directly handle this situation.

3.4.6.8 Transverse Reinforcement

Transverse steel is only needed to hold longitudinal bars in place during construction. The effects of transverse reinforcement on CRCP crack patterns are not directly considered in this Guide, but field studies have indicated that transverse crack locations often coincide with the location of the transverse steel, particularly when the steel is placed in two layers. Most agencies using CRC pavements have established transverse reinforcement configuration standards that will control longitudinal cracks that develop due to problems with forming the lane-to-lane joint or settlements along the highway.

3.4.6.9 Longitudinal Joint Load Transfer and Ties

The load transfer of the longitudinal traffic lane/tied shoulder joint affects the magnitude of the transverse bending stress at the top of the slab (between the wheel loads). Basically, this load transfer affects the critical transverse stress at the slab surface, which controls the development of longitudinal cracking between transverse cracks and, consequently, the development of punchout distress. Since most shoulders for CRCP are not CRCP and are placed separately and tied into the CRCP, the long-term load transfer is fairly low due to the difficulty in securing a permanent tie.

3.4.6.10 Formed Depth of Longitudinal Joints

Current design procedures do not directly consider the formed depth of longitudinal joints in the prediction of longitudinal cracking or punchout development. However, the formed depth does affect the cracking of the joints and the load transfer achieved. It is desirable to keep formed depth to the minimum that will still ensure that the joints will crack effectively and not randomly. A formed depth of one-third the slab thickness is recommended.

3.4.6.11 Base

The base type and material characteristics are critical features that affect the crack spacing pattern, slab support and loss of support (erosion), punchouts, smoothness, and construction costs. For heavily trafficked CRCP, strong base support is considered very important. Field studies have shown that, because of the widely varying base stiffness and base friction with the CRCP, a wide variation in cracking patterns and spacing can result. In addition, the erosion potential of different bases and their material characteristics can vary widely.

Bonding of the CRCP to the base is needed to provide a desired crack spacing (otherwise crack spacing would be too long). For example, CRCP placed directly on an asphalt stabilized base usually results in adequate friction to achieve a good crack spacing. CRCP placed on unbound aggregate base may have much longer crack spacing as friction is much lower. In fact, many CRCP designs have successfully used a relatively thin asphalt concrete base as a layer over a cement-stabilized base layer (*17*). When the CRCP is placed directly on a cement stabilized or lean concrete base, some type of partial bond breaker may be needed such as a double wax curing compound to reduce the bond and avoid the potential for reflection cracking from the base.

The width of the base is also important; it should extend beyond the CRCP slab edge to provide increased edge support and reduce erosion potential.

Base modulus also affects transverse stress in the PCC slab. Obviously, greater base course resistance to erosion from pumping action reduces the potential for loss of support and wear-out of aggregate interlock (from loss of support), which can lead to premature longitudinal cracking and punchouts. One field study showed that increasing the compressive strength of a lean concrete base significantly reduced the incidence of punchouts (*31*) because erosion was reduced. Open-graded bases should be used with caution due to their possible effect on crack pattern and structural stability of the pavement.

Base type must be selected within the context of other design features, including slab thickness, crack width, PCC materials properties, crack spacing, erosion resistance, truck traffic level, and costs. Generally speaking, the goal is to select the lowest cost base course that provides an acceptable level of support, design crack spacing and crack width, resistance to erosion, and smoothness over the design life at the desired level of reliability.

3.4.6.12 Subbase

The use of a subbase beneath the base course depends on several factors, including the type and stiffness of the subgrade, the type of base course (unbound or stabilized base), and the use of an open-graded drainage layer. Field studies have shown that for JPCP slabs constructed on a stabilized base, the erosion can take place beneath the stabilized base. For such designs, providing a granular subbase is important to minimize the potential for erosion and loss of support beneath the stabilized base. Several agencies specify such a granular layer beneath a stabilized base course. An aggregate subbase may also be used as a measure to protect the aggregate base against contamination by fines on very soft, fine-grained subgrade. Beneath a permeable base, the use of a dense-graded aggregate subbase meeting the gradation requirements for a filter layer is essential to prevent infiltration of fines into the open-graded drainage layer.

3.4.6.13 Subsurface Drainage

CRCP may have special problems when placed on a stiff stabilized open-graded drainage layer. The infiltration of PCC into the open-graded base increases the effective thickness of the CRCP slab that would affect crack spacing and width. If a permeable layer (with lower permeability) is used in a CRCP, consideration should be given to placing it below an asphalt treated base course and on top of a granular subbase to prevent infiltration of fines from the subgrade. This design has been used successfully on heavily trafficked freeways.

3.4.6.14 Shoulder Design

A CRCP can be designed successfully with a variety of shoulder types and designs. A typical shoulder design for CRCP traffic lanes is either a JPCP (placed after the mainline traffic lanes) without dowels or an AC shoulder. In either case, the load transfer over time may be poor and thus should not be counted on to have any significant effect unless major efforts are made to increase the long-term load transfer of lane/shoulder joint. However, shoulder design will affect the construction cost and the performance of the pavement. Key design aspects include the tie between the shoulder and the traffic lane, the erodibility of the underlying base materials of the shoulder, the use of the shoulder for regular traffic for emergencies, to increase capacity, and for parking.

3.4.6.15 Subgrade Improvement

The improvement of the top of a soft wet subgrade provides improved support and uniformity to the pavement and aids construction. Subgrade improvement can be accomplished by stabilizing the upper portion or the placement of a thick granular layer. Current design procedures can directly consider subgrade improvement in terms of increased moduli that reduce slab deflections slightly. They also consider the reduced variability in support along the project if the designer believes that this will occur. Another benefit of an improved subgrade may be to reduce the potential of erosion at the top of the subgrade. PART 1, Chapter 1 describes foundation improvement techniques in more detail.

3.4.7 CRCP DESIGN PROCEDURE

The design of CRCP involves selecting design features that ensure the pavement will meet all performance criteria at an acceptable level of reliability. The designer must select an initial trial design and analyze its performance. If the performance criteria are not met at the desired level of reliability, the design must be adjusted until all of the selected criteria are satisfied. This section describes the required design features, materials, performance criteria, distress predictions, and design adjustments for CRCP design.

3.4.7.1 CRCP Performance Criteria

Design performance criteria are required to help ensure that the CRCP will perform successfully over the design period. Two important criteria have been established for CRCP: punchout development and smoothness (IRI). An addition criterion that can be directly considered is crack width if desired. In addition, the level of design reliability should be considered in conjunction with selection of the performance criteria. For example, if a very high level of design reliability is chosen a higher level of punchouts or smoothness might be selected than if a lower level of design reliability was used. This would avoid the possibility of selecting a combination of performance criteria and design reliability that is unattainable.

<u>Crack Width and LTE</u>

Inadequate crack width design has resulted in punchouts and necessitated early rehabilitation in some CRCP. The designer could consider a maximum crack width that would occur during the cooler months at the end of the design life. This value would have to be determined by experience but would be less than 0.02 in at the steel depth based on calibration experience. Such a value could be used as a general guide for the designer because crack width has a great effect on loss of LTE of cracks and during the design life it may be desirable to limit the extent of LTE loss, especially when the CRCP is subjected to very heavy number of trucks. Mean crack LTE should be maintained above 95 percent.

<u>Punchouts</u>

Development of punchout distress is a significant factor that causes a loss of smoothness for a CRCP, and smoothness is very critical to the traveling public. The punchout definition and database used in calibration of the punchout model showed that over 90 percent of the punchouts were of low severity. Thus, a higher performance criteria than is normally considered may be appropriate since most of them would be of low severity. Values ranging from 10 to 20 per mile may be appropriate as initial values to consider at 95 percent reliability or lower. This input needs local calibration to select a proper value.

Smoothness

CRCP has been shown to exhibit smoothness after long time periods (25). The smoothness of CRCP (as measured by IRI) is the most critical consideration for the traveling public. It is desirable to place limits on IRI to ensure that a CRCP design will perform as desired over the design period. The critical level of smoothness should depend on its effect on highway users' assessment of ride quality. These values are chosen by the designer and should not be exceeded at the design level of reliability. Smoothness over the life of the CRCP is greatly affected by that achieved at construction. Therefore, this initial IRI input must be chosen considering the smoothness specifications under which the CRCP will be constructed.

3.4.7.2 Trial Design

The trial design should be selected considering the factors described in 3.4.6 CRCP Design Considerations of this chapter. The local experience with pavement designs for various design conditions may be the most valuable resource in selecting trial design. The design catalog developed under NCHRP Project 1-32 (*19*) may also be helpful in selecting trial design. A typical trial section may include the following features:

- PCC strength – typical design strength. Note that the proper design input is the expected mean strength, not the lower minimum required strength for construction.
- Trial slab thickness – depends on traffic level, PCC properties, and climate. Suggested initial trial thicknesses for CPCP without edge supports (tied PCC shoulder or widened slab) are:
    - Low traffic (2-way ADTT < 1000) – 8 in or less.
    - Moderate traffic (2-way ADTT up to 3000) – 9 to 10 in.
    - Heavy traffic (2-way ADTT > 3000) – 10 in or more.

  A thicker slab is needed in dry-nonfreeze areas than in wet or wet-freeze areas. The trial thickness may be reduced by 1 in for CRCP with edge support.
- Percent reinforcement – in general, reinforcement should be adequate to keep crack widths very tight over the design life (e.g., less than 0.02 in at steel depth). Trial values may range from 0.60 to 0.70 percent for moderate truck traffic and 0.70 to 0.80 for heavy truck traffic.
- Base and subbase – normally an asphalt or cement stabilized base is recommended for heavy trafficked highways for CRCP.
- Edge support – separately constructed but tied JPCP shoulders are commonly used with CRCP and are effective in reducing critical deflections and stresses.

3.4.7.3 Punchouts Prediction Model

Development of punchout distress is directly related to the formation of a longitudinal crack between two adjacent closely spaced transverse cracks. This crack initiates at the top of the slab and propagates downward through the CRCP after the transverse cracks have lost LTE. The development of the longitudinal crack is, in turn, related to the accumulated fatigue damage caused by a slab bending in the transverse direction. Therefore, the prediction of punchouts can be considered in the design process in terms of the accumulated fatigue damage associated with the formation of longitudinal cracks (*25, 28, 29, 31, 32*).

<u>Punchout Model</u>

CRCP punchouts are predicted using a calibrated model, which predicts punchouts as a function of accumulated fatigue damage due to top-down stresses in the transverse direction. The nationally calibrated model is as follows:

$$PO = \frac{A}{1 + \alpha \cdot FD^{\beta}} \tag{3.4.47}$$

where,

PO	=	total predicted number of punchouts per mile.
FD	=	accumulated fatigue damage (due to slab bending in the transverse direction) at the end of y^{th} year.
A, α, β	=	calibration constants (105.26, 4.0, -0.38, respectively).

Model Statistics:

R^2	=	0.67
SEE	=	4.73 punchouts/mile
N	=	220

This CRCP punchout model was calibrated based on performance of 74 field sections from 23 states. The calibration sections consist of 57 LTPP GPS-5 sections, 6 sections from the Vandalia experimental site, and 11 heavily trafficked sections near Chicago. Time-series data were available for many of the sections, making the total number of field punchout observations at 220. The punchout predictions given by equation 3.4.47 are shown in figure 3.4.48. Figure 3.4.49 shows predicted punchouts versus age for an example case. These predictions are valid only when the fatigue damage is calculated according to the procedure described in this section.

Loss of support along CRCP longitudinal joints has been identified as a key factor in the development of punchout distress (*25, 26, 32*). It plays a prominent role, since it directly affects top-of-slab tensile stress and crack shear stress on the faces of transverse cracks where aggregate interlock occurs to transfer load between adjacent slab segments. An increase in shear stress increases the rate of aggregate wear-out that ultimately leads to lower load transfer and increased lateral bending stress. However, as long as support conditions can be maintained and wear-out of aggregate interlock minimized, bending stresses in CRCP systems will be relatively small—which results, for all practical purposes, in infinitely long fatigue lives. For this reason, it is critical to maintain high load transfer across the cracks and full support conditions beneath the CRCP slab.

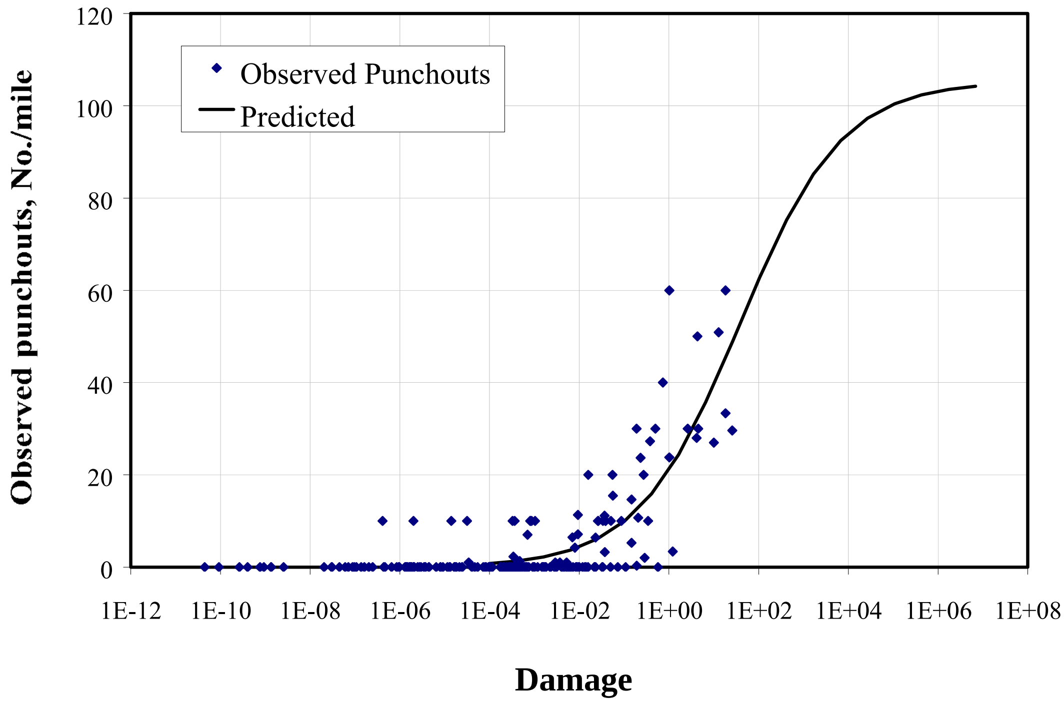

Figure 3.4.48. Observed punchouts versus accumulated damage.

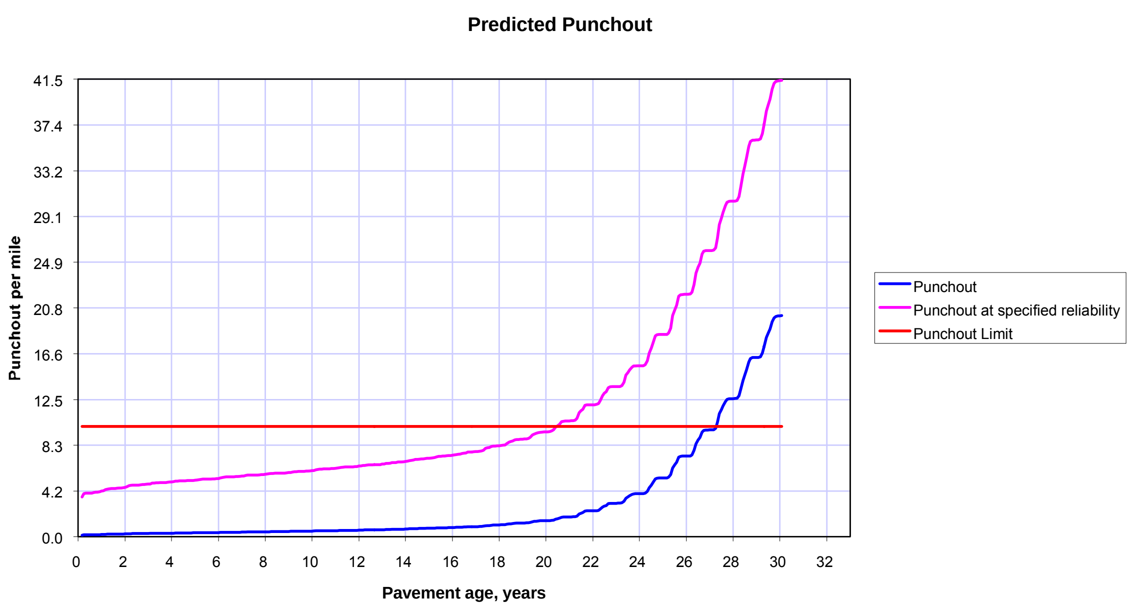

Figure 3.4.49. Example CRCP punchout prediction for a given section.

Drying shrinkage is a primary contributor to early crack initiation in CRCP. The amount of drying shrinkage that takes place depends greatly on the amount of evaporation, the quality of curing, and the water/cement ratio used to place the concrete pavement. Drying shrinkage is usually greater if concrete is placed under hot weather paving conditions and if favorable mix design features exist (e.g., a high paste content or high water/cement ratio). If evaporation rates are too low, then a potential for longer crack spacing exists. If the evaporation is too high, then shorter crack spacing and reduced concrete strengths can result. The minimum and maximum curing limits need to be established to promote optimum crack development in CRCP systems. Moisture measurements in field slabs have indicated that the drying process in concrete tends to concentrate shrinkage development in the upper portion of the concrete slab (*33, 7*). These measurements have also indicated a certain amount of non-linearity of the humidity profile vertically through a pavement slab due to wetting and drying cycles caused by rainfall and varying humidity conditions.

Coefficient of thermal expansion is also a major factor in crack spacing and crack opening, thus the lower its value the better.

Erosion potential is greatest where upward curling and warping along the edge and corner areas pump trapped water back and forth along the slab/subbase interface under applied wheel loads. When combined with the relatively viscous nature of water, this pumping action creates a shearing stress that erodes the subbase material. Representation of erosion performance in the design of CRCP focuses on the use of material models and equation forms suggested in past research (*29, 34, 35*). Erosion of the base along the CRCP slab edge has been approximately related to material erodibility potential, precipitation, and presence of a granular layer beneath a stabilized base. PART 2, Chapter 2 describes the model for predicting loss of support beneath the slab edge over time. The following factors have been shown to affect CRCP punchout development:

- Presence of sufficient amount of reinforcement.
- PCC thickness.
- Use of stabilized base layers and the strength and durability of the materials.
- Base and subgrade type.
- Placement of vehicle loads near unsupported pavement edges.
- Poor slab edge support (e.g., lack of widened paving lanes, tied PCC shoulders, or edge beams).
- Subsurface drainage including an open-graded base course.
- Freezing index/number of freeze-thaw cycles.
- Construction conditions, including PCC zero-stress temperature and built-in "construction" curling/warping.
- CRCP curling and/or warping (including combined effects of slab geometry and temperature/moisture gradients).

Structural Response Modeling

Critical truck axle loading includes a single, tandem, tridem, or quad axle located as close as possible to the corner formed by transverse crack and slab edge possible, as shown in figure

3.4.8. The magnitude of the stresses induced at the top surface of the CRCP is greater at nighttime when CRCP panels are curled upward. Loss of LTE across transverse cracks due to temperature movements and crack deterioration, accelerated by base/subbase erosion, also significantly increase critical tensile stresses.

The following factors affect the magnitude of bending stresses at the top surface of the CRCP slab:

- PCC thickness.
- PCC modulus of elasticity.
- PCC Poisson's ratio.
- PCC unit weight.
- PCC coefficient of thermal expansion.
- Base thickness.
- Base modulus of elasticity.
- Interface condition between the PCC slab and base – assumed unbonded.
- Mean crack spacing (assumed equal to 2 ft for critical segment).
- Subgrade stiffness.
- Crack LTE.
- Equivalent difference between top and bottom PCC slab surface temperature.
- Moisture distribution through the slab.
- Magnitude of permanent curl/warp gradient.
- Axle type (single or tandem).
- Axle weight.
- Axle position (distance from the critical slab edge) – varied between 0 and 18 in from the longitudinal edge.

Note 1. Since an unbonded interface is assumed between the PCC slab and the base, base unit weight is set equal to 0. This reflects that no normal tension exists between the PCC slab and the base at the unbonded interface and, therefore, the base cannot load the PCC slab.
Note 2. The coefficient of thermal expansion of the base layer is assumed equal to the PCC coefficient of thermal expansion.
Note 3. Deflection LTE of the longitudinal lane-to lane joint is assumed to be equal to 50 percent.

While many of the parameters above remain constant throughout the design period (e.g., slab thickness and joint spacing), others vary seasonally, monthly, hourly, or with pavement age. For accurate fatigue analysis results, all cases that produce significantly different stresses must be evaluated separately. The fatigue damage increments defined in this Guide were determined to account for those cases as follows:

- Pavement age – accounts for the changes in PCC modulus with age.
- Month – accounts for monthly variations in base stiffness, foundation stiffness (including the effects of moisture and temperature on the base and subbase layers incorporated in the effective k-value), and the effects of monthly variation in relative humidity on slab warping due to differential shrinkage.
- Load configuration (axle type)

- Load level
  - Single axles – 3,000 to 41,000 lb in 1,000-lb increments.
  - Tandem axles – 6,000 to 82,000 lb in 2,000-lb increments.
  - Tridem axles – 12,000 to 102,000 lb in 3,000-lb increments.
  - Quad axles – 12,000 to 102,000 lb in 3,000-lb increments.
- Temperature – the effects of temperature gradient, permanent curl/warp, and monthly variation in moisture warping expressed as the effective temperature difference (top minus bottom) – 0 °F to the minimum (most negative) value that occurs in the section in 2 °F steps.
- Load position – the procedure developed to account for the effects of traffic wander calls for calculating the damage at the critical damage location caused by the loads placed at specific lateral offsets (approximately 48-in from edge of slab).

A finite element analysis program is required to adequately solve for these critical CRCP stresses. The stress calculations in the Design Guide software is accomplished using neural networks developed based on a large number of finite element analysis runs made using ISLAB2000. The ranges of input parameters covered in the neural networks are shown in table 3.4.9. These ranges represent practical limits for each parameter.

Table 3.4.9. Ranges of input parameters for the neural network computing critical PCC stresses at the top the CRCP.

Input Parameter	**Minimum Value**	**Maximum Value**
Radius of relative stiffness [a]	22.5 in	80 in
Transverse LTE	0%	95%
Axle offset from the slab edge	0 in	18 in
Wheel aspect (width-to-length) ratio	10	0.5
Temperature difference (top – bottom)	-55 °F [b]	0 °F
Axle weight, single axle	0 lb	45,000 lb
Axle weight, tandem axle [c]	0 lb	90,000 lb
Size of the void	0 in	36 in

[a] The radius of relative stiffness of highway pavements typically fall between 22.5 and 80 in. Analyses based on plate theory become increasingly inaccurate for the radius of relative stiffness values beyond the limit shown above.

[b] Depends on PCC coefficient of thermal expansion, k-value, PCC unit weight, PCC thickness, and radius of relative stiffness.

[c] Tandem spacing is assumed equal to 51 in.

Punchout Prediction Procedure

The calibrated CRCP punchout prediction model is valid only if the fatigue damage is calculated following the procedures outlined in this section. Presented in this section is the step-by-step procedure for predicting CRCP punchouts. The steps involved include the following:

1. Tabulate input data – summarize all inputs needed for predicting CRCP punchouts.
2. Process traffic data – the processed traffic data needs to be further processed to determine equivalent number of single, tandem, and tridem axles produced by each passing of tandem, tridem, and quad axles.
3. Process pavement temperature profile data – the hourly pavement temperature profiles generated using EICM (nonlinear distribution) need to be converted to distribution of equivalent linear temperature differences by calendar month. Temperatures also used to compute the dynamic modulus of asphalt stabilized base courses.
4. Calculate crack spacing – accurate prediction of the transverse cracking pattern is extremely important for a successful CRCP design. Transverse cracking is characterized by crack spacing and crack opening. Generally, larger crack spacing results in wider crack opening and loss of LTE. Several parameters affect crack spacing and crack opening including PCC shrinkage, PCC thermal contraction, PCC tensile strength, PCC zero-stress temperature at construction, amount and depth of steel reinforcement, and base layer friction.
5. Calculate crack width and crack LTE for one month.
6. Calculate loss of support along longitudinal edge of slab for one month.
7. Calculate critical stress – calculate critical top of slab transverse stress corresponding to each load configuration (axle type), load level, lateral load position, and temperature difference for one month.
8. Calculate deterioration of crack stiffness for the month.
9. Process monthly relative humidity data – the effects of seasonal changes in moisture conditions on differential shrinkage is considered in terms of monthly deviations in slab warping, expressed in terms of effective temperature difference.
10. Calculate fatigue damage – calculate damage for each damage increment and sum to determine total damage.
11. Determine the amount of punchouts – use punchout prediction equation 3.4.47.

Steps 5 through 9 are performed for each month in the design period. Details of these steps are included as follows.

Step 1: Tabulate Input Data

Tabulate all input required for CRCP punchout prediction. The required parameters are summarized in table 3.4.10. In addition to the inputs listed in this table, the processed inputs from steps 2, 3 and 4 below are needed for the fatigue analysis.

Table 3.4.10. Summary of input parameters for CRCP punchout prediction.

Input	Variation*	Source
Design life (yr)	Fixed	Direct design input
Month of project opening	Fixed	Direct design input
PCC age at opening (mo)	Fixed	Direct design input
PCC strength for each month (psi)	Design mo	Result of PCC strength input processing (section 3.4.3.6 *Pavement Structure Input*)
PCC modulus for each month (psi)	Design mo	
Reinforcement content (%)	Fixed	Direct design input
Longitudinal reinforcement bar diameter(in)	Fixed	Direct design input
Longitudinal reinforcement bar spacing (in)	Fixed	Direct design input
Loss of bond age (mo)	Fixed	Direct design input
Type of shoulder (AC or tied PCC)	Fixed	Direct design input
PCC Poisson's ratio	Fixed	Direct design input
PCC unit weight (pcf)	Fixed	Direct design input
PCC Coefficient of thermal expansion (/°F)	Fixed	Direct design input
Ultimate shrinkage strain (10^{-6})	Fixed	Direct design input or calculated value based on PCC mix properties
Reversible shrinkage (% of ultimate shrinkage)	Fixed	Direct design input
Time to 50% ult. Shrinkage (days)	Fixed	Direct design input
Base thickness (in)	Fixed	Direct design input
Base unit weight (pcf)	Fixed	Direct design input
Monthly base modulus (psi)	Calendar mo	Result of Seasonal Analysis (section 3.4.3.6 *Pavement Structure Input*)
Monthly effective subgrade k-value (psi/in)	Calendar mo	Results of "E-to-k" conversion (section 3.4.3.6 *Pavement Structure Input*)
PCC permanent curl/warp (°F)	Fixed	Direct design input
PCC zero-stress temperature	Fixed	Direct design input or estimated from construction month and cement content
Edge-to-edge (outside) axle width (ft)	Fixed	Direct design input
Lane width (ft)	Fixed	Direct design input
Mean wheelpath (in)	Fixed	Direct design input
Traffic wander standard deviation (in)	Fixed	Direct design input
Slab width (ft)	Fixed	Direct design input
Tire pressure (psi)	Fixed	Direct design input
Axle spacing (in)	Fixed	Direct design input
Dual wheel spacing (in)	Fixed	Direct design input
Tire width (in)	Fixed	Direct design input

* Design mo: parameters that vary with pavement age; Calendar mo: parameters that vary seasonally.

Step 2: Process traffic data

The traffic inputs are first processed to determine the expected number of single, tandem, tridem, and quad axles in each month, day, and hour within the design period. This procedure is described in detail in PART 2, Chapter 4. For CRCP, each passing of an axle may cause one or more occurrences of critical loading as shown in table 3.4.11. Thus, tridem axles and quadruple axles are converted into equivalent numbers of single and tandem axles for computational purposes. The number of single and tandem axle loads over the full axle load spectrum is thus calculated and ready for use in calculation of critical stresses and fatigue damage.

Table 3.4.11. Traffic loading conversion rules for CRCP response model.

Axle Type	**Efficient number of passes**
Single	1 pass
Tandem	1 pass of tandem axle segments plus 1 pass of single axle loaded to ½ tandem axle load magnitude
Tridem	2 passes of tandem axle loaded to 2/3 tridem axle load magnitude plus 1 pass of single axles loaded to 1/3 of tridem axle load magnitude
Quadruple	3 passes of tandem axles loaded to ½ of quad axle load magnitude plus 1 pass of single axles loaded to 1/4 quad axle load magnitude

Step 3: Process temperature profile data

The EICM produces temperatures at 11 evenly spaced points through the thickness of the PCC layer on an hourly basis for every day available from the weather station database selected for the project. The equivalent linear temperature gradient is computed for each hour of every day over the period for which data is available from the weather station(s). These linear temperature gradients are then extrapolated over the design life. This data is then used to compute combined temperature curling, moisture warping, and load stresses at the top of the CRCP.

Step 4: Crack Spacing

Crack spacing is required for the determination of crack opening and for prediction of the critical tensile stresses for fatigue accumulation prediction. Crack spacing may be determined using several methods based on the construction method. If CRCP is to be constructed using a crack control option, mean crack spacing should be used for crack width and fatigue computations. If CRCP is allowed to crack randomly, external software like CRCP8 or the procedure presented herein can be used. To predict the mean crack spacing, the following is used:

$$\overline{L} = \frac{\left\{ f_t - C\sigma_0 \left(1 - \frac{2\zeta}{H} \right) \right\}}{\frac{f}{2} + \frac{U_m P_b}{c_1 d_b}} \qquad (3.4.48)$$

where,

$\overline{L}$ = mean crack spacing, in.
f_t = concrete tensile strength, psi.
f = AASHTO subbase friction coefficient from the table below based on subbase type.

U_m = peak bond stress, psi
P_b = percent steel, fraction equal to area of steel reinforcement (A_s) per area of concrete (A_c), percent. $P_b = A_s/A_c$.
d_b = reinforcing steel bar diameter, in
c_1 = first bond stress coefficient
σ_{env} = tensile stress in the PCC due to environmental curling, psi.
H = slab thickness, in.
ζ = depth to steel layer, in.
C = Bradbury's curling/warping stress coefficient (*36*).
σ_0 = Westergaard's nominal stress factor.

$$\sigma_0 = \frac{E_{PCC}\Delta\varepsilon_{tot}}{2(1-\mu_{PCC})} \tag{3.4.49}$$

μ_{PCC} = PCC Poisson's ratio.
$\Delta\varepsilon_{tot}$ = unrestrained curling and warping strain.

$$\Delta\varepsilon_{tot} = \alpha_{PCC}\Delta t_{eqv} + \varepsilon_{\infty}\Delta\left(1 - rh_{PCC}^3\right)_{eqv} \tag{3.4.50}$$

α_{PCC} = PCC coefficient of thermal expansion, /°F.
Δt_{eqv} = equivalent temperature.
ε_{∞} = ultimate shrinkage of PCC.
$\Delta\left(1 - rh_{PCC}^3\right)_{eqv}$ = relative humidity differences between the pavement surface and bottom based on formulations given by Mohamed and Hansen (*37*).

Step 5: Crack Width and Crack LTE

To predict the mean estimate of the opening of the transverse cracks at the level of the steel due to shrinkage, thermal contraction, and counteracted by the restraint of the reinforcing steel and the subbase friction, the following crack width formula is used in this design procedure:

$$cw = Max\left(L \cdot \left(\varepsilon_{shr} + \alpha_{PCC}\Delta T_{\varsigma} - \frac{c_2 f_{\sigma}}{E_{PCC}}\right) \cdot 1000 \cdot CC,\ 0.001\right) \tag{3.4.51}$$

where,
cw = average crack width at the depth of the steel, mils.
L = crack spacing based on design crack distribution, in.
ε_{shr} = unrestrained concrete drying shrinkage at the depth of the steel, $\times 10^{-6}$.
α_{PCC} = PCC coefficient of thermal expansion, /°F.
ΔT_{ζ} = drop in PCC temperature from the concrete "zero-stress" temperature at the depth of the steel for each season, °F.
c_2 = second bond stress coefficient.
f_{σ} = maximum longitudinal tensile stress in PCC at the steel level, psi.
E_{PCC} = PCC elastic modulus, psi.
CC = local calibration constant (CC = 1 for the national calibration).

The unrestrained shrinkage strain at any time t at the reinforcing steel level for an atmospheric relative humidity corresponding to a month i is given by the following equation:

$$\varepsilon_{shr}(t) = \varepsilon_{su} \cdot \left\{ 1 - \left(\frac{RH_c}{100} \right)^3 \right\} \tag{3.4.52}$$

where,

$\varepsilon_{shr}(t)$ = unrestrained shrinkage strain for month *i* at any time t days from placement, x 10^{-6}

ε_{su} = ultimate shrinkage strain (discussed in PART 2, Chapter 2), x 10^{-6}

RH_c = relative humidity in the concrete, percent

$$RH_c = RH_{ai} + (100 - RH_{ai})\, f(t) \tag{3.4.53}$$

where,

RH_{ai} = atmospheric relative humidity for month i, percent

$f(t)$ = $1/(1 + t/b)$

where,

t = time since concrete placement in days

b = $35d^{1.35}(w/c - 0.19)/4$

d = depth to steel, mm

w/c = water-to-cement ratio

The maximum longitudinal tensile stress in PCC at the steel level are calculated using the following equation:

$$f_\sigma = L\frac{f}{2} + \frac{LU_m P_b}{c_1 d_b} + C\sigma_0\left(1 - \frac{2\zeta}{H}\right) \tag{3.4.54}$$

where,

f_σ = tensile stress in the PCC due to environmental curling, psi.

L = crack spacing, in.

f = subbase friction coefficient from table 3.4.2.

U_m = peak bond stress, psi.

P_b = percent steel, fraction equal to area of steel reinforcement (A_s) per area of concrete (A_c), percent. $P_b = A_s/A_c$.

c_1 = first bond stress coefficient.

d_b = reinforcing steel bar diameter, in.

C = Bradbury's curling/warping stress coefficient (*36*).

σ_0 = Westergaard's nominal stress factor obtained using equation 3.4.49.

ζ = depth to steel layer, in.

H = PCC thickness, in.

The degree of load transfer and stiffness across the transverse cracks is key to CRCP performance, since these cracks receive the greatest magnitude of the traffic loads. As indicated in equation 3.4.51, the width of the transfer cracks is expected to vary as the average temperature of the concrete varies, which implies that load transfer will vary according to daily and seasonal temperature conditions. Average monthly temperatures at steel depth predicted by the EICM module are used to predict seasonal (monthly) changes in crack opening and changes in load transfer capacity.

Crack opening is related to the ability of crack to transfer vertical shear loads. Crack shear capacity varies with the crack opening and season as it affects crack LTE over the life of the pavement. Initial shear capacity of a non-damaged joint could be expressed using the following relation:

$$s_{0i} = 0.05 \cdot h_{PCC} \cdot e^{-0.032 cw_i} \qquad (3.4.55)$$

where,

s_{oi} = dimensionless initial shear capacity based on crack width for time increment i.
h_{PCC} = thickness of the slab, in
cw_i = crack width as a function of time and crack spacing for time increment i, mils.

The current shear capacity of the transverse cracks for any given instance in pavement life i can be characterized using the following formula:

$$s = s_{0i} - \Delta S_{i-1} \qquad (3.4.56)$$

where,

s = current crack shear capacity computed for time increment i
s_{0i} = initial crack shear capacity based on crack width for time increment i.
ΔS_{i-1} = loss in shear capacity accumulated from all previous time increments, as computed at the end of the previous time increment ($i-1$). Set equal to 0 for the first month.

Transverse crack stiffness is determined from known crack shear capacity using the following equation:

$$Log(J_c) = ae^{-e^{-\left(\frac{J_s - b}{c}\right)}} + de^{-e^{-\left(\frac{s-e}{f}\right)}} + ge^{-e^{-\left(\frac{J_s - b}{c}\right)}} \cdot e^{-e^{-\left(\frac{s-e}{f}\right)}} \qquad (3.4.57)$$

where,

J_c = joint stiffness on the transverse crack for current time increment.
a = -2.2
b = -11.26
c = 7.56
d = -28.85
e = 0.35

f = 0.38
g = 49.8
s = dimensionless shear capacity
J_s = load transfer across lane-shoulder joint; typical values are given in table 3.4.12. These values are implemented in the Design Guide software.
s = current joint shear capacity.

Table 3.4.12. Typical joint stiffness for different shoulder types.

Shoulder type	J_s
Granular	0.04
Asphalt	0.04
Tied PCC	4

Before LTE could be used in a mechanistic model for prediction of critical fatigue stresses, effect of base layer and, to some extent effect of steel reinforcement, is added to the model as follows:

$$LTE_{TOT} = 100 * \left(1 - \left(1 - \frac{1}{1 + \log^{-1}\left[(0.214 - 0.183\frac{a}{\ell} - \log(J_c) - R)/1.18 \right]} \right) \left(1 - \frac{LTE_{Base}}{100} \right) \right) \quad (3.4.58)$$

where,

LTE_{TOT} = total crack LTE due to aggregate interlock, steel reinforcement, and base support, percent.
l = radius of relative stiffness computed for time increment i, in
a = radius for a loaded area, in
R = residual dowel-action factor to account for residual load transfer provided by the steel reinforcement
= $2.5Pb - 1.25$
Pb = percent of longitudinal reinforcement
LTE_{Base} = the base layer contribution to the LTE across transverse crack, %. Typical values are given in table 3.4.8.

Step 6: Calculation of loss of support along longitudinal edge of slab

Procedures to estimate the amount of loss of support along the longitudinal edge of the CRCP slab are provided in PART 2, Chapter 2. The loss of support is calculated monthly over the design life of the CRCP. If there is significant loss of support the critical stress will increase resulting in more fatigue damage and eventually increased punchout development.

Step 7: Process monthly relative humidity data

Moisture warping is adjusted monthly based on atmospheric relative humidity. The effects of monthly variation in moisture warping are expressed in terms of equivalent temperature difference and are added to the equivalent linear temperature difference during stress calculations.

$$ETG_{SHi} = \frac{3 \cdot (\varphi \cdot \varepsilon_{su}) \cdot (S_{hi} - S_{h\,ave}) \cdot h_s \cdot \left(\frac{h}{2} - \frac{h_s}{3} \right)}{\alpha \cdot h^2 \cdot 100} \tag{3.4.59}$$

where,

ETG_{Shi}	=	temperature difference equivalent of the deviation of moisture warping in month i from the annual average, °F.
φ	=	reversible shrinkage factor, fraction of total shrinkage. Use 0.5 unless more accurate information is available.
ε_{su}	=	ultimate shrinkage (ε_{su} may be estimated based on PCC mix properties using the equation presented in PART 2, Chapter 2), x 10^{-6}:
S_{hi}	=	relative humidity factor for month i:

$S_{hi} = 1.1 \cdot RH_a$ for $RH_a < 30\%$

$S_{hi} = 1.4 - 0.01 \cdot RH_a$ for $30\% < RH_a < 80\%$

$S_{hi} = 3.0 - 0.03 \cdot RH_a$ for $RH_a \geq 80\%$

RH_a	=	ambient average relative humidity, percent.
Sh_{ave}	=	annual average relative humidity factor. Annual average of S_{hi}.
h_s	=	depth of the shrinkage zone (typically 2 in).
h	=	PCC slab thickness, in.
α	=	PCC coefficient of thermal expansion, /°F.

The temperature-difference equivalent of the monthly deviations in moisture warping (ETG_{Shi}) given by equation 3.4.59 is based on ultimate shrinkage, which takes time to develop. The ETG_{Shi} at any time t days from placement is

$$ETG_{SHt} = S_t \cdot ETG_{SHi} \tag{3.4.60}$$

where,

ETG_{Shi}	=	ETG_{Shi} at any time t days from PCC placement, °F.
ETG_{Shi}	=	temperature difference equivalent of the deviation of moisture warping in month i from the annual average, °F.

$$S_t = \frac{Age}{n + Age} \tag{3.4.61}$$

S_t	=	time factor for moisture-related slab warping.
Age	=	PCC age, days since placement.
n	=	time to develop 50% of ultimate shrinkage strain, days. Use 35 (the ACI recommended value), unless more accurate information is available (*6*).

Step 8: Calculate critical stress

Calculate the critical top of slab transverse stress for all cases that needs to be analyzed. For CRCP punchouts, the following increments are considered:

- Load configuration – axle type.
- Load level – discrete load levels in 1,000- to 3,000-lb increments, depending on axle type.
- Temperature gradient – equivalent linear temperature difference between PCC top and bottom temperatures from each hour superimposed with the equivalent temperature difference due to PCC shrinkage (equation 3.4.7) and permanent curl/warp temperature difference.
- Lateral load position – 6 specific locations for both top-down and bottom-up cracking.

The calculation of critical stresses is described in more detail in the subsection titled *Structural Response Modeling* in this section (3.4.7.3).

Step 9: Deterioration of Transverse Crack Stiffness and Crack LTE

As the concrete slab is subjected to axle load applications, vertical crack surfaces are subjected to repetitious shear loading between the two sides of the crack that leads to aggregate wear-out and decreases crack load transferring capacity. Crack shear capacity shows sufficient deterioration potential if the crack width-to-PCC thickness ratio is greater than 0.0037 (crack width and PCC thickness are expressed in the same units). The loss of shear at the end of a time increment is determined using the following equations:

$$\Delta s_i = \sum_j \left(\frac{0.005}{1 + 1 \cdot \left(\frac{cw_i}{h_{PCC}} \right)^{-5.7}} \right) \left(\frac{n_{ji}}{10^6} \right) \left(\frac{\tau_{ij}}{\tau_{ref\,i}} \right) ESR_i \qquad if \quad \frac{cw_i}{h_{PCC}} < 3.7$$

$$\Delta s_i = \sum_j \left(\frac{0.068}{1 + 6 \cdot \left(\frac{cw_i}{h_{PCC}} - 3 \right)^{-1.98}} \right) \left(\frac{n_{ji}}{10^6} \right) \left(\frac{\tau_{ij}}{\tau_{ref\,i}} \right) \cdot ESR \qquad if \quad \frac{cw_i}{h_{PCC}} > 3.7 \tag{3.4.62}$$

where,

Δs_i	=	loss in shear capacity for crack spacing as a summation over shear capacity losses due to each load application in each weight/axle group *j*.
cw_i	=	crack width for time increment *i*, mils.
h_{PCC}	=	slab thickness, in.
n_{ji}	=	number of axle load applications for load level *j*
τ_{ij}	=	shear stress on the transverse crack at the corner due to load *j*, psi.
$\tau_{ref\,i}$	=	reference shear stress derived from the PCA test results, psi.
ESR	=	equivalent shear ratio to adjust traffic load applications for lateral traffic wander.

$$ESR = a + \frac{b}{\frac{L}{\ell}} + C\frac{LTE_{crack}}{100}$$

$$a = 0.0026\overline{D}^2 - 0.1779\overline{D} + 3.2206 \qquad (3.4.63)$$

$$b = 0.1309Ln(\overline{D}) - 0.4627$$

$$c = 0.5798Ln(\overline{D}) - 2.061$$

where,

L	=	crack spacing, in.
ℓ	=	radius of relative stiffness, in.
LTE_{crack}	=	load transfer efficiency on transverse crack, percent.
$\overline{D}$	=	distance from pavement edge to the center of wheel path, in.

Reference shear stresses (τ_{ref}) are computed as follows:

$$\tau_{ref} = 111.1 \cdot e^{-e^{x'}} \qquad (3.4.64)$$

$$x' = \alpha e^{-(\lambda Ln(J_c))^{\gamma}} \qquad (3.4.65)$$

where,

Jc	=	computed joint stiffness on the transverse crack.
α	=	0.9988, a regression constant.
λ	=	0.1089, a regression constant.
γ	=	1.0, a regression constant.

The coefficients of this function may vary for different aggregate types, but preliminary test results indicate little difference in the shear wear-out behavior among mixes made with different coarse aggregate types.

As a concrete slab is subjected to more load applications, losses in shear capacity calculated for each time increment are accumulated as following:

$$\Delta S_i = \sum_{i=1}^{i=current} \Delta s_i = \Delta S_{i-1} + \Delta s_i \qquad (3.4.66)$$

where,

ΔS_i	=	loss in shear capacity accumulated over all previous time increments, including current time increment *i*
Δs_i	=	loss in shear capacity during current time increment *i* due to all weight/axle type group *j*.
ΔS_{i-1}	=	loss in shear capacity accumulated over all previous time increments excluding the current time increment *i*.

Step 10: Calculate Fatigue Damage

An incremental analysis is used to evaluate accumulated fatigue damage due to slab bending in the transverse direction, which is the main parameter used to predict CRCP punchout. The analysis period is subdivided into time increments based on pavement design life, concrete strength gain, subgrade support, and climatic conditions relative to their effect on crack width and load transfer. A separate analysis is carried out in steps for every monthly increment. The effects of temperature gradients are evaluated on hourly basis. The temperature conditions in PCC pavements vary continuously throughout each day and have a dramatic effect on the pavement structural response.

Total fatigue damage is computed by summing fatigue damages incurred during each analysis increment. Several input parameters are adjusted for different time increments, as shown in figure 3.4.50. A list of these parameters and reasons for varying their values are given in table 3.4.13.

For every time increment, the number of applied traffic loads (n_{ij}) in the traffic lane is computed using input traffic data for the analysis period. Traffic load spectra are estimated and axle load distributions developed for each axle type (single, tandem, tridem). Lateral offsets from the slab edge are also considered. Axle load distributions are used in the response model to compute maximum top of slab transverse tensile stresses for each time increment.

The maximum bending stresses (σ_{ij}) and bending strength are used to compute the number of allowable axle load applications (N_{ij}) and aggregate interlock wear due to each design wheel load (j) for each time increment (i) using the following relation:

$$\log\left(N_{i,j,k,l,m,n}\right) = C_1 \cdot \left(\frac{MR_i}{\sigma_{i,j,k,l,m,n}}\right)^{C_2} - 1 \qquad (3.4.67)$$

where,

$N_{i,j.}$	=	allowable number of load applications during time increment i due to load of magnitude j.
MR_i	=	PCC modulus of rupture at age i, psi
$\sigma_{i,j}$	=	applied stress at time increment i due to load of magnitude j.
C_1	=	calibration constant = 2.0.
C_2	=	calibration constant = 1.22.

The fatigue damage due to all design wheel loads and all traffic increments can be accumulated according to Miner's damage hypothesis by summing the damage over the entire design period using following equation:

$$FD = \sum \frac{n_{i,j}}{N_{i,j}} \qquad (3.4.68)$$

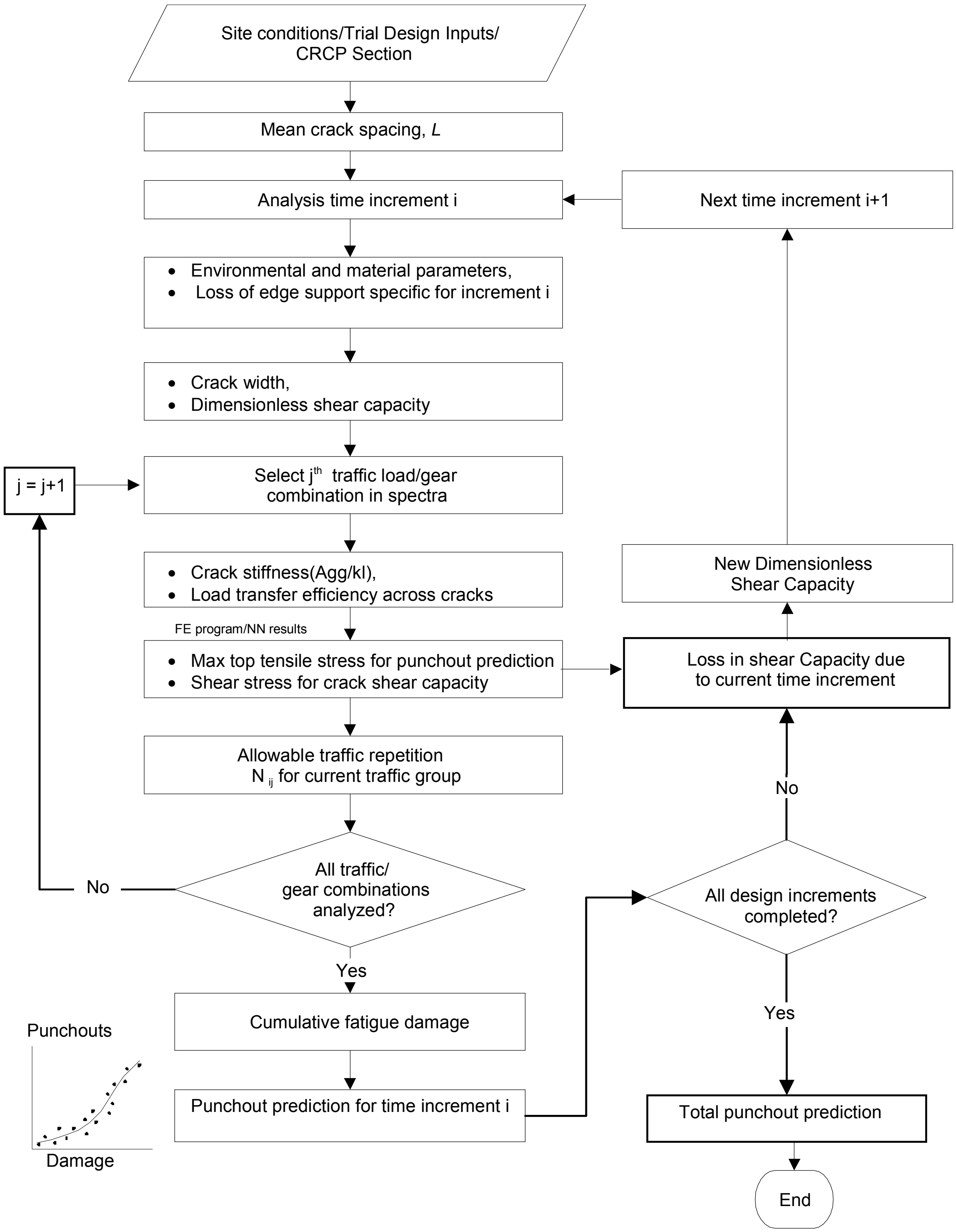

Figure 3.4.50. Punchout prediction algorithm for CRCP.

Table 3.4.13. Input parameters that change with analysis period increment.

Input Parameter	Basis for Change	Variation Considered
Number of load applications	Traffic growth through design period and seasonal variation.	Monthly increase
Temperature gradient	Changes in temperature conditions in the PCC layer.	Hourly change
Ambient relative humidity	Seasonal changes in moisture conditions.	Average value for each month of the year
Subgrade modulus	Seasonal changes in subgrade stiffness due to moisture and temperature conditions	Average value for each month of the year
Pavement support conditions	Loss of support due to erosion throughout design period	Monthly variation
Crack LTE	Incremental wear out of crack aggregate interlock	Monthly variation
Concrete strength	Incremental strength gain throughout design period	Monthly increase
Transverse crack width	(1) Increasing opening over time due to continuous drying shrinkage. (2) Monthly/seasonal variation (as function temperature and moisture).	Monthly variation

where,

FD = accumulated fatigue damage over the design period for current crack spacing occurring at the critical fatigue location in the slab.
n_{ij} = number of applied axle load applications of the j^{th} magnitude evaluated during the i^{th} traffic increment.
N_{ij} = number of allowable axle load applications of the j^{th} magnitude evaluated during the i^{th} traffic increment to crack initiation in PCC.
i = counter for number of analysis time increments.
j = counter for the magnitude of load.

Step 11: Determine the amount of punchouts

After total damage is computed, the mean number of punchouts per mile is predicted using the nationally calibrated model given in equation 3.4.47.

Design Reliability for CRCP Punchouts

CRCP pavements designed with the punchout model given in equation 3.4.47 will have 50 percent design reliability. That is, they are just as likely to fail before the design life as after the design life. For design purposes a higher reliability than 50 percent will normally be specified. In these circumstances the predicted punchouts must be adjusted upwards to ensure the desired level of reliability. The equations used to adjust predicted mean punchouts at any given level of reliability is presented below:

$$PO_R = PO + Z_R S_P \tag{3.4.69}$$

where,

PO_R	=	predicted punchouts at reliability level R, no./mile.
PO	=	incremental change (monthly) in mean punchouts, no./mile.
Z_R	=	standard normal deviate for the given reliability level R.
S_P	=	standard deviation of PO at the predicted mean punchout level, no./mile.

$$S_P = 4.04 * \mathrm{PO}^{0.3825} \tag{3.4.70}$$

Equation 3.4.70 may be modified based on local calibration. Figures 3.4.51 and 3.4.52 (two different CRCP projects) show that increased reliability level results in increased predicted punchouts. This means that modification of design may be needed to increase reliability that the CRCP will meet punchout performance criteria at the end of the design life.

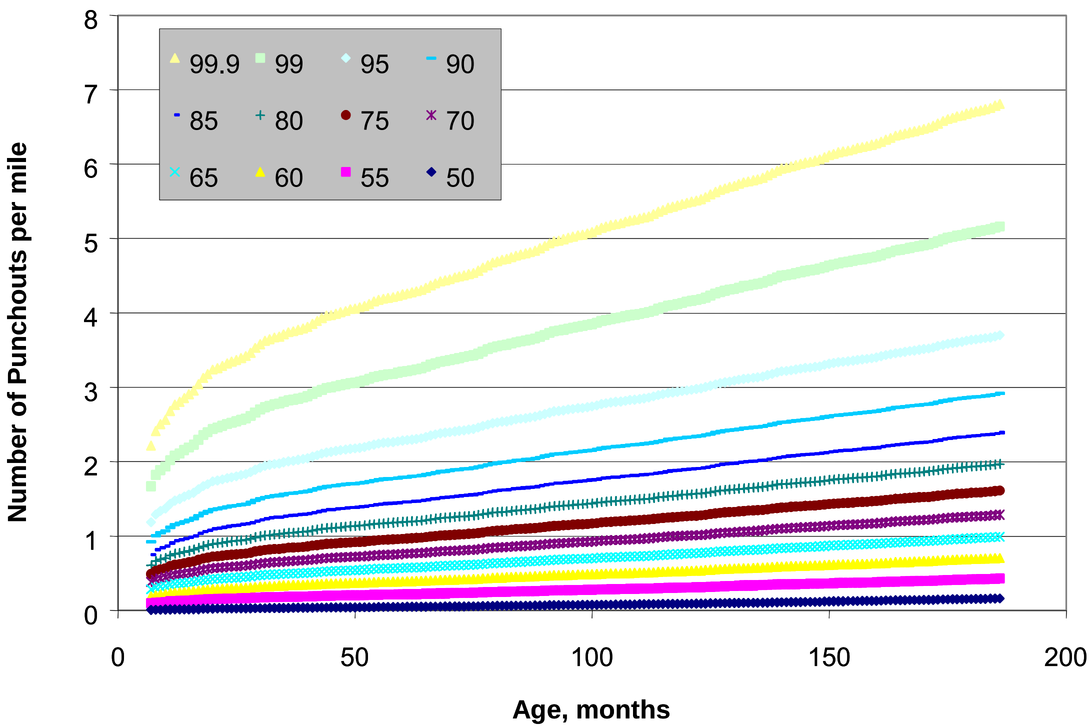

Figure 3.4.51. Illustration of effect of design reliability on punchout prediction (case 1).

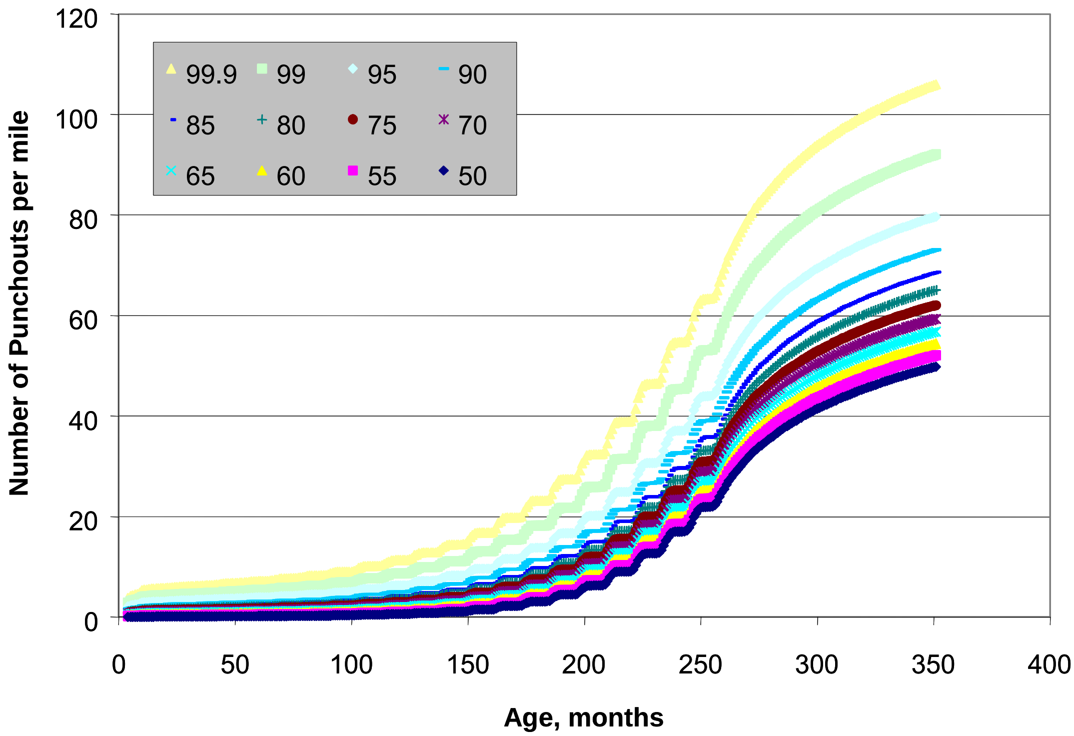

Figure 3.4.52. Illustration of effect of design reliability on punchout prediction (case 2).

<u>Modification of CRCP Design Features to Reduce Punchouts</u>

The CRCP design procedure requires the selection of a trial design. This design is then analyzed and punchouts and smoothness (IRI) are predicted over the design life. If these exceed their design criteria, the trial design must be modified. Crack spacing, associated crack width, slab thickness, and poor support conditions are the primary factors affecting CRCP performance and punchout development. The following summarizes potential modifications of design features to reduce punchout occurrence:

- **Increase slab thickness**. An increase in CRCP slab thickness will reduce punchouts based on (1) a decrease in tensile stress at the top of the slab, (2) an increase in shear capability and a greater tolerance to maintain a high load transfer capability at the same crack width that also allows for reduced tensile stress at top of the slab, and (3) improvement of shear capacity of transverse cracks and reduced damage. Figure 3.4.53 shows an example illustrating the significant effect of slab thickness on punchout development.
- **Increase percent longitudinal reinforcement**. Even though an increase in steel content will reduce crack spacing, it has been shown to greatly reduce punchouts overall due to tightly closed cracks and less loss of LTE. Figure 3.4.54 shows the significant effect of the percent reinforcement on punchout development.

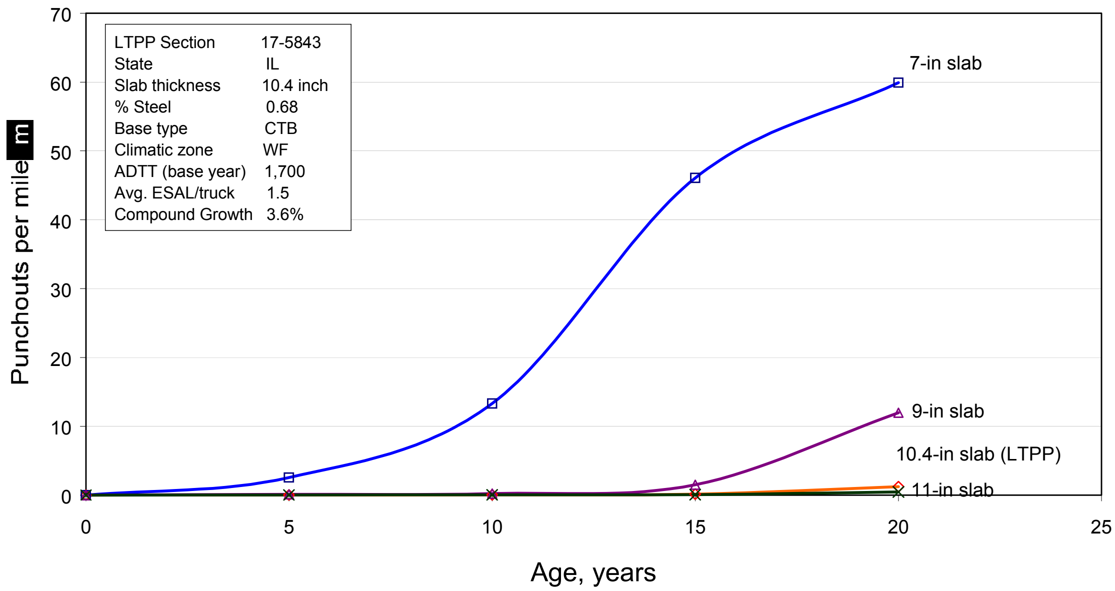

Figure 3.4.53. Predicted number of punchouts for sections with various CRCP slab thickness.

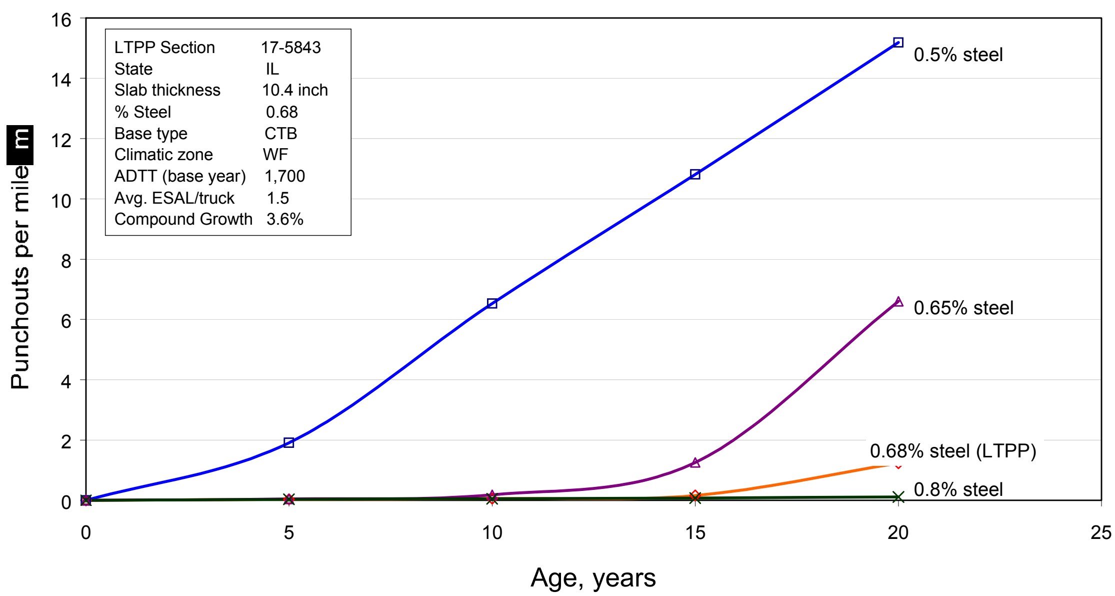

Figure 3.4.54. Predicted number of punchouts for sections with various percent of longitudinal reinforcement.

- **Reduce the depth of reinforcement**. Placement of steel closer to the pavement surface reduces punchouts through keeping cracks tighter. (However, do not place closer than 3.5 in from the surface to avoid construction problems and limit damage from infiltration of chlorides.) Figure 3.4.55 shows an example of the effect of depth of reinforcement on punchout development.
- **Increase PCC strength**. An increase in PCC strength will result in lower fatigue damage in the PCC. Figure 3.4.56 shows an example plot showing the relative effect of PCC flexural strength on punchout development. However, if increased strength is gained by increased cement content, the increased α_{PCC} and shrinkage will result.
- **Reduce coefficient of thermal expansion**. Use of a lower thermal coefficient of expansion concrete will reduce crack width opening for the same crack spacing. Figure 3.4.57 shows an example of the effect of the coefficient of thermal expansion of PCC on punchout development. Optimizing the mix design can lead to a reduction in punchouts.
- **Increase maximum aggregate size**. The larger the maximum size, the better the aggregate interlock.
- **Provide an erosion-resistant base**. Use of a strong and erosion resistant base system will provide a more uniform and structural adequate support. Use of bases with high friction coefficient reduces mean crack spacing and provides tighter cracks.
- **Minimize permanent curl/warp.** The magnitude of permanent curl/warp can have a very significant effect on punchout development. Figure 3.4.58 shows an illustration of this significant effect.

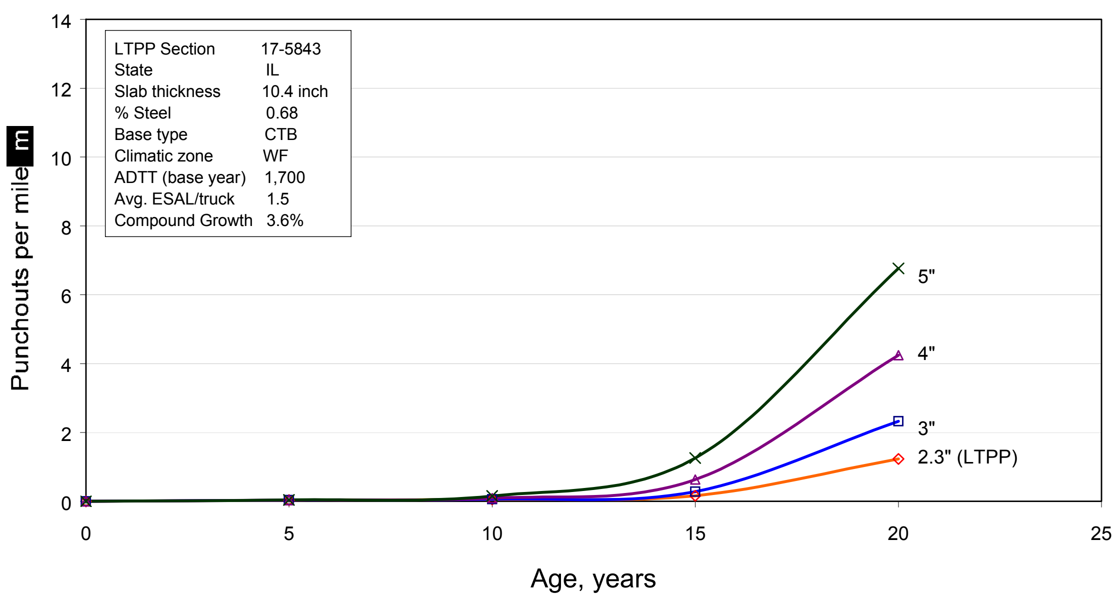

Figure 3.4.55. Predicted number of punchouts for sections with various reinforcement depths.

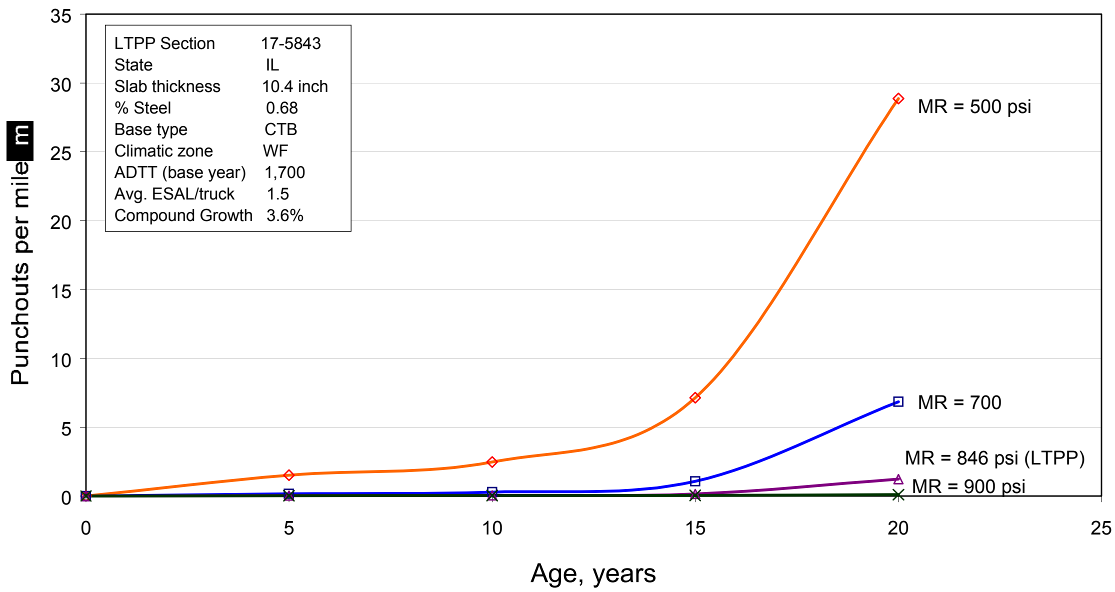

Figure 3.4.56. Predicted number of punchouts for sections with various PCC modulus of rupture (does not reflect the impact of increased shrinkage or α_{PCC}).

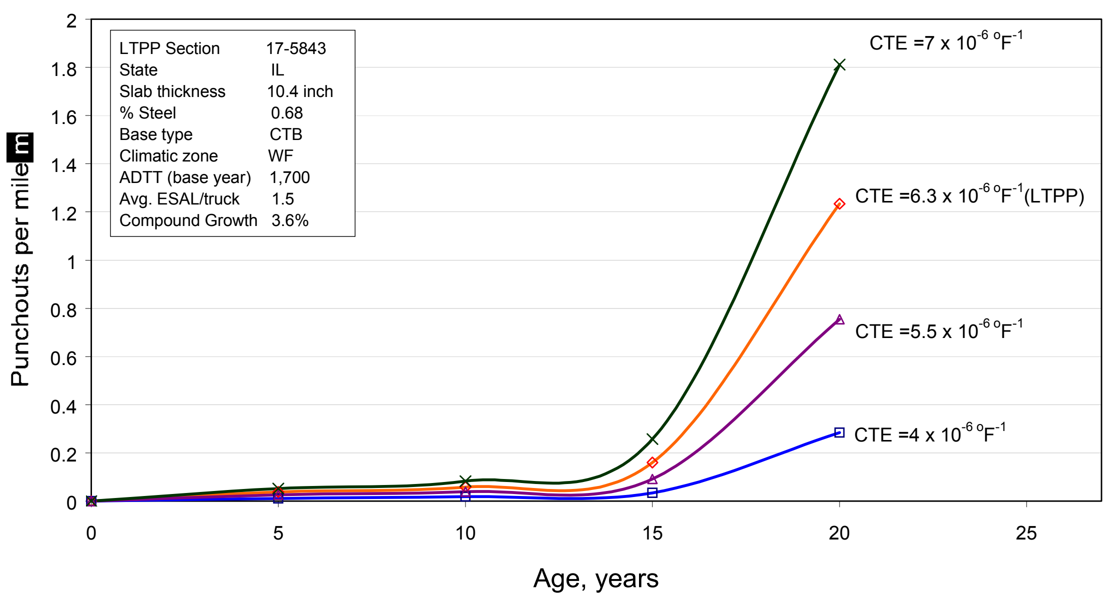

Figure 3.4.57. Predicted number of punchouts for sections with various PCC coefficient of thermal expansion.

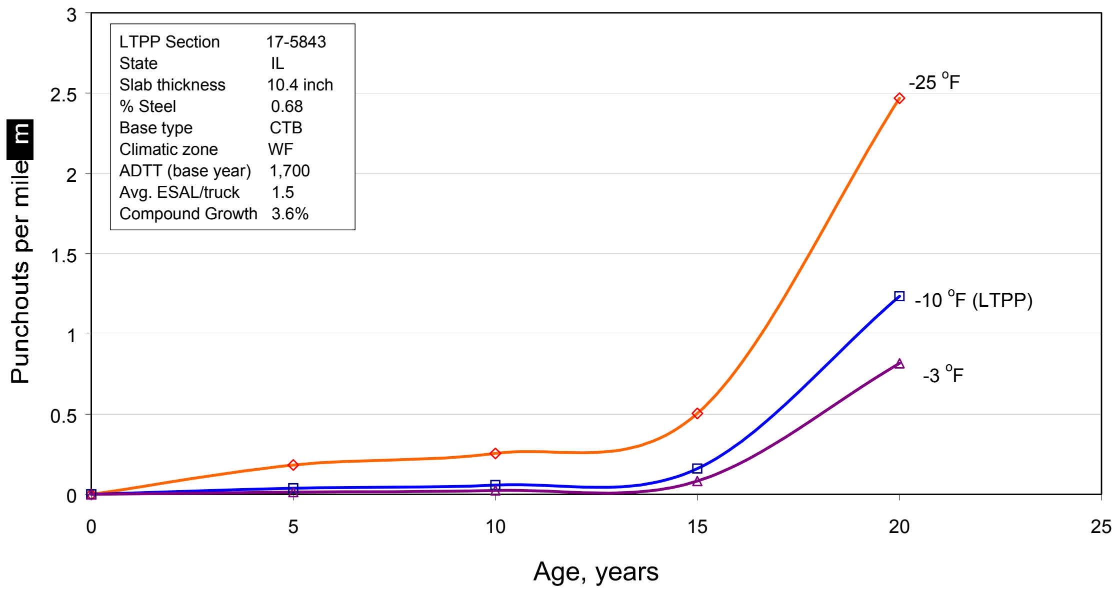

Figure 3.4.58. Predicted number of punchouts for sections for a range of permanent curl/warp effective temperature gradients.

3.4.7.4 CRCP Smoothness

The smoothness of CRCP is the most critical consideration for the traveling public. A typical highway pavement loses smoothness over time until it requires rehabilitation or restoration. Smoothness has normally not been a problem with CRCP unless punchout distress (along with poor full-depth repairs of these punchouts) becomes too high. For example, the CRCP included in the LTPP program have demonstrated very low IRI values over many years. Nonetheless, it is desirable to place limits on smoothness to ensure that a CRCP will perform as required over the design period. The critical level of smoothness should depend on its effect on highway users' assessment of ride quality.

<u>Factors Affecting CRCP Smoothness</u>

In the Design Guide approach CRCP smoothness is estimated based on initial smoothness, punchouts, and site conditions. The effects of punchouts and some site factors, e.g., subgrade percent passing the number 200 sieve and freezing index are presented in figure 3.4.59 and discussed in the following paragraphs.

Effect of Punchouts

Low-severity punchouts are described as the area enclosed by two closely spaced (usually less than 2 ft) transverse cracks, a short longitudinal crack, and the edge of the pavement or a longitudinal joint. The "Y" cracks that exhibit spalling, breakup, and faulting are also described as punchouts. Medium- and high-severity punchouts are heavily spalled and faulted, and the concrete within the punchout is punched down or broken up in pieces.

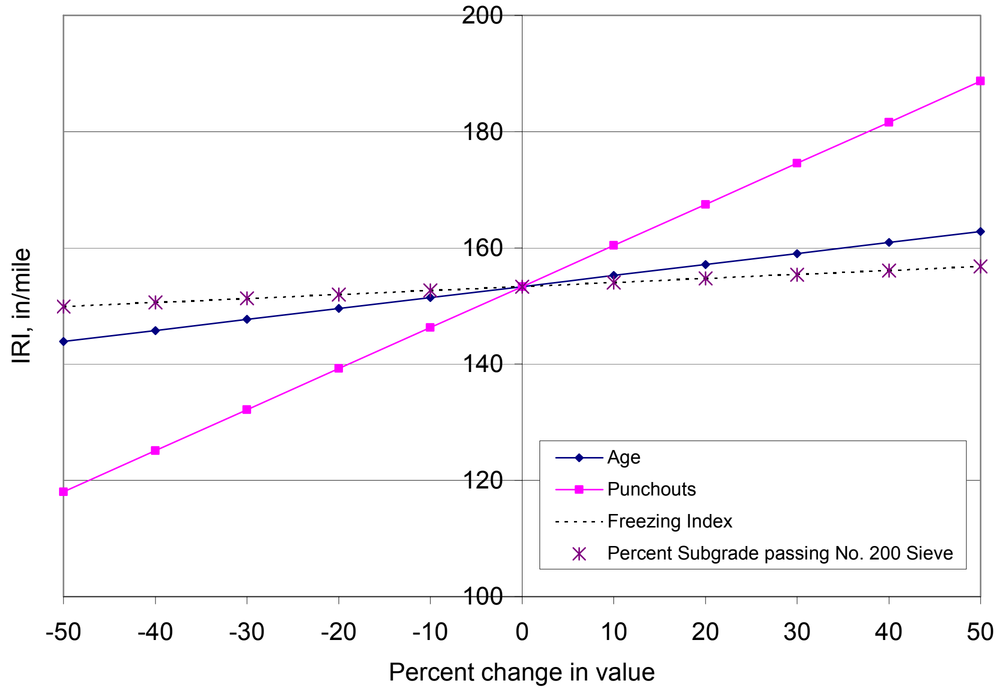

Figure 3.4.59. Effect of distress and site variables on CRCP smoothness.

This leads to very rough sections of pavement and, hence, a decrease in smoothness. Punchouts are often patched before reaching high severity. Figure 3.4.59 shows the effect of an increasing number of punchouts (of all severities) on pavement smoothness. As is evident, the predicted IRI is very sensitive to the number of punchouts per mile.

Effect of Pavement Site Conditions

The influence of pavement site conditions on smoothness of CPCP is similar to that for JPCP. Figure 3.4.59 shows that the influence of freezing index and subgrade fines on predicted CRCP smoothness.

<u>Smoothness Prediction</u>

Smoothness is the result of a combination of the initial as-constructed profile of the pavement and any change in the longitudinal profile over time and traffic. These changes can occur for many reasons, but the development of certain pavement distresses will affect smoothness greatly. Key distresses affecting the IRI for CRCP include punchouts and transverse cracking. Thus, building a smooth pavement and then preventing distresses from occurring is a key design objective. The IRI model for CRCP is given as follows:

$$IRI_M = IRI_I + \mathrm{C1} \bullet PO + \mathrm{C2} \bullet SF \qquad (3.4.71)$$

where,

IRI_I = initial IRI, in/mi.
PO = number of punchout/mi at all severity levels (low, medium, and high).

SF = site factor

= $AGE \cdot (1 + 0.556\ FI) \cdot (1 + P_{200}) * 10^{-6}$

AGE = pavement age, yr.

FI = freezing index, °F days.

P_{200} = percent subgrade material passing No. 200 sieve.

$C1$ = *3.15*

$C2$ = *28.35*

Model Statistics:

R^2 = 0.60

SEE = 14.6 in/mile

N = 94

CRCP Smoothness Reliability

The predicted CRCP smoothness given by equation 3.4.71 has 50 percent design reliability. The equations used to adjust predicted mean smoothness at any given level of reliability is presented below:

$$IRI_R = IRI_M + Z_R STD_{IRI} \quad (3.4.72)$$

where,

IRI_R = predicted IRI at reliability level R, percent, in/mi.

IRI_M = predicted IRI at 50 percent reliability level, in/mi.

Z_R = standard normal deviate for the given reliability level R (one tail distribution).

STD_{IRI} = standard deviation corresponding to the predicted IRI level, in/mi.

$$STD_{IRI} = \left(Var_{IRIi} + C1^2 \cdot Var_{PO} + S_e^2\right)^{0.5} \quad (3.4.73)$$

Var_{IRIi} = variance of initial IRI (obtained from LTPP) = 29.16 $(\text{in/mi})^2$.

Var_{PO} = variance of punchout [equation 3.4.70]) $(\text{No./mi})^2$.

S_e^2 = variance of overall model error = 213.2 $(\text{in/mi})^2$.

Equation 3.4.73 may be modified based on local calibration.

Modification of CRCP Design to Improve Smoothness

When the trial design produces an IRI that does not meet the performance criteria selected by the designer, the trial design can be modified to lower the IRI. Some of the most effective ways to accomplish this are as follows:

- **Construct the pavement very smooth**. Smoothness specifications that offer significant incentives to build a smooth pavement are standard in many states. These specifications have had a dramatic effect, decreasing the mean IRI over a period of several years of implementation. Thus, it is well known now that a very smooth pavement can be

constructed. This will provide the customer with a smoother pavement over a long period of time.
- **Minimize or eliminate punchouts**. The smoothness prediction model shows that smoothness loss occurs from the development of punchouts. The effect of punchouts can be very significant. All factors affecting punchouts can be varied to minimize their occurrence. Particularly, maintaining small crack widths are critical.

3.4.8 SPECIAL LOADING SITUATIONS

The Design Guide software traffic inputs allows for a wide range of truck type, tire, and axle configurations as follows:

- Ten different vehicle types (class 4 to 13).
- Single, tandem, tridem, and quad axles with variable spacing between axles (for multiple axle configurations).
- Either dual tires or a single tire with variable spacing of the dual tires.
- Variable tire pressure.
- Definable truck tractor axle spacing between steering and drive axles.

Normal design conditions include the consideration of a wide mix and range of single, tandem, tridem, and quad axles of widely varying weights. However, the traffic input also allows the designer to conduct an analysis with a single special vehicle type (10 vehicle types are available) with specific axle weights and tire configurations as described above. For example, a user can analyze the impact of a truck having a single steering axle with weight of 16 kips and a tridem axle weighing 100,000 pounds with super single tires with a tire pressure of 145 psi.

The Design Guide software handles special vehicles, either separately or in combination with other vehicles, by explicitly defining traffic volume, axle spacing, axle distribution, tire pressure, and vehicle distribution in main traffic dialog boxes.

For example, a special vehicle (say of approximately Class 7 configuration) analyzed separately could be modeled as follows:

- Entering the Traffic dialog box and entering volume values for the vehicle.
- Entering the Traffic Volume Adjustment Factors dialog box including the Vehicle Class Distribution and setting values to the desired percentage (e.g., 100% Class 7 vehicle).
- Entering the Axle Load Distribution Factors dialog box and setting the appropriate single, tandem, tridems, and/or quads to 100% for the desired special vehicle axle weights (note, there is not need to set other class vehicle axle weights to zero because this can be more simply handled buy entering appropriate zeros in the Number Axles/Truck dialog box as described under the next item.
- Enter the Number of Axles/Truck dialog box and enter zeros for all vehicles except the special vehicle (e.g., Class 7), then enter the appropriate mean axles/truck for the special vehicle for each axle.

- Enter the Axle Configuration and Wheel Base dialog boxes and set the proper values for the special vehicle.

The advantage of using this method, which is included for both rigid and flexible pavements, is that this special vehicle can be directly mixed and modeled with other traffic on the pavement (i.e. it can be run with and without the special vehicle, to determine the change in performance due to allowing a special vehicle in the traffic mix.)

If a completely nonstandard axle configuration needs to be analyzed (such as a quad axle with 12 tires spread across the traffic lane) a separate analysis is required to determine an equivalent single, tandem, tridem, or quad axle that would produce the same stress or deflection. The can be accomplished using the following procedure:

1. Conduct a finite element analysis to compute critical bending stress at the top or bottom surface of the PCC slab or PCC slab corner deflections for the nonstandard axle and tire configuration.
2. Determine the standard single, tandem, tridem, or quad axle that produces the same critical stress (or deflection).
3. The damage caused by the nonstandard axle can be analyzed either by (a) adding the number of additional passes of the equivalent standard axles to the normal axle distributions, or (b) considering only the special vehicle.

If the different basis of equality (stress or deflection) produces different equivalent axle loads, then the analysis of cracking and faulting for JPCP should be conducted separately.

3.4.9 CALIBRATION TO LOCAL CONDITIONS

Any agency interested in adopting the design procedure described in this guide should prepare a practical implementation plan. The plan should include achieving full departmental support, selecting procedures to obtain all inputs and establishing local data and defaults for inputs, training of staff, acquiring of needed equipment, acquiring of needed computer hardware, and calibration/validation to local conditions.

The mechanistic-empirical design procedure in this guide represents a major improvement and paradigm shift from existing empirical design procedures (e.g., AASHTO 1993), both in design approach and in complexity. The use of mechanistic principles to both structurally and climatically (temperature and moisture) model the pavement/subgrade structure requires much more comprehensive input data to run such a model (including axle load distributions, improved material characterization, construction factors, and hourly climatic data such as ambient temperatures, precipitations, solar radiation, cloud cover, and relative humidity). Thus, a significant effort will be required to evaluate and tailor the procedure to the highway agency. This will make the new design procedure far more capable of producing more reliable and cost-effective designs, even for design conditions that deviate significantly from previously experienced (e.g., much heavier traffic).

It is important to realize that even the original (relatively simple) AASHTO design procedures, originally issued in 1962 and updated several times since, required many years of implementation by State highway agencies. The agencies focused on obtaining appropriate inputs (such as mean PCC modulus and flexural strength), applying calibration values for parameters like the "regional" or climatic factor, subgrade support and its correlation with common lab tests, traffic inputs to calculate equivalent single axle loads, and many other factors. In addition, many agencies set up test sections that were monitored for 10 or more years to further calibrate the design procedure to local conditions. Even for this relative simple procedure by today's standards, many years were required for successful implementation by State highway agencies.

3.4.9.1 Need for Calibration to Local Conditions

Clearly, the mechanistic-empirical Design Guide procedure will require an even greater effort to successfully implement a useful design procedure. Without calibration, the results of mechanistic calculations (fatigue damage and differential energy) cannot be used to predict slab cracking, joint faulting, crack width, or punchouts. For JPCP slab cracking, none of the direct pavement responses (deflection, stress, or strain) can be used directly to predict the rate of crack development because a complex algorithm is required to model the cracking mechanism that produces "damage". This damage must be correlated with actual cracking in the field. Actually, the distress mechanisms are far more complex than can be practically modeled; therefore, the use of empirical factors and calibration is necessary to obtain realistic performance predictions.

The Design Guide is largely based on mechanistic engineering principles that provide a fundamental basis for the structural design of pavement structures. The JPCP and CRCP design procedures have been calibrated using design inputs and performance data largely from the national LTPP database, which includes sections located throughout significant parts of North America. The distress models specifically calibrated included:

- JPCP joint faulting.
- JPCP transverse cracking.
- CRCP punchouts (with limited crack width calibration).

This calibration effort was a major iterative work effort that resulted in distress prediction models with national calibration constants. The calibration curves generally represent "national" performance of JPCP and CRCP in the LTPP database and other national data. Whatever bias included in this calibration data is naturally incorporated into the distress prediction models. The national calibration may not be entirely adequate for specific regions of the country and a more local or regional calibration may be needed.

The IRI models for both JPCP and CRCP are empirical in nature and were developed directly from the LTPP data available for each family of pavements (JPCP, CRCP). Further validation for a local agency may not be needed, but could be accomplished if desired as described in this section.

3.4.9.2 Approach to Calibration

Because this design procedure is based on mechanistic principles the procedures should work reasonably well within the inference space of the analytical procedure and the performance data from which the procedure was calibrated. However, this is a very complex design procedure and it must be carefully evaluated by highway agencies wishing to implement. The following is the recommended calibration/validation effort required to implement this mechanistic-empirical design procedure for rigid pavements:

1. Review all input data.
2. Conduct sensitivity analysis.
3. Conduct comparative studies.
4. Conduct validation/calibration studies.
5. Modify input defaults and calibration coefficients as needed.

Review All Input Data

All inputs to the Design Guide software should be reviewed with two major goals in mind.

- Determine the desired level and procedures for obtaining each input on various types of design projects (low volume as compared to high volume, where achieving an adequate design is more critical). The Design Guide allows three levels of inputs and each level has different procedures for many inputs.
    - Level 1—site-specific testing data such as laboratory testing of soils and materials, FWD testing and backcalculation, and ATC and weigh-in-motion (WIM) testing on site.
    - Level 2—regional factors and material properties from available testing procedures or correlation equations (e.g., use of compressive strength to estimate modulus of rupture).
    - Level 3— typical local values (if known) or default values based on experience.

    Note that the LTPP data available for the calibration of this Design Guide procedure was a mixture of all levels. Several inputs are very critical but are not well defined and these are the ones where the agency should conduct sensitivity analysis as described below.
- Determine if defaults provided with the Design Guide software are appropriate for the agency and if not, modify as needed.
- Select allowable ranges for inputs for various types of projects within the geographical area of the agency (low volume, high volume, different geographic areas within the state).
- Select procedures to obtain these inputs for regular design projects (e.g., traffic volume and weight inputs). Determine the effects of the accuracy of input values on the resulting design.
- Conduct necessary testing to establish specific inputs (e.g., PCC coefficient of thermal expansion for different aggregate types, mean PCC elastic modulus, mean PCC modulus of rupture for various paving mixtures, PCC ultimate shrinkage for various paving mixtures, axle load distributions for types of axles), acquire needed equipment for any testing required.

- Conduct analyses to establish the desired level of design reliability for various types of highways (e.g., Interstate, primary, secondary) or levels of traffic. Typical values are provided in PART 1, Chapter 1 but these need to be evaluated by each agency. This will require running the software for various projects over a range of design reliability levels and examining what experienced engineers believe is a reasonable level of design reliability for each type of project.

Sensitivity Analysis

Each agency should conduct sensitivity analysis of the new design procedure. This is accomplished by selecting a typical design situation with all design inputs. The software is run and the mean distresses and IRI predicted over the design period. Then individual inputs are varied, normally one at a time (unless two or more are correlated and then two or more are varied in unison as would occur in nature such as PCC modulus of elasticity and strength) and the change in all outputs observed. Appropriate tables and plots are prepared and the results evaluated. Inputs can be divided into three groups for example:

1. Those that have very significant effect on one or more outputs.
2. Those that have a moderate effect on one or more outputs.
3. Those that have only minor effect on one or more outputs.

Those inputs that belong to group No. 1 must be selected more carefully than No. 3, as they will have a very significant effect on design. The above sensitivity may be repeated for low, medium and high traffic project designs to see if that has an effect on inputs.

Comparative Studies

Conduct comparisons of designs from the Design Guide with those of the existing procedure in use by the agency. Select typical design situations (previous designs would be ideal) and obtain the design inputs for the Design Guide. Run the software and determine the distresses and IRI over the analysis period. Evaluate the adequacy of the design based on the results and agency performance experience. If deficiencies exist in the design guide predictions, determine the reasons if possible.

Calibration to Local Conditions

The national calibration-validation process was been successfully completed for both JPCP and CRCP and several types of PCC rehabilitations. Although this effort was very comprehensive, further validation study is highly recommended as a prudent step in implementing a new design procedure that is different from current procedures. A validation database should be developed to confirm that the national calibration factors or functions are adequate and appropriate for the construction, materials, climate, traffic, and other conditions that are encountered within the agencies highway system.

Prepare a database of agency performance data and compare the new design procedure results with the performance of these "local" sections. This will require the selection of at least 20 JPCP or 20 CRCP sections around the state. If the state has very distinct climates this should be done in each climate.

The goal of the calibration-validation process is to confirm that the performance models accurately predict pavement distress and ride quality on a national basis. For any specific geographic area, adjustments to the national models may be needed to obtain reliable pavement designs.

<u>Modify the Calibrations/Inputs</u>

If significant differences are found between the predicted and measured distresses and IRI for the agencies highways, appropriate adjustments must be made to the calibration coefficients. This study will also establish the level of accuracy desirable for key input parameters and default input values. Make modifications to the new procedure as needed based on all of the above results and findings. These results could then be used to establish a new standard deviation model for use in reliability design as subsequently discussed to provide a more cost effective design.

3.4.9.3 Performance Prediction Models

The Design Guide includes the following three performance models for JPCP design:

- Slab cracking (from fatigue damage).
- Joint faulting.
- Smoothness (IRI).

The following performance models are used for CRCP design:

- Punchouts and crack width.
- Smoothness (IRI).

<u>Slab Cracking (JPCP)</u>

Fatigue cracking is the main basis of slab thickness design in the Design Guide. Two modes of cracking failure are considered: top-down and bottom-up. Numerous factors affect fatigue cracking in JPCP. For calibration and validation of the cracking model, evaluation of the following factors is important:

- PCC properties—various PCC properties are very important to accurate modeling of JPCP slab cracking. A few of the more significant properties are presented.
- Coefficient of thermal expansion—curling stress is a dominant factor that affects cracking performance. Accurate value of thermal coefficient is very important to ensure reliable results. Testing should be conducted to determine typical values for the type of aggregates and PCC mixes. Based on testing results, recommendations can be made on whether the use of typical value (based on mix design and aggregate type) is sufficient or project-specific testing is needed.

- PCC modulus of rupture and elastic modulus—the mean strength and modulus are the required inputs, not the minimum required for construction (which is often much lower than the mean achieved on projects). Testing results from previous projects (if they exist) or from new lab tests should be used to build a database of these values. Strength and modulus gain over time is very important since fatigue damage is calculated incrementally. The validation study should include a testing program to verify the PCC strength-gain model. An increase in PCC strength is typically accompanied by an increase in elastic modulus, α_{PCC}, and shrinkage which must be taken into consideration to obtain accurate analysis results. The testing program should include the modulus testing to ensure that the correlation between PCC strength and modulus is reasonable.
- PCC shrinkage—the surface of PCC pavements can dry significantly, while the relative humidity within the PCC remains constant at 85 percent or higher at 2 in or greater depths, even in very dry areas. This difference in moisture condition can cause significant warping of PCC slabs, which affects curling stresses. Testing should be conducted to determine the shrinkage characteristics of PCC used by the agency.
- Temperature profiles—the temperature conditions in PCC pavements vary continuously throughout a 24-hour day. For accurate fatigue damage assessment, consideration of hourly temperature profiles is highly desirable. In the Design Guide, this is accomplished through the use of an analytical model (Enhanced Integrated Climatic Model [EICM]) that predicts temperature profile in PCC slabs based on hourly climatic data, which are readily available from the National Oceanic and Atmospheric Administration. This model is capable of producing accurate results, but local calibration is highly recommended to ensure that the model predictions closely match actual temperature profiles. The calibration of EICM involves making adjustments to model parameters (e.g., thermal conductivity, heat capacity, emissivity) to match measured temperatures.
- Permanent curl/warp effective temperature difference—as a result of temperature gradients built into the PCC slabs during construction and differential permanent shrinkage, PCC slabs are not flat even when no temperature gradient is present. The magnitude of permanent curl/warp can be variable even along a given project as climatic conditions and PCC mixtures change. In the Design Guide, the magnitude of effective permanent curl/warp was determined by optimization based on national calibration results. The magnitude of effective permanent curl/warp for differing curing procedures and construction temperatures can be determined through local field studies.

<u>Joint Faulting (JPCP)</u>

Faulting is a key performance factor that affects ride quality of JPCP. All of the parameters outlined for slab cracking are also applicable to faulting performance. In addition, calibration and validation study for the faulting model should include the following parameters:

- Dowel diameter—the dowel diameter is the most dominant factor affecting the faulting performance of doweled PCC pavements. The performance of pavements with various size dowels should be evaluated to verify model predictions.
- Base type—base type and quality (resistance to erosion) is a significant factor affecting faulting performance, especially on nondoweled pavements. The performance of

pavements constructed on different types of bases should be evaluated to verify model predictions and erosion index.

- Joint opening—joint movements is an important parameter in the Design Guide faulting model; however, the faulting model was calibrated using calculated joint opening values because measured values were unavailable. The testing program for the validation study should include monitoring of the joint movements to ensure that the values used in calibration are realistic. The PCC zero-stress temperature minus the actual PCC slab temperature is an influential input to joint opening. Further verification of this parameter would be very helpful.

<u>Punchouts (CRCP)</u>

Practically all of the factors for slab cracking and joint faulting are also important to CRCP. Specifically, crack width (predicted at steel depth), and crack load transfer efficiency should be carefully controlled within the climate and materials of the local agency. These depend on crack spacing prediction, which is dependent on many of the above parameters and slab/base friction. The PCC zero-stress temperature minus the actual PCC slab temperature is an influential input to crack opening. Further verification of this parameter would be very helpful. The permanent curl/warp discussion for JPCP applies also to CRCP. Reduction of this factors is beneficial to CRCP.

One approach is to obtain data from previous CRCP projects constructed and run the software to predict crack spacing, crack width, and crack LTE to see how close to reality they actually predict. This leads to review of the various inputs for CRCP (such as the slab/base friction factor to more accurately predict crack spacing) and a modification of the crack width calibration constant (which has a default of 1.0 but can be varied lower or higher depending on which way the adjustment is needed).

<u>Smoothness (JPCP, CRCP)</u>

Ride quality/smoothness is one of the more common performance indicators used by State highway agencies for both design and pavement management purposes. One key concept included in the Design Guide is that there is a defined relationship between distress and smoothness (as measured by IRI). In other words, certain distresses have a significant effect on the IRI measured over time. Thus, smoothness is considered a key element or parameter in the experiment. Initial smoothness is a direct design input to the Design Guide and has a major effect on future smoothness. This input is highly dependent upon the smoothness specifications under which the project is constructed. Obtaining data from recently constructed projects is important to establishing this input.

For rigid pavements, two models are included in the guide. The models are suitable for use in new pavement and rehabilitation design. Inputs for these models include cracking, faulting, initial smoothness, and site conditions for JPCP. The models for rehabilitation design include maintenance related variables such as patching.

Design Reliability

The design reliability and its associated standard deviation for each of the distress models are based on the results from the national database. Specifically, the residual error (or standard deviation) of the difference between "predicted" distress and "observed" or measured distress is computed as a function of predicted distress from the national calibration database. This error can be quite large and it essentially results in a more costly pavement design for a local agency.

If a highway agency makes improvements to the inputs and calibration of the models using local pavement sections, this may reduce this error of prediction. A new relationship for the standard deviation used in design reliability could be developed using the local calibration data from the agency. The effect of this improvement could be a more cost effective pavement design since there is less uncertainty or error in the design.

Agency should not use the same design reliability level as in previous Guide. This should be established by the agency based on local condition.

REFERENCES

1. Khazanovich, L., H. T. Yu, S. Rao, K. Galasova, E. Shats, and R. Jones. (2000). *ISLAB2000 - Finite Element Analysis Program for Rigid and Composite Pavements*. User's Guide. ERES Consultants Division of Applied Research Associates, Inc., Champaign, IL.
2. Yu, H. T., K. D. Smith, M. I. Darter, J. Jiang and L. Khazanovich (1998). *Performance of Concrete Pavements Volume III - Improving Concrete Pavement Performance*. Final Report, FHWA-RD-95-111, Federal Highway Administration, McLean, VA.
3. Poblete, M. (1986). *Informe Anual 1986*, Control y Seguimiento de Pavimentos de Hormigon, IDIEM-Direccion de Vialidad, Universidad de Chile.
4. Darter, M. I., J. M. Beck, M. B. Snyder, and R. E. Smith (1985). *Portland Cement Concrete Pavement Evaluation System-COPES*, NCHRP Report 277, Transportation Research Board, Washington, D.C.
5. Khazanovich, L., M. Darter, R. Bartlett, and T. McPeak (1998). *Common Characteristics of Good and Poorly Performing PCC Pavements*. Report FHWA-RD-97-131. Federal Highway Administration, Washington, D.C.
6. Mindess, S., and J. F. Young (1981). *Concrete*. Prentice-Hall, Englewood Cliffs, NJ.
7. Janssen, D. J. (1987). "Moisture in Portland Cement Concrete," *Transportation Research Record 1121*. Transportation Research Board, Washington, D.C.
8. Rao, C., E. J. Barenberg, M. B. Snyder, and S. Schmidt (2001). "Effects of Temperature and Moisture on the Response of Jointed Concrete Pavements." *Proceedings*, *7th International Conference on Concrete Pavements*, Orlando, Florida.
9. Springenschmid, R. and W. Fleischer (2001). "Recent Developments in the Design and Construction of Concrete Pavements for German Expressways," *Proceedings*, *7th International Conference on Concrete Pavements*, Orlando, Florida.
10. Springenschmid, R., and E. Hiller (September 1998). "Influence of Temperature During Curing on Stresses in Concrete Pavements," *Proceedings, 8th International Symposium on Concrete Roads*, Theme II, Lisbon, Portugal.
11. Springenschmid, R. and M. Mangold (1994). "Curing of Concrete Pavements to Control Thermal Stresses," *Proceedings, 7th International Symposium on Concrete Roads*, Vienna, Austria.
12. Hall, K. T., M .I. Darter, T. E. Hoerner, and L. Khazanovich (1997). *LTPP Data Analysis—Phase I: Validation of Guidelines for k-Value Selection and Concrete Pavement Performance Prediction*. Technical Report FHWA-RD-96-198, Federal Highway Administration, McLean, VA.
13. Owusu-Antwi, E. B., L. Titus-Glover, L. Khazanovich, and J. R. Roesler. (1997). *Development and Calibration of Mechanistic-Empirical Distress Models for Cost Allocation*. Final Report, Federal Highway Administration, Washington, D.C.
14. McGhee, K.H. (1995). *Design, Construction, and Maintenance of PCC Pavement Joints*. Synthesis of Highway Practice 211. Transportation Research Board, National Research Council, Washington, DC.
15. Christory, J. P. (1990). "Assessment of PIARC Recommendations on the Combating of Pumping in Concrete Pavements." *Sixth International Symposium on Concrete Roads*. Madrid, Spain, 1990.

16. Permanent International Association of Road Congresses (1987). *Combating Concrete Pavement Slab Pumping by Interface Drainage and Use of Low-Erodability Materials: State of the Art and Recommendations*, Permanent International Association of Road Congresses, Paris, France.
17. Darter, M. I. (1992). *Report on the 1992 U.S. Tour of European Concrete Highways*, Report FHWA-SA-93-012, Federal Highway Administration, Washington, D.C.
18. Larson, R.M., S. Vanikar, and S. Forster (date). *Summary Report—U.S. Tour of European Highways (U.S. Tech)—Follow-up Tour of Germany and Austria*. Report FHWA-SA-93-080. Federal Highway Administration, Washington, D.C.
19. Darter, M. I., H. L. Von Quintus, Y. J. Jiang, E. B. Owusu-Antwi, and B. M. Killingsworth (1997). *Catalog of Recommended Design Features* (CD-ROM). NCHRP Project 1-32. Transportation Research Board, National Research Council, Washington, D.C.
20. Chou, Y.T. (1981). *Structural Analysis Computer Programs for Rigid Multicomponent Pavement Structures with Discontinuities- WESLIQID and WESLAYER; Report 1: Program Development and Numerical Presentations; Report 2: Manual for the WESLIQID Finite Element Program; Report 3: Manual for the WESLAYER Finite Element Program*. Technical Report GL-81-6, U.S. Army Engineer Waterways Experiment Station, May.
21. ERES Consultants (1998). *Pavement SubsurfaceDrainage Design*. Reference Manual, NHI Course No. 13126. National Highway Institute, Washington, D.C.
22. Miner, M. A. (1945). "Cumulative Damage in Fatigue," *Transactions*, American Society of Mechanical Engineers, Vol. 67, pp. A159-A164.
23. Khazanovich, L. (1994). *Structural Analysis of Multi-Layered Concrete Pavement Systems*. Ph.D. Thesis, University of Illinois at Urbana-Champaign.
24. Hoerner, T. E, M. I. Darter, L. Khazanovich, L. Titus-Glover, and K. L. Smith (2000). *Improved Prediction Models for PCC Pavement Performance Specifications, Volume I: Final Report.* Report No. FHWA-RD-00-130, Federal Highway Administration, Washington, D.C.
25. Zollinger, D. G., N. Buch, D. Xin, and J. Soares (1999). *Performance of Continuously Reinforced Concrete Pavements: Volume VII: Summary*. Final Report, FHWA-RD-98-102, PCS/Law Engineering.
26. Gharaibeh, N. G., M. I. Darter, and L. B. Heckel (1999). "Field Performance of CRCP in Illinois," Report FHWA-IL-UI-268, Illinois Department of Transportation.
27. Simpson, A. L., Rauhut, J.B., Jordahl, P.R., Owusu-Antwi, E., Darter, M.I., Ahmad, R., Pendleton, O., Lee, Y-H., (1994). "Sensitivity Analysis for Selected Pavement Distresses," Report SHRP-P-393, Strategic Highway Research Program.
28. LaCourseiere, S. A., M. I. Darter, and S. A. Smiley (1978). *Structural Distress Mechanisms in Continuously Reinforced Concrete Pavement*, Transportation Engineering Series No, 20, University of Illinois at Urbana-Champaign.
29. Zollinger, D. G., and E. J. Barenberg (1990). *Continuously Reinforced Pavements: Punchouts and Other Distresses and Implications for Design*, Project IHR - 518, Illinois Cooperative Highway Research Program, University of Illinois at Urbana-Champaign.
30. Tang, T., D. G. Zollinger, and B. F. McCullough (1996). "Field Tests and Analyses of Concrete Pavement in Texarkana and La Porte, Texas," Research Report 1244-7, Texas Transportation Institute, Texas A&M University, College Station, TX.
31. Darter, M. I. (1988). "CRCP Distress Study on I-77 Fairfield and Chester Counties, South Carolina," ERES Consultants, Inc., Champaign, IL.

32. Selezneva O. I., D. Zollinger, and M. Darter (2001). "Mechanistic Analysis of Factors Leading to Punchout Development for Improved CRCP Design Procedures," *Proceedings of the 7th International Conference on Concrete Pavements*, pp. 731-745.
33. Parrott, L. J. (July 1988). "Moisture Profiles in Drying Concrete," *Advances in Cement Research,* Vol. 1, No. 3.
34. Van Wijk, A. J. and C. W. Lovell (1986). "Prediction of Subbase Erosion Caused by Pavement Pumping," *Transportation Research Record No. 1099*, Washington, D.C., pp. 45 – 57.
35. Van Wijk, A. J. (1985). "Rigid Pavement Pumping: (1) Subbase erosion and (2) Economic Modeling," Joint Highway Research Project File No. 5-10, School of Civil Engineering, Purdue University, West Lafayette, IN.
36. Bradbury, R. D. (1938). "Reinforced Concrete Pavements," Wire Reinforcement Institute, Washington, D.C.
37. Mohamed, A. R., and W. Hansen (1997). "Effect of Nonlinear Temperature Gradient on Curling Stress in Concrete Pavements," *Transportation Research Record No. 1568,* Washington, D.C., pp. 65-71.
38. Poblete, M, R. Salsilli, R. Valenzuela, A. Bull, and P. Spratz (1988). "Field Evaluation of Thermal Deformations in Undoweled PCC Pavement Slabs," *Transportation Research Record No. 1207,* Washington, D.C., pp. 217-228.
39. Hansen, W., E.A. Jensen, and P. Mohr (2001). *The Effects of Higher Strength and Associated Concrete Properties on Pavement Performance*. Report No. FHWA-RD-00-161, Federal Highway Administration, Washington, D.C.
40. Personal correspondence with Dr. Dan Zollinger (Texas A&M University).
41. Eisenmann, J. and G. Leykauf, "Effect of Paving Temperatures on pavement Performance," Procedings 2nd International Workshop on the Theoretical Design of Concrete Pavements," Siquenza, Spain, 1990.
42. Eisenmann, J. and G. Leykauf, "Simplified Calculation Method of Slab Curling Caused by Surface Shrinkage," Proceedings 2nd International Workshop on the Theoretical Design of Concrete Pavements," Siquenza, Spain, 1990